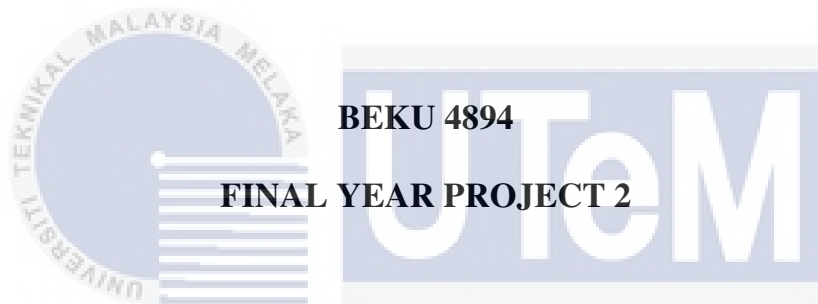**FAKULTI KEJURUTERAAN ELEKTRIK**

UNIVERSITI TEKNIKAL MALAYSIA MELAKA

SEM 2 SESSION 2014/2015

BEKU 4894

FINAL YEAR PROJECT 2

DESIGN OF LOWER LIMB EXOSKELETON ROBOT

NAME	:	**TAN CHEE JUN**
MATRIX NO.	:	
SERIAL NO.	:	**19**
COURSE	:	**4-BEKM S1**
DATE	:	**1/6/15**
SUPERVISOR	:	**NUR LATIF AZYZE BIN MOHD SHAARI AZYZE**

" I hereby declare that I have read through this report entitle "Design of Lower Limb Exoskeleton Robot" and found that it has comply the partial fulfilment for awarding the degree of Bachelor of Mechatronics Engineering With Honours.
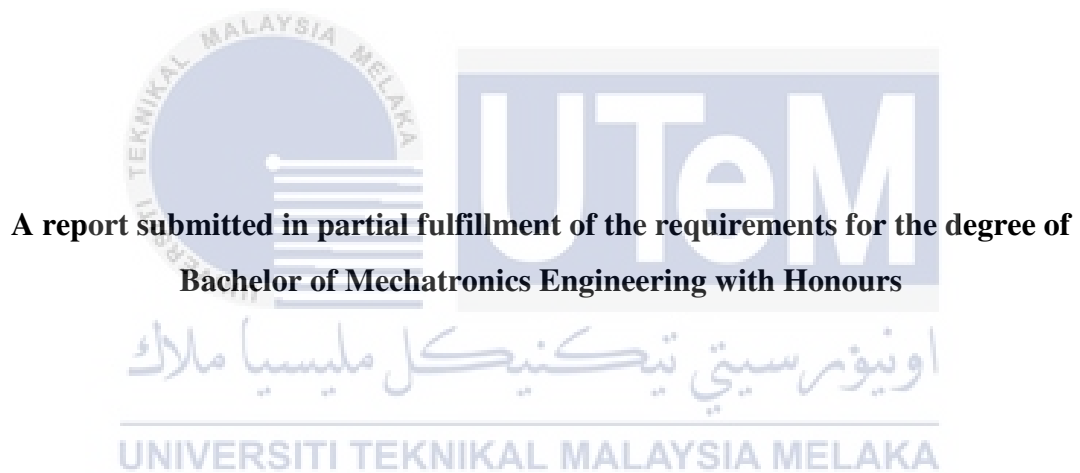

Signature   : ....

Supervisor's Name   : ....

Date   : ....
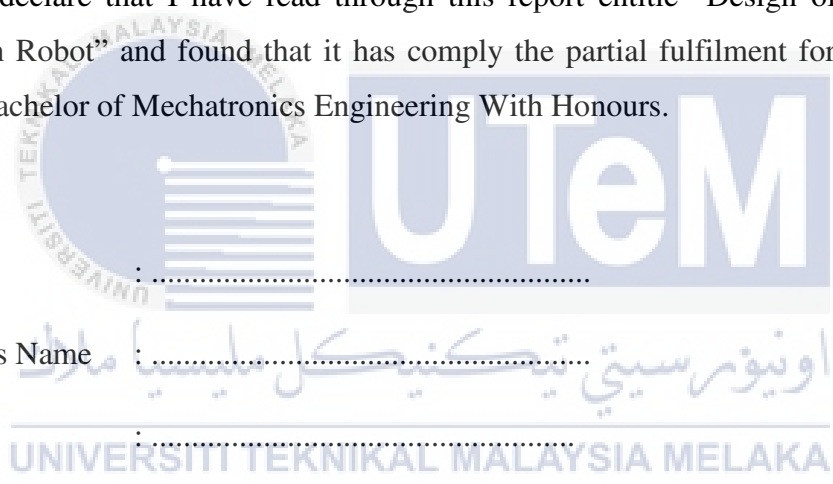
DESIGN OF LOWER LIMB EXOSKELETON ROBOT

TAN CHEE JUN

**A report submitted in partial fulfillment of the requirements for the degree of
Bachelor of Mechatronics Engineering with Honours**

Faculty of Electrical Engineering

UNIVERSITI TEKNIKAL MALAYSIA MELAKA

JUNE 2015

iii

"I declare that this report entitle "Design of Lower Limb Exoskeleton Robot" is the result of my own research except as cited in the references. The report has not been accepted for any degree and is not concurrently submitted in candidature of any other degree."

Signature : ....

Name : ....

Date : ....

ACKNOWLEDGEMENT

First of all, I would like to thank my parents for giving me endless supports during the toughest time in my life. I owe my parents my sincerest gratitude as they went through all kinds of hardship to support me throughout the course of pursuing knowledge. Next, I would like to thank my supervisor, En. Nur Latif Azyze bin Mohd. Shaari Azyze for providing me valuable guidance to pass through the mist of confusion and ignorance. En Latif had also lessened the stress for me by giving me the freedom to do this project in my own pace. Besides that, I would like to thank all my friends for sharing their valuable opinions on my projects and inspired me with different ideas that proved to be useful. They also provide support and help when I needed the most by sharing useful information and teaching me. I would also like to thank all the lecturers that I've met by any reasons for giving me guidance and sharing their knowledge relentlessly throughout the whole time I've spent in UTeM. They are always there to help me when I required their enlightenment and they've always managed to widen my knowledge. Finally, I would like to thank those whom I've failed to mention that had helped me in this project whether directly or indirectly. Thank you all for being part of the pushing hands the pushed this project into completion no matter how big or small your contribution is.

ABSTRACT

Every year, many workers suffer from work-related musculoskeletal disorders (MSD) cases that are caused by long term walking and standing. This problem can be overcome by using exoskeleton which is a type of wearable robots that can augment the performance of an able-bodied user. A lower limb exoskeleton can be used to improve muscle endurance of the user by providing support torque to the limbs. There are many studies that use hydraulic actuator to actuate the lower limb exoskeleton which have several drawbacks like dirty, noisy and high power consumption. Therefore, electrical actuators that are clean, silent and less power consuming are used in designing the lower limb exoskeleton in this project. Hence, to design an electrical actuated exoskeleton, this project is aimed to derive the mathematical model and joint torque equations, to design a lower limb exoskeleton using electrical motors from the market and to validate the design of the lower limb exoskeleton by simulation. In order to achieve the objectives, mathematical model of the exoskeleton are derived using kinematic analysis and the required joint torque are derived using force analysis. Besides that, motors and gearboxes are selected and incorporated into the design of the exoskeleton. After that, finite element analysis (FEA) and motion analysis test on the design model of the exoskeleton are conducted using SolidWorks. The FEA test shows that the structural strengths of all the exoskeleton links are able to support the user under maximum torque condition. Besides that, the motion analysis done also shows that the actuator units selected are able to support a 100kg user and the exoskeleton to walk. However, there are limitations for the actuator units selected which requires further testing and improvement. In conclusion, all the objectives are achieved but the exoskeleton still requires further studies and improvements.

ABSTRAK

Setiap tahun, ramai pekerja mengalami malasah gangguan muskuloskeletal disorder(MSD) yang disebabkan oleh berdiri dan berjalan untuk jangka masa panjang. Masalah ini boleh diatasi dengan menggunakan Exoskeleton yang merupakan jenis robot boleh pakai yang boleh meningkatkan prestasi seorang pengguna yang berbadan sihat. Exoskeleton untuk kaki boleh digunakan untuk meningkatkan daya tahan otot pengguna dengan menyediakan sokongan tork kepada anggota badan. Terdapat banyak kajian yang menggunakan penggerak hidraulik untuk menggerakkan Exoskeleton mempunyai beberapa kelemahan seperti kotor, bising dan penggunaan tenaga yang tinggi. Oleh itu, penggerak elektrik yang bersih, senyap dan kurang memakan kuasa digunakan dalam mereka bentuk Exoskeleton dalam projek ini. Oleh itu, untuk mereka bentuk sebuah kulit luar digerakkan elektrik, projek ini bertujuan untuk memperolehi model matematik dan persamaan tork bersama, untuk mereka bentuk Exoskeleton menggunakan motor elektrik dari pasaran dan untuk mengesahkan reka bentuk Exoskeleton dengan simulasi. Dalam usaha untuk mencapai objektif, model matematik Exoskeleton telah diperolehi dengan menggunakan analisis kinematik dan tork bersama yang diperlukan telah diperolehi dengan menggunakan analisis kuasa. Selain itu, motor dan kotak gear telah dipilih dan dimasukkan ke dalam reka bentuk Exoskeleton. Selepas itu, Finite Element Analysis (FEA) dan analisis pergerakan kepada model Exoskeleton telah dijalankan menggunakan SolidWorks. Ujian FEA menunjukkan bahawa kekuatan struktur semua anggota Exoskeleton dapat menyokong pengguna di bawah keadaan tork maksimum. Selain itu, analisis pergerakan yang dilakukan juga menunjukkan bahawa unit penggerak dipilih mampu menyokong pengguna 100kg dan Exoskeleton untuk berjalan. Walau bagaimanapun, terdapat batasan bagi unit penggerak terpilih yang memerlukan ujian lanjut dan penambahbaikan. Kesimpulannya, semua objektif tercapai tetapi Exoskeleton ini masih memerlukan kajian lanjut dan penambahbaikan.

TABLE OF CONTENTS

LIST OF TABLES

LIST OF ABBREVIATIONS

MSD	-	Musculoskeletal Disorder
LLD	-	Lower Limb Musculoskeletal Disorder And Injuries
DC	-	Direct Current
EMG	-	Electromyography
DH	-	Denavit-Hartenberg
m	-	Mass
l	-	Length
T	-	Torque
FEA	-	Finite Element Analysis
s	-	Step Length
H	-	Maximum Lift Height

LIST OF FIGURES

LIST OF APPENDICES

CHAPTER 1

INTRODUCTION

1.1 Motivation

Musculoskeletal disorders (MSD) are a form of injury or discomfort that normally involves our body parts below the skull including joints, muscles and so on. This form of injuries normally befalls on our limbs, neck and back. MSD commonly arises from acute trauma which happens when the body supporting structure is subjected to a large single load that exceeds the body's limitations for instance like heavy lifting and moving heavy stuffs. Besides that, MSD are also caused by the overuse trauma which happens when the body is subjected to repetitive movement while under loading condition for example like unloading goods from trucks.

In year 2005, out of 1012000 cases of work related MSD reported in the United Kingdom, there are 18%, which is about 185000 people that suffers from the lower limb musculoskeletal disorder and injuries (LLD). [1] LLD poses a great effect on the patients; it can affect the patient in level from causing discomfort to immobility and thus decreasing the quality of life. Besides that, LLD also affects the employer in terms of work time lost and decrease in production rate. This shows that LLD possesses a great threat to not only the society but also the industry and the consequences of it are critical.
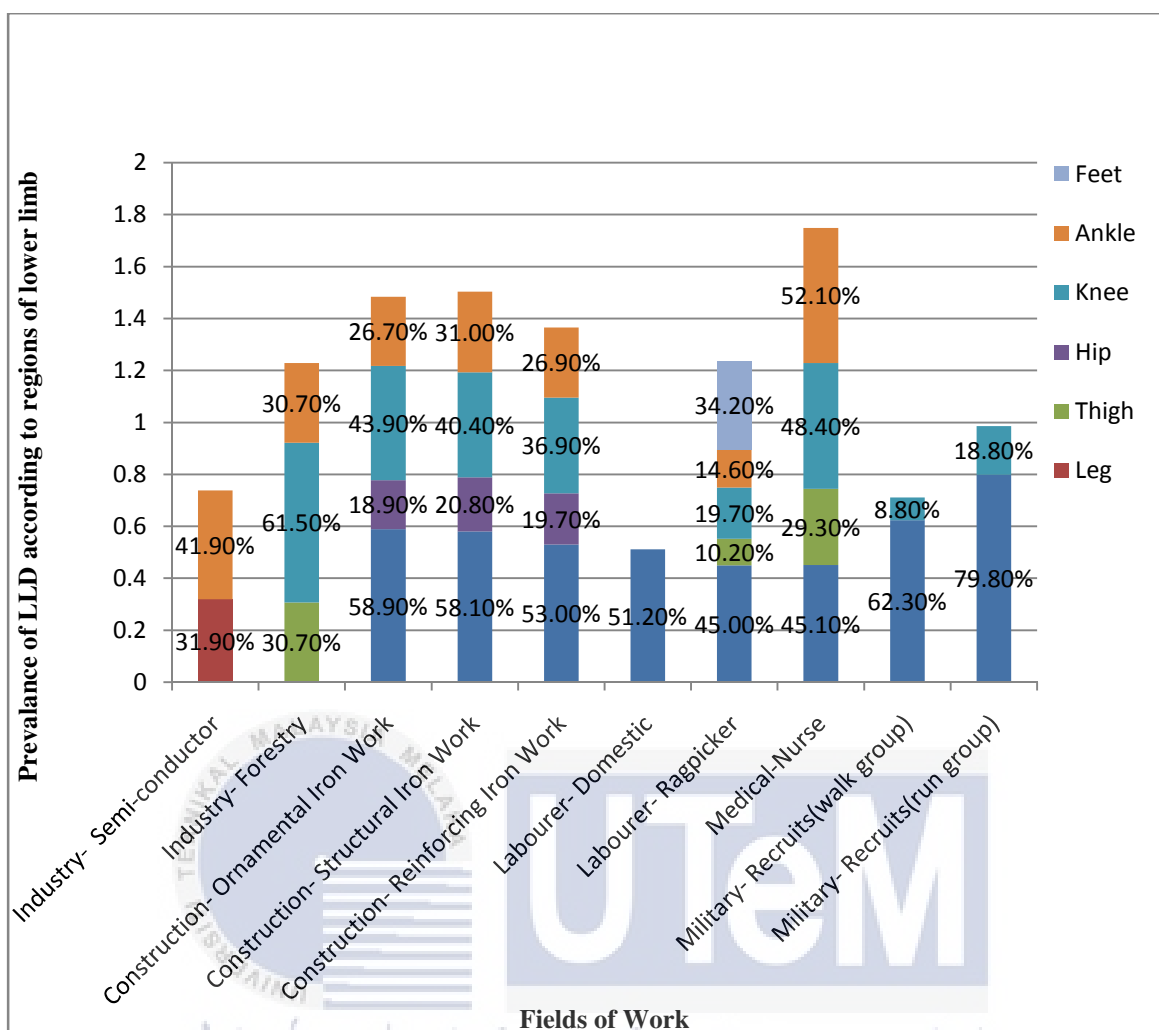
Figure 1.1: Prevalence of LLDs reported for different field of work. [2]

Figure 1.1 shows the prevalence of LLD reported in different field of work. The statistics shows that more than 50% of the LLD reported involve the injuries of the full lower limb in the field of construction field. This is probably due to the heavy lifting and long term standing that the work requires. Besides that, the medical field also shows a high prevalence of LLD which about half of the injuries reported involve ankle, knee and lower limb. This is caused by the long term walking and standing working as a nurse. Apart from that, the military field also shows the highest prevalence of LLD which is more than 60% in the form of full lower limb pain. This is no surprise as the soldiers need to carry heavy loads and walk or run for a long distance. For the industry worker however, only parts of the lower limb like ankle and knee shows a high prevalence of LLDs reported. [2]

This shows that how common are LLDs occurs in not only the industry but also some other fields of work. This project can help in reducing the occurrence of the LLDs by providing the support to the workers lower limb.

1.2 Problem Statement

With the widespread presence of lower limb musculoskeletal disorder and injuries, it is not an issue that can be ignored. Patients that suffer from lower limb musculoskeletal disorder and injuries (LLD) have reduced mobility due to conditions like osteoarthritis and bursitis. [2] These conditions that lower mobility will cause inconvenience in life for the patients as they cannot perform daily life activities as they used to be. This project of designing an electrical powered exoskeleton will help in preventing the development of LLDs in fields of work with high risk like construction and military. This will help to reduce the number of LLD cases in the society.

Some of the previous studies have incorporated hydraulic cylinders in their designs to actuate the exoskeleton. However, using hydraulic actuators to provide actuation have their downsides. One of it being the complexity of the system due to the reason it needs both hydraulic system for the actuation and electrical system for the sensors and control of the exoskeleton. Besides that, oil leakage can occur which will reduce the performance and soil the user. Moreover, hydraulic actuation's power consumption is almost 2 times of that of electrical actuation. [4,5]

Although electrical powered exoskeleton can provide the ideal operation condition for the user, it has a problem that needs to be overcome. The problem being that it is difficult to find the suitable sized electrical motor in the market to provide actuation. For instance, the hip of a 75kg man requires a maximum of 80Nm of joint torque during a walking cycle. [3] It is possible to find a servomotor that can produce 80Nm but it is difficult to find a servomotor that produce that amount of torque that is small and light. [5]

However, a drive system can be incorporated to the design to produce sufficient amount of torque with smaller sized electrical motor. Hence, this project is purposed to provide a design of electrical powered exoskeleton with clean operation, less power consuming and less complex of the overall system.

1.3 Objectives

1. To derive mathematical model of lower limb using kinematic analysis and formulate joint torque.
2. To design an electrical powered lower limb exoskeleton using Solid Works.
3. To validate the design of exoskeleton in terms of structural strength as well as joint torque base on the motor available on the market.

1.4 Scope

The scope of this project is to design a lower limb exoskeleton actuated by electrical actuator. Since the average weight of adult Malaysian men is 61.8kg, the lower limb exoskeleton should be able to support user up to 100kg. [36] This project will focus on supporting a 100kg able-bodied user at ground level walking by lifting the limbs. The lower limb exoskeleton will be actuated by electrical actuator available on the market. In this project, the kinematics of lower limb exoskeleton will be derived. Besides that, the mechanical design of the lower limb exoskeleton will be discussed. Apart from that, the lower limb exoskeleton will be simulated to test the structural strength and torque requirement.

CHAPTER 2

LITERATURE REVIEW

2.1 Introduction

Exoskeleton is a device that can augment the performance of an able-bodied wearer. It is used to augment the strength or the endurance of the wearer through various means. There are many types of exoskeleton which are mainly grouped into either full body exoskeleton or partial exoskeleton which further divides into upper limb exoskeleton and lower limb exoskeleton. As the name suggested, full body exoskeleton improves the performance of both the upper and lower limb of the user be it the strength or the endurance. For upper limb exoskeleton, the exoskeleton will augment the performance of user from the waist up including torso and arms. Whereas, the lower limb exoskeleton will improve the performance of the user's legs. This research will focus on the lower limb exoskeleton. [6]

The lower limb exoskeleton is further divided into two types which are series and parallel. Series lower limb exoskeletons are the ones that are applied in series with human legs to store energy and release far greater strain energy. [8] This type of exoskeleton works by storing energy when the user's feet are striking the ground and release it by pushing the user to lift. By doing this, it reduces the effort for the user to move and hence reduce the metabolic cost. The most common example of this type of exoskeleton is the elastic shoes.

The other type of exoskeleton is known as parallel exoskeleton which is applied in parallel with human lower limb to change the limitations of the human body. For this type of exoskeleton there are various designs that serve different purposes for the wearer. One of which is for load transfer. This design transfer load as well as the body weight directly to the ground which will reduce the metabolic cost of the wearer for loads carrying and ultimately enhance the endurance of the wearer. One of the examples for this type of exoskeleton is Berkeley Lower Limb Exoskeleton (BLEEX) developed by University of California, Berkeley. [3, 8] There is another design that is intended for torque and work augmentation. This sort of design augments joints torque and power of the user allowing them to lift heavy thing and perform daily activities with ease. Besides that, it also helps in reduce joint pain for user. However, this design normally does not transfer substantial load to the ground unlike the previous design mentioned. An example of this type of exoskeleton is the Hybrid Assistive Limb (HAL) developed by Cyberdyne [7, 8]. Besides that, there is another designed that aimed to increase the users muscle endurance. This type of exoskeleton utilizes the fact that only a small portion of our muscles are fatigue during an exhaustive exercise. It redistributes the work load over a greater number of muscles, particularly the muscles that are not easily fatigue. This design simply uses spring that will stretch by unused muscles to store energy and then release it to assist the muscles that are easily fatigue. Hence, the muscle endurance of the wearer can be increased using this design. [8]

Since there are so many designs for exoskeleton, a design suitable for an intended application should be determined and suitable components of the exoskeleton should be selected to make sure that the exoskeleton designed works as it should.

2.2 Biomechanics of Human
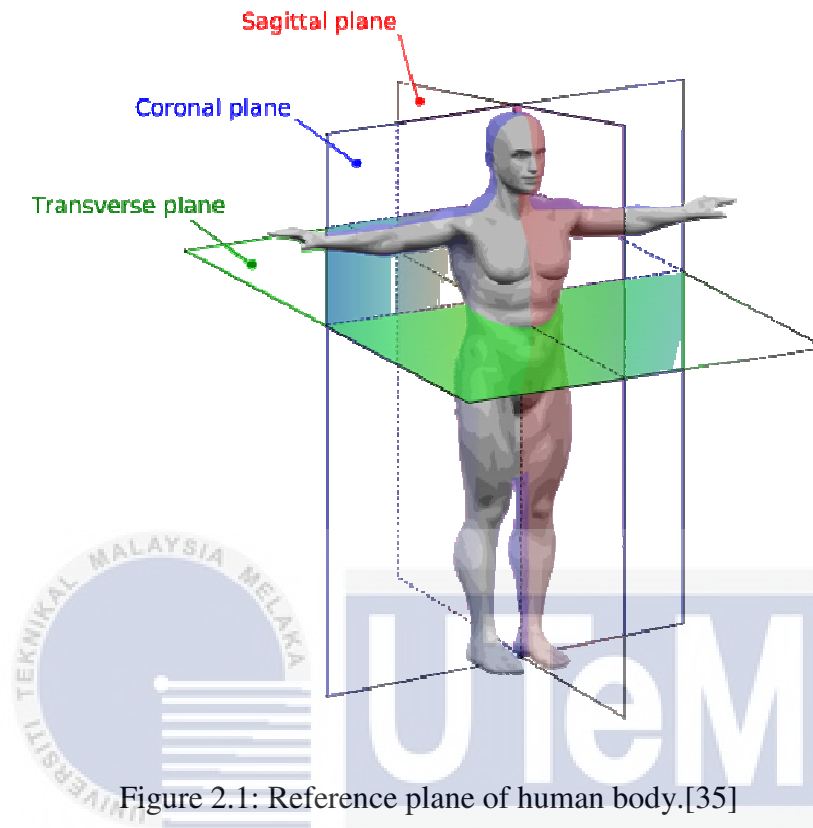
Figure 2.1: Reference plane of human body.[35]

Human's movement and motion are very complex due to the vast number of degree of freedom of our body. However, most of our daily life motions that require large torque and power are performed in the Sagittal plane. [34] These motions include walking, running, standing up and more. This is the reason why many of the previous studies focused on actuation of joint in Sagittal plane particularly in flexion/extension of hip, knee and ankle as seen in [30].

There are many degrees of freedom for human's lower limb. However, it would be a waste to actuate all of them as some of them do not require high power. According to [30], the flexion/extension of hip, knee and ankle requires the most power which needs to be actuated.

In conclusion, actuations should be provided to the flexion/extension of hip, knee and ankle whereas the other un-actuated joints are left to rotate freely to minimize the hindrance of the user's movements.

2.3 Actuators

Actuators are the device that provide motion for the exoskeleton and hence support the wearer's limb motion. It takes the command from the controller and provides motion according to the requirement at a certain instant. Electrical Actuator is one of the most popular choices due to its clean and silent operation as well as lower power consumption than others [5]. Some of the electrical actuators used by previous studies include DC Servomotor, Linear Actuator and Series Elastic Actuator.

DC Servomotor is a popular choice in providing actuation for robots as well as exoskeletons. It is essentially a motor with built-in position feedback. One of the reasons it is often used as an actuator is because of its simplicity and convenience to apply. [21] DC Servomotor can be easily controlled by controller which sends signal to it. Unlike any other actuator, the direction, speed and even position of the motor can be easily controlled by electronics. Moreover, DC servomotor provides precise positioning because of its built-in position feedback which gives an accurate control of its motion and position. . It provides clean and silent actuation of exoskeleton compared to the other which makes it suitable for application in any environment, indoor or outdoor. Apart from that, it is relatively compact compared to other electrical actuators is also one of the reason why it is such popular choice. [21] This is why it is normally positioned on the exoskeleton's joint that need to be actuated as seen in [18, 19, 21, 27]. However, there are some studies that position it away from the joint and transmit power through a drive system like chain or cable. [20, 23] Despite the compact size, a DC Servomotor with high torque and small size is not very easy to find. That is why Servomotors are normally coupled with suitable reducers to provide high torque and fast response motion in a small package. DC

Servomotors are chosen to be used by previous studies are also because of its high energy efficiency. [21]

There are studies that use linear actuator as their actuation system for their exoskeleton. [22, 23] Linear actuator consists of an electric motor and a leadscrew which translate the rotational motion provided by the motor into linear motion. It is chosen by studies in [22, 23] because of its high load capacity which means it can provide high force output. Apart from that, reasonable price is also one of the advantages of the linear actuators. However, there are some drawbacks of this type of actuator. One of it being that it is normally large and bulky because it needs to house the components like leadscrew, motor, gearing, bearing and other components. Besides that, the moving parts of the actuator are prone to wear and tear due to frictions. The linear actuator also has a limited range of motion as the leadscrew can only extend for a limited length only.
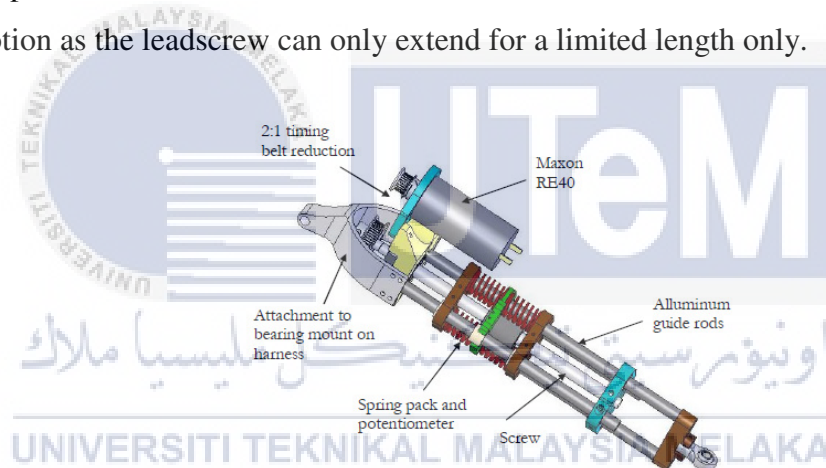
Figure 2.2: Linear series elastic actuator[25]

Linear Series Elastic Actuator is also a type of actuator used to provide motion for the exoskeleton. This actuator utilizes an electric motor coupled with lead ball screw and spring pack to provide linear motion as shown in Figure 2.2. It has a spring pack in series with the output of the motor. Some studies chose this type of actuator because it provides a better way to implement light and inexpensive force control. [25] Apart from that, it is said to be shock tolerant, low impedance and provides energy storage due to the spring pack incorporated in the design. [10] However, the size of Series Elastic Actuator is usually larger than other alternatives because it the components it needs. It is very hard to fit an

electric motor, lead ball screw, spring pack, gearing and frames into a small package. Hence, it would increase the size of the exoskeleton which makes it not ideal for commercial applications. Like the linear actuator, the series elastic actuator also suffers from the same problem in range of motion due to the design.

Table 2.1: Comparison between actuators.

	DC Servomotor	Linear Actuator	Series Elastic Actuator
Advantages	-Compact -Easy To Control -High Precision -Accurate Positioning -High Energy Efficiency -Silent -Can Be Coupled With Drives To Produce High Torque	-Cheap -High Load Capability	-Low Impedance -Accurate Force Feedback -Shock Tolerance -Energy Storage
Disadvantages	-Expensive -Size Could Be Large	-Large And Bulky -Wear And Tear Of The Ball Screw(Friction)	-Low Bandwidth At High Force -Bulky -Custom Built, Not Available On Market
Range Of Motion	Wide	Limited by the length of leadscrew	Limited by the length of leadscrew

The comparisons between the actuators are summarized in Table 2.1. As a conclusion, DC servomotor is chosen for this project due to the facts that it has wider range of motion, more compact size and less prone to wear and tear compact to the other alternatives.

2.4 Drive System

Harmonic drive system is a power transmission system that is a very popular choice in electrical actuated exoskeleton as seen in [4, 18, 19, 27]. It decreases the output speed as well as increases the output torque for an actuation system and hence reduces the size of the motor required. The reason why it is chosen by many of the previous studies is due to its advantages of no backlash, excellent positional accuracy and high torque/reduction ratio. [4, 16] Besides that, compact size is also one of the main advantages of harmonic drives. This is due to the special design that makes it input concentric with its output. However, all that advantages come with a great price; the cost of a harmonic drive unit is often very high.

In [19], chain drive is chosen to be the drive system for the exoskeleton. Chain drive is a long distance power transmission system that utilizes the chain to transmit power. It possesses the advantages of simple to implement and flexible length of power transmission. However, chain drive system can take up a lot of space for the chain means that it is not suitable for exoskeleton application.

In [23], cable-pulley drive is used to transmit power for actuation. Depending on designs, the cable-pulley drive can have very limited range of motion and takes up a lot of space. However, this sort of drive system does not have problems like backlash and friction unlike chain drive system.

Table 2.2: Comparison between drive used by previous studies.

	Harmonic Drive	Chain Drive	Cable-Pulley Drive
Features	-short distance power transmission -speed reduction	-transmit power over long distance -speed reduction	-transmit power over long distance -speed reduction
Advantages	-compact -no backlash -excellent positional accuracy -high reduction ratio	-simple to use -any length can be achieved	-no backlash -no friction
Disadvantages	-expensive	-takes space	-limited range of motion -takes space

Table 2.2 summarizes the comparison between the drive systems. Each solution has its own trade off, an appropriate trade-off should be considered to select the most suitable solution for an application. In this case, harmonic drive unit is the most suitable drive system simply because of the facts that it has the most compact size, possess high accuracy and also high reduction capability.

2.5 Control Scheme

To control the motion of an exoskeleton, a good control strategy is required to be implemented so that the user can control the exoskeleton smoothly. There are many types of applications for exoskeletons for instance like rehabilitation or power augmentation which makes development of a generalized control strategy for all exoskeleton would be very challenging. [11] Hence, a suitable control scheme for the application is vital to make the exoskeleton operate smoothly.

Many of the previous studies [11, 24, 27] based their control scheme on motion intent recognition. This type of control strategy determines user's intention using combination of sensors and generates appropriate trajectories with the exoskeleton.

In [28, 29, 30], the control scheme for the lower limb exoskeleton minimizes the use of sensory data from the human-exoskeleton interactions and uses sensory data from the exoskeleton. This means that no sensors are applied on the user's body and data are taken from the exoskeleton only. The control system utilises data from linear accelerometer, encoders and foot load distribution sensor to determine the suitable trajectory for the exoskeleton to move. The main advantage of this control scheme is the elimination of problem with measuring muscle activities or interaction forces. [30] However, this control scheme has a one drawback which is accurate dynamic models are required for different situations to make the exoskeleton function well. [11]

In [24, 27], researchers proposed a control scheme based on surface electromyography (EMG). The control system of the exoskeleton uses data from EMG sensors, encoders, ground reaction force sensors and gyroscope to determine the user's intentions. The control algorithm divides a series of motion into phases like walking, standing and sitting. The control system determines the phase that the user is in as well as the phase they intended to change into utilizing the sensory data from the exoskeleton and actuate the exoskeleton accordingly. The main advantage of using this control scheme is that is has the ability to predict intended movement even if the muscle is too weak to perform the movement. [13] However, this control scheme has a drawback which is not suitable to be applied to exoskeleton with too many degree of freedom as the EMG sensor are prone to noise caused by neighbouring muscles.[12,13]

In [14], a control scheme based on manual controlling was implemented. The study uses hand-held controllers to control the air pressure send to the pneumatic actuator and thus actuate the orthotics device. The air pressure send into the pneumatic actuator is proportional to the displacement of the push button. This means that the user's intentions are input by the user itself, not the measurements from the users like studies mentioned

above. The main advantage of this control scheme is that it is easy to implement without many sensors needs. However, this type of control strategy needs high level of manual supervision by the user which is one of the disadvantages of it. [11]

The truth is there is no prefect control scheme despite the fact that there are many types of control scheme done by different studies. There's always a disadvantage possess by the control strategy. However, considering the facts that the control scheme based on EMG is extracting user's intentions directly and it can predict movement even with weak muscle conditions make it suitable for exoskeleton with many applications.

2.6 Sensors

Sensors are the device that senses various data about the exoskeleton and the wearer and send it to the controller for it to make decisions. Sensors are important to make sure that the exoskeleton operate as desired by the user. Different combinations of sensors are used by different researchers to achieve their desired operation of the exoskeleton.

2.6.1 Intention Detection

To control the exoskeleton, sensors that are able to detect the user's intentions are important to in order to make the exoskeleton to be controlled as intended. Table 2.3 shows the comparison between sensors used to detect intentions.

Table 2.3: Comparison between intention detection sensors

	EMG	Force sensor	Pressure sensor
Features	-Measure muscle activity	-Measure force -Measure load distribution	-Measure pressure distribution -Measure load distribution
Advantages	-Measure only users intention, contact surface does not affect -Proper interpretation can predict user's intention, reduce delay	-Simple to use -Low cost	-Low cost
Disadvantages	-Requires work on interpretation	-Noise when contact with different surface -Slight delay	-Noise when contact with different surface

In [21, 24, 26, 27], force sensors are applied to measure forces on the exoskeleton. It is normally incorporate in to the design of the footpad of the exoskeleton. Each footpad will have 2-4 force sensors distributed across the area of the footpad. These force sensors in footpads are responsible to measure load distribution or ground reaction forces which are analysed to determine the user's intentions. This is because the force distribution will differ with different user intentions for instance like lifting your leg or standing still. One of the reasons why it is used in many studies is because it is low cost and it is simple to use. [9] However, there are a few drawbacks in applying force sensors in footpads to determine the user's intentions. One of which is the problem when the contact surface is rough, it is very hard to the forces exert by the user and the force exert by the rough surface. Thus, there might be error in determining the user's intentions. [9] Apart from that, the natural delay in control loop that are caused by the nature of neuronal signal travels from brain to muscle is also one of the drawback as mentioned in [9].

In [18, 19], the force sensors on footpads are replaced with pressure sensors to measure the pressure distribution between the user's feet. In [18], it is not only used to measure pressure, force and contact area but also provide gait timing parameters which are used in controlling the exoskeleton. However, since it is also applied in the footpad, it might also suffer from the same problem with force sensors when the contact surface is rough.

In [24, 27], EMG is used to determine the user's intention in motion. It is applied on flexor and extensor muscles to measure muscle activity and hence determine the user's intentions. Unlike force sensors or pressure sensors on footpad, EMG sensors does not affect by the changes in contact surface as it only measure muscle activity generate by the intentions of the user. Therefore, the problem with contact surface is avoided with the use on EMG sensors. [9] According to [9], the delay problem existed in the use of force sensors can be reduced with proper interpretation of the EMG signals. Proper interpretation of EMG signal can allow calculated prediction of the user's desired motion in advance and hence reduce in delay. However, using EMG sensors come with one drawback which is in interpretation of EMG signal into useful data. Conversion of EMG signals into muscle force requires substantially more work than using force or pressure sensors.

Considering that each solutions has their own advantages and disadvantages, a combination of using EMG sensors and force sensors is chosen for this project to make the detection of user's intentions more accurate and smoother operation of the exoskeleton.

2.6.2 Joint Angle

To control the joints, sensors that detect the joint angle are very important. In [19, 24, 24], rotary encoders are chosen as the sensor to detect the joint angle for the exoskeleton. It is a sensor that translates rotary motion into electrical signal that contains

information about the position, speed and acceleration.[16] The reason it is a popular choice it because of it advantages like significantly wear free, wide range of motion and high precision. However, encoders also have disadvantages like high cost and complex to implement. [15]

In [20, 25], potentiometer are used to take measurement of the joint angle. It is basically a variable resistor with different resistance value at different position. It is often chosen for its advantages like low cost, low power consumption, simple to implement as well as small and light. Although it has limited range of motion, but it is suitable to be implement on joints that rotate in a small angle range. However, due to its rotating contact, it is prone to wear and tear compared to encoder. [15]

Table 2.4: Comparison between angular sensors.

	Rotary Encoder	Potentiometer
Features	-Unlimited range of motion -Digital -Output as data signal	-Limited range of motion -Analog -Output as unit value
Advantages	-Wear free - High precision	-Low cost -Low power consumption -Small and light -Simple to use
Disadvantages	-High cost -Complex to implement	-Wear and tear

The comparisons between joint angle sensors are shown in Table 2.6.2.1. After considerations, rotary encoder is chosen to measure the joint angles due to the fact that it is wear free and has unlimited range of motion compared to potentiometer.

2.7 Material

In designing an exoskeleton, a material that is light and strong is required to form the frame of the exoskeleton. This is because lighter frame means lesser power is required to actuate the body part. However, the frame of the exoskeleton should be hard enough to withstand the torque generated by the actuator and also the body weight of the wearer.

In many of the studies [18, 21, 25, 27], aluminium alloys are chosen as their main material for the frame of the exoskeleton. Although different types of aluminium alloys are used in different studies, the main reason aluminium alloys is one of the most popular material is because of its lightness and strength. [21, 27]

In [6], combination of Duralumin or aluminium 2024 and stainless steel is used to construct the structure of the exoskeleton. The duralumin is used to from the frame and the stainless steel is used to form the joints. On the other hand, combination of aluminium alloy 7075 and polyamide 6 are used to form the structure of the exoskeleton in [21]. The aluminium alloy 7075 are used in high load structure whereas the polyamide 6 are applied in low load structure to make the exoskeleton as light as possible. In [25], combination of carbon fiber and prosthetic aluminium tubing which uses aluminium 7068 is used to construct the exoskeleton. The prosthetic aluminium tubing is chosen because it is designed for human use and very light. Carbon fibers are only used in a small portion because it is very expensive despite the fact that it is lighter than aluminium alloys.

Table 2.5: Comparison of properties between aluminium alloys.

	Duralumin (Aluminium 2024) [31]	Aluminium 7075 [32]	Prosthetic Aluminium (Aluminium 7068) [33]
Yield strength (MPa)	393	503	683
Density (g/cc)	2.77	2.80	2.85
Machinability	High	Medium	Medium
Availability	High	High	Low

Table 2.5 shows the comparison between aluminium alloys used by previous studies. As seen from table 4, Aluminium 7068 has significant higher yield strength than other aluminium alloys. The yield strength of the material is very important as the frame of exoskeleton needs to be strong enough to actuate limbs without breaking. Although aluminium 7068 has the highest density, the difference is not as significant as the yield strength. Apart from that, aluminium 7068 and 7075 has lower machinability from aluminium 2024 which is expected from a harder alloy.

Aluminium 7068 would be the right material to be used to form the frame of exoskeleton due to its strength despite the fact that it has the highest density and lower machinability among the others. However, due to its low availability, the aluminium 7075 with higher availability, lower yield strength as well as density is chosen to be the material to form the exoskeleton in this project.

CHAPTER 3

METHODOLOGY

3.1 Flow Chart

The process of this project is depicted as shown in Figure 3.1. The flow chart shows the steps to complete in order for this project to be done. First, the project's processes are planned. Next, the journal previous studies are analysed to gain more information that are useful in this project. Then, the parameters or scope for the lower limb exoskeleton are set. After that, the mathematical model and equations are derived by following the parameters set. After deriving the mathematical model and equations, the lower limb exoskeleton is designed using the values calculated from the equations derived. Then, the designed exoskeleton model is simulated and tested for its performance in terms of structural strength and ability to actuate the user. If the exoskeleton's performance is not satisfied, the problem that causes its poor performance will be identified and the exoskeleton will be redesigned. Once the exoskeleton's performance is satisfied, the design is finalized and the project ends with it.
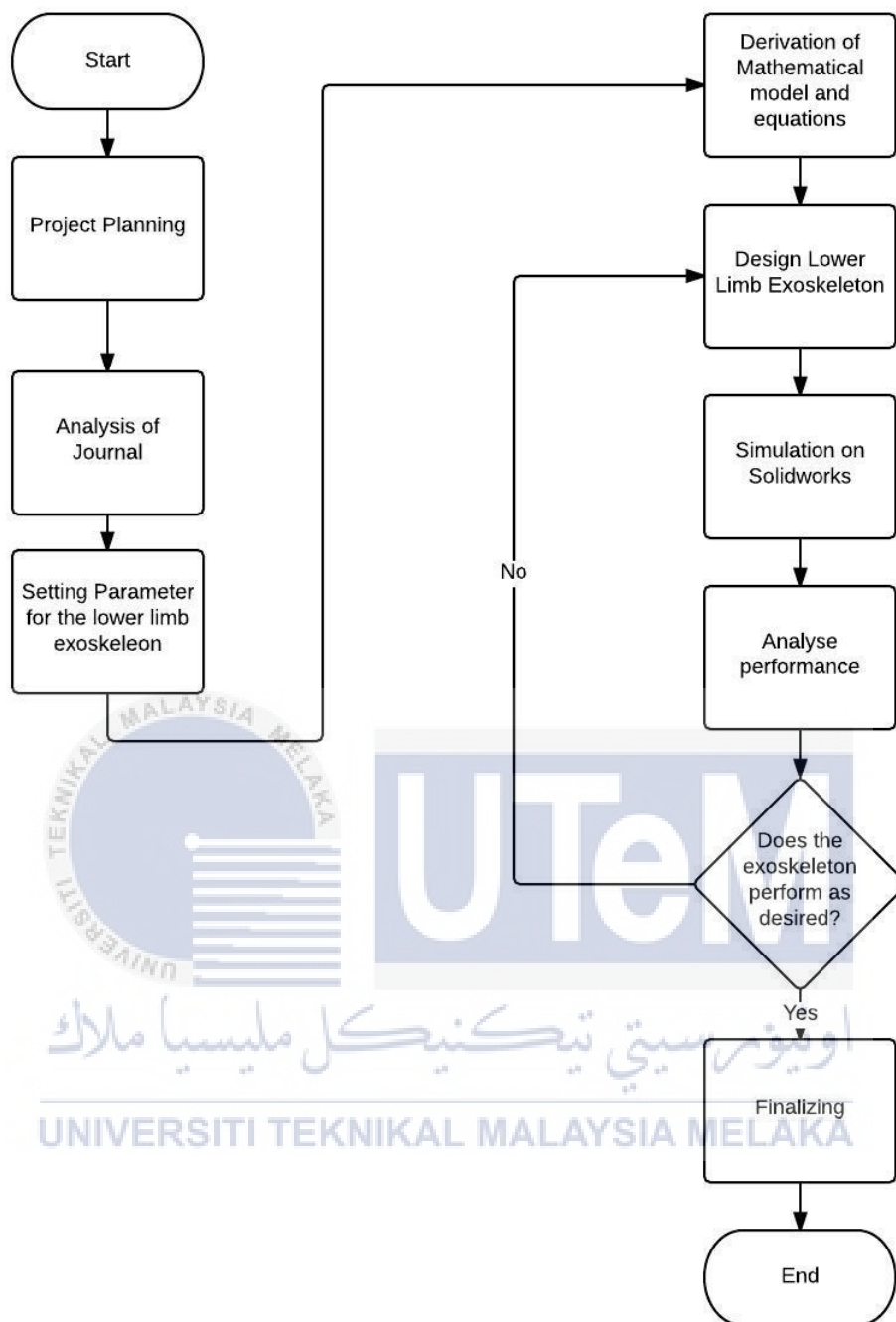
Figure 3.1: Flow chart of the project

3.2 K-chart

A K-chart as shown in Figure 3.2 is used to illustrate the planning for this project. The planning in this K-chart includes title selection, scope, methodology, result and analysis. The block and arrow in red indicate the flow of the planning for this project. First, the title that is chosen is Exoskeleton and the scope focused the project to parallel lower limb electrical actuated exoskeleton. Then, the hardware design and the theory are covered in the methodology. The hardware design includes the design of the lower limb exoskeleton using SolidWorks whereas the theory part covers the derivation of mathematical model and equations. The mathematical model derived is verified using Matlab and the result from the design are simulated and tested using SolidWorks Motion Analysis tools.
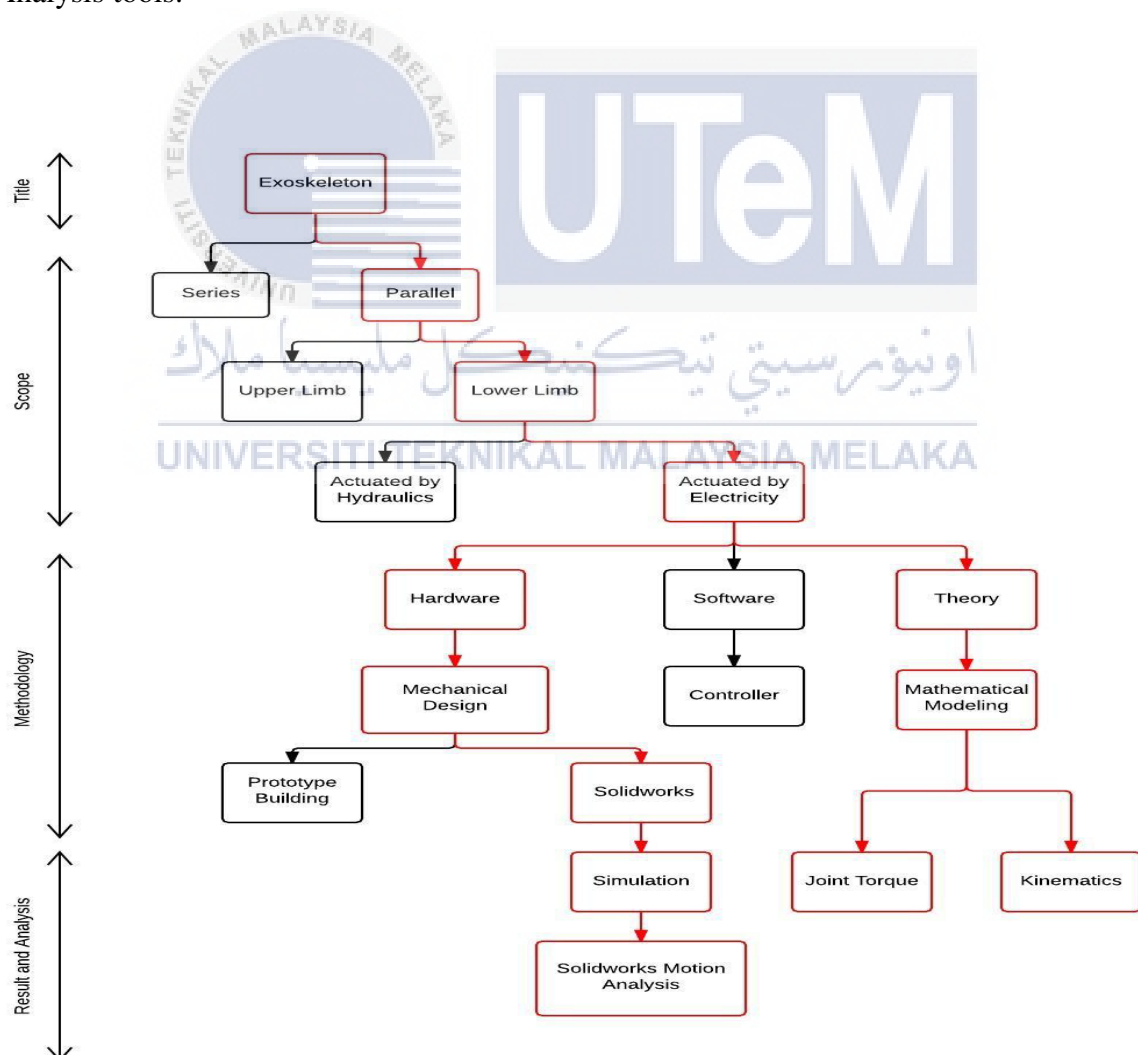
Figure 3.2: K-chart of the project

3.3 Derivation of mathematical model of lower limb exoskeleton using Kinematic Analysis and Formulation of joint torque equation

3.3.1 Kinematic Analysis

In order to control the lower limb exoskeleton, the relationship between joint angles and the position of the foot must be identified. The exoskeleton leg is considered to be a Rotational-Rotational-Rotational (RRR) series planar robot due to its movement on Sagittal plane only. Forward kinematics is applied to find the position of the foot if the values for the joint angles are given. First, reference frames are assigned to the hip, knee and ankle joint as shown in Figure 3.3.
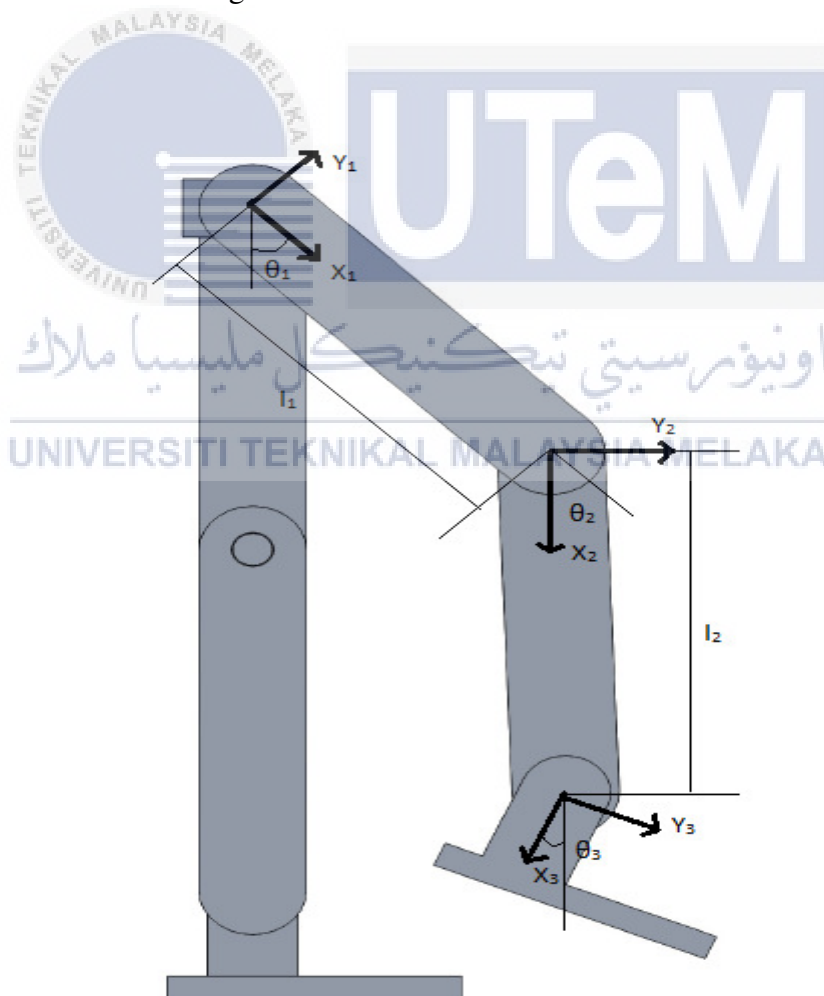
Figure 3.3: Exoskeleton leg with reference frames assigned

By using the reference frame assigned, the Denavit-Hartenberg(DH) table that represents the translational and rotational relationship between links are constructed as shown in Table 3.1.

Table 3.1: Denavit-Hartenberg Parameters of the lower limb exoskeleton

	Joint	α_{i-1}	a_{i-1}	d_i	θ_i
Hip	1	0	0	0	θ_1
Knee	2	0	l_1	0	θ_2
Ankle	3	0	l_2	0	θ_3

Then, the transformation matrix for each link is determined by substituting the values in the DH table into the general form of the transformation matrix, $^{i-1}_iT$.

$$^{i-1}_iT = \begin{bmatrix} cos\theta_i & -sin\theta_i & 0 & a_{i-1} \\ sin\theta_i cos\alpha_{i-1} & cos\theta_i cos\alpha_{i-1} & -sin\alpha_{i-1} & -sin\alpha_{i-1}d_i \\ sin\theta_i sin\alpha_{i-1} & cos\theta_i sin\alpha_{i-1} & cos\alpha_{i-1} & cos\alpha_{i-1}d_i \\ 0 & 0 & 0 & 1 \end{bmatrix} \tag{3.1}$$

$$^0_1T = \begin{bmatrix} cos\theta_1 & -sin\theta_1 & 0 & 0 \\ sin\theta_1 & cos\theta_1 & 0 & 0 \\ 0 & 0 & 1 & 0 \\ 0 & 0 & 0 & 1 \end{bmatrix} \tag{3.2}$$

$$^1_2T = \begin{bmatrix} cos\theta_2 & -sin\theta_2 & 0 & l_1 \\ sin\theta_2 & cos\theta_2 & 0 & 0 \\ 0 & 0 & 1 & 0 \\ 0 & 0 & 0 & 1 \end{bmatrix} \tag{3.3}$$

$$
{}_3^2T = \begin{bmatrix} cos\theta_3 & -sin\theta_3 & 0 & l_2 \\ sin\theta_3 & cos\theta_3 & 0 & 0 \\ 0 & 0 & 1 & 0 \\ 0 & 0 & 0 & 1 \end{bmatrix}
$$ (3.4)

Next, by multiplying the transformation matrixes in order, the transformation matrix that relates the transformation of the end effector (foot) and the base (hip), ${}_3^0T$ *is* determined.

$$
{}_3^1T = {}_2^1T \cdot {}_3^2T
$$

$$
= \begin{bmatrix} cos\theta_2 & -sin\theta_2 & 0 & l_1 \\ sin\theta_2 & cos\theta_2 & 0 & 0 \\ 0 & 0 & 1 & 0 \\ 0 & 0 & 0 & 1 \end{bmatrix} \begin{bmatrix} cos\theta_3 & -sin\theta_3 & 0 & l_2 \\ sin\theta_3 & cos\theta_3 & 0 & 0 \\ 0 & 0 & 1 & 0 \\ 0 & 0 & 0 & 1 \end{bmatrix}
$$

$$
= \begin{bmatrix} cos(\theta_2 + \theta_3) & -sin(\theta_2 + \theta_3) & 0 & l_2 cos\theta_2 + l_1 \\ sin(\theta_2 + \theta_3) & cos(\theta_2 + \theta_3) & 0 & l_2 sin\theta_2 \\ 0 & 0 & 1 & 0 \\ 0 & 0 & 0 & 1 \end{bmatrix}
$$ (3.5)

$$
{}_3^0T = {}_1^0T \cdot {}_3^1T
$$

$$
= \begin{bmatrix} cos\theta_1 & -sin\theta_1 & 0 & 0 \\ sin\theta_1 & cos\theta_1 & 0 & 0 \\ 0 & 0 & 1 & 0 \\ 0 & 0 & 0 & 1 \end{bmatrix} \begin{bmatrix} cos(\theta_2 + \theta_3) & -sin(\theta_2 + \theta_3) & 0 & l_2 cos\theta_2 + l_1 \\ sin(\theta_2 + \theta_3) & cos(\theta_2 + \theta_3) & 0 & l_2 sin\theta_2 \\ 0 & 0 & 1 & 0 \\ 0 & 0 & 0 & 1 \end{bmatrix}
$$

The transform matrix is simplified by representing ,

$$c_1 = cos\theta_1$$

$$c_2 = cos\theta_2$$

$$s_1 = sin\theta_1$$
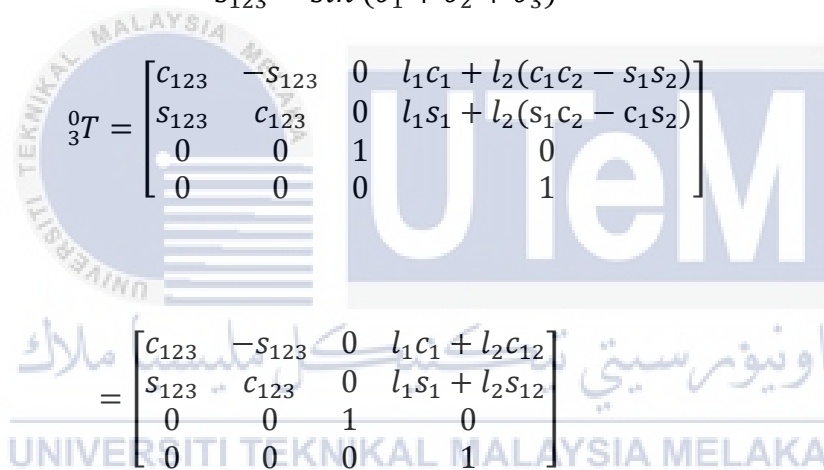
$$s_2 = sin\theta_2$$

$$c_{12} = \cos(\theta_1 + \theta_2)$$

$$s_{12} = \sin(\theta_1 + \theta_2)$$

$$c_{123} = \cos(\theta_1 + \theta_2 + \theta_3)$$

$$s_{123} = \sin(\theta_1 + \theta_2 + \theta_3)$$

$$^0_3T = \begin{bmatrix} c_{123} & -s_{123} & 0 & l_1c_1 + l_2(c_1c_2 - s_1s_2) \\ s_{123} & c_{123} & 0 & l_1s_1 + l_2(s_1c_2 - c_1s_2) \\ 0 & 0 & 1 & 0 \\ 0 & 0 & 0 & 1 \end{bmatrix}$$

$$= \begin{bmatrix} c_{123} & -s_{123} & 0 & l_1c_1 + l_2c_{12} \\ s_{123} & c_{123} & 0 & l_1s_1 + l_2s_{12} \\ 0 & 0 & 1 & 0 \\ 0 & 0 & 0 & 1 \end{bmatrix} \tag{3.6}$$

The position of the foot relative to the base in the x-axis and y-axis can be obtained from the position vector in the transformation matrix. That means an equation of x and y in terms of hip angle and knee angle can be obtained.

The position of the end effector relative to the base,

$$x = l_1c_1 + l_2c_{12} \tag{3.7}$$

$$y = l_1s_1 + l_2s_{12} \tag{3.8}$$

After that, inverse kinematics are applied to find the joint angle if given the position of the foot. For inverse kinematics of the leg, the position of the end effector relative to the base serves as the input and the rotation of the hip and knee serve as the output. From the forward kinematics done on the leg, we know that

From equation (3.7) and (3.8)

$$x = l_1 c_1 + l_2 c_{12}$$

$$y = l_1 s_1 + l_2 s_{12}$$

By squaring both x and y, we obtain

$$x^2 = (l_1 c_1)^2 + 2(l_1 c_1)(l_2 c_{12}) + (l_2 c_{12})^2$$

$$y^2 = (l_1 s_1)^2 + 2(l_1 s_1)(l_2 s_{12}) + (l_2 s_{12})^2$$

Adding x^2 and y^2,

$$x^2 + y^2 = (l_1 c_1)^2 + 2(l_1 c_1)(l_2 c_{12}) + (l_2 c_{12})^2 + (l_1 s_1)^2 + 2(l_1 s_1)(l_2 s_{12})$$

$$+ (l_2 s_{12})^2$$

$$= (l_1 c_1)^2 + (l_1 s_1)^2 + (l_2 c_{12})^2 + (l_2 s_{12})^2 + 2(l_1 c_1)(l_2 c_{12}) + 2(l_1 s_1)(l_2 s_{12})$$

$$= l_1^2 (c_1^2 + s_1^2) + l_2^2 (c_{12}^2 + s_{12}^2) + 2 l_1 l_2 (c_1 c_{12} + s_1 s_{12})$$

Using the trigonometry identities,

$$(cos\theta)^2 + (sin\theta)^2 = 1$$

$$cosa \cdot cosb \mp sina \cdot sinb = \cos(a \pm b)$$

$$\cos(-\theta) = cos\theta$$

$$x^2 + y^2 = l_1^2 + l_2^2 + 2l_1l_2\cos(\theta_1 - (\theta_1 + \theta_2))$$

$$= l_1^2 + l_2^2 + 2l_1l_2\cos(-\theta_2)$$

$$= l_1^2 + l_2^2 + 2l_1l_2\cos\theta_2$$

$$\cos\theta_2 = \frac{x^2 + y^2 - (l_1^2 + l_2^2)}{2l_1l_2} \qquad (3.9)$$

Using the trigonometry identities,

$$(cos\theta)^2 + (sin\theta)^2 = 1$$

$$(cos\theta_2)^2 + (sin\theta_2)^2 = 1$$

$$sin\theta_2 = \pm\sqrt{1 - (cos\theta_2)^2} \qquad (3.10)$$
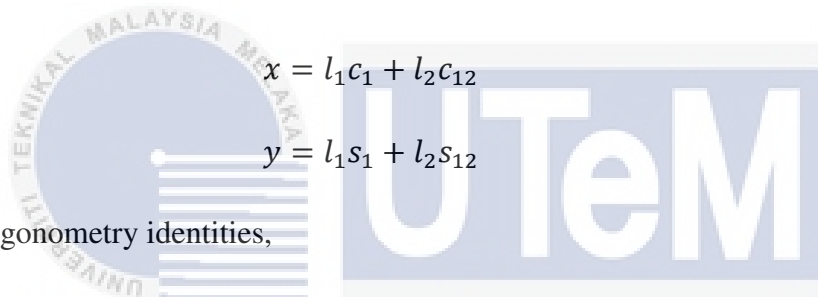
Divide equation (3.10) with equation (3.9),

$$tan\,\theta_2 = \frac{sin\theta_2}{\cos\theta_2} = \frac{\pm\sqrt{1 - (cos\theta_2)^2}}{cos\theta_2}$$

$$\theta_2 = \frac{\pm\sqrt{1 - \left(\frac{x^2+y^2-(l_1^2+l_2^2)}{2l_1l_2}\right)^2}}{\frac{x^2+y^2-(l_1^2+l_2^2)}{2l_1l_2}}$$

$$\theta_2 = \frac{\pm\sqrt{(2l_1l_2)^2 - [x^2 + y^2 - (l_1^2 + l_2^2)^2]}}{x^2 + y^2 - (l_1^2 + l_2^2)} \tag{3.11}$$
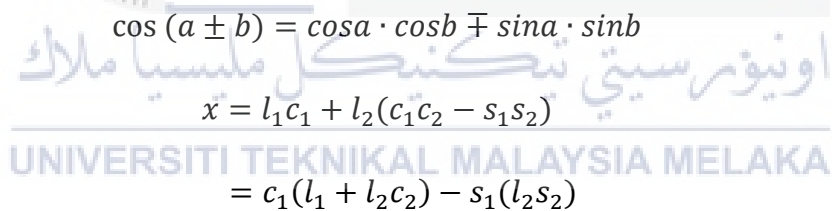
To Find θ_1,

$$x = l_1c_1 + l_2c_{12}$$

$$y = l_1s_1 + l_2s_{12}$$

Using the trigonometry identities,

$$\cos(a \pm b) = cosa \cdot cosb \mp sina \cdot sinb$$

$$x = l_1c_1 + l_2(c_1c_2 - s_1s_2)$$

$$= c_1(l_1 + l_2c_2) - s_1(l_2s_2) \tag{3.12}$$

$$y = l_1s_1 + l_2(c_1s_2 + c_2s_1)$$

$$= c_1(l_2s_2) - s_1(l_1 + l_2c_2) \tag{3.13}$$

Now , let

$$k_1 = l_1 + l_2c_2$$

$$k_2 = l_2s_2$$

$$r = \sqrt{k_1^2 + k_2^2}$$
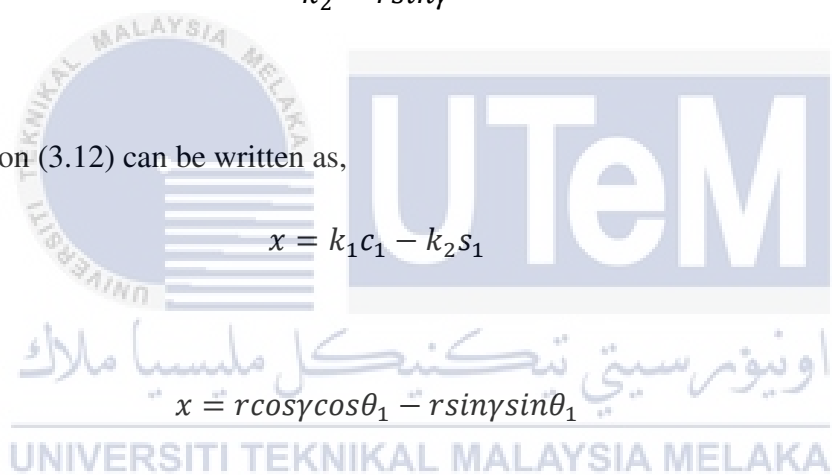
$$\gamma = \tan^{-1}\frac{k_2}{k_1}$$

$$k_1 = r\cos\gamma$$

$$k_2 = r\sin\gamma$$

Then equation (3.12) can be written as,

$$x = k_1 c_1 - k_2 s_1$$

$$x = r\cos\gamma\cos\theta_1 - r\sin\gamma\sin\theta_1$$

$$\frac{x}{r} = \cos\gamma\cos\theta_1 - \sin\gamma\sin\theta_1$$

$$\frac{x}{r} = \cos(\gamma + \theta_1) \tag{3.14}$$

Whereas equation (3.13) can be written as,

$$y = k_2 c_1 + k_1 s_1$$

$$y = r\sin\gamma\cos\theta_1 + r\cos\gamma\sin\theta_1$$
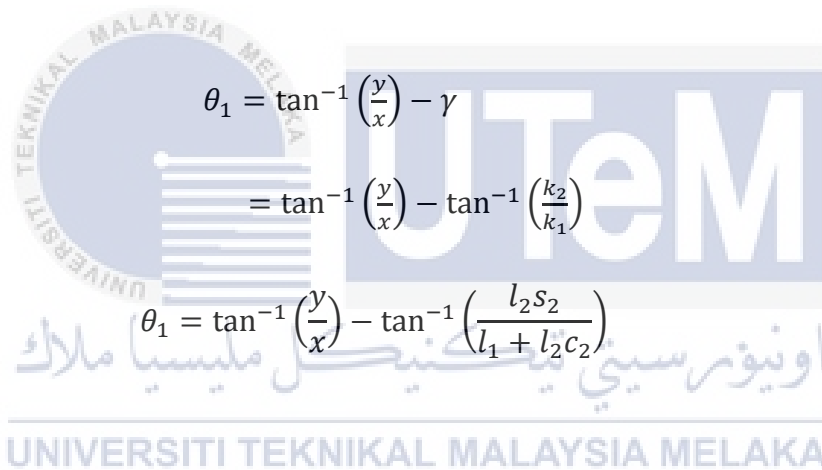
$$\frac{y}{r} = \sin\gamma\cos\theta_1 - \cos\gamma\sin\theta_1$$

$$\frac{y}{r} = \sin(\gamma + \theta_1)$$

(3.15)

Divide equation (3.15) with equation (3.14)

$$\tan(\gamma + \theta_1) = \frac{\sin(\gamma + \theta_1)}{\cos(\gamma + \theta_1)} = \frac{y}{x}$$

$$\theta_1 = \tan^{-1}\left(\frac{y}{x}\right) - \gamma$$

$$= \tan^{-1}\left(\frac{y}{x}\right) - \tan^{-1}\left(\frac{k_2}{k_1}\right)$$

$$\theta_1 = \tan^{-1}\left(\frac{y}{x}\right) - \tan^{-1}\left(\frac{l_2 s_2}{l_1 + l_2 c_2}\right)$$

(3.16)

Besides the relationship between the joint angle and the foot position, the joint torque required to move the user is also formulated. The torque in hip, knee, and ankle joints that are required are formulated.

3.3.2 Joint Torque Equation

The torque required at each joint can be determined by using free body diagrams of different joints. Figure 3.4, Figure 3.5, Figure 3.6 shows the forces acting on hip, knee and ankle joint respectively.
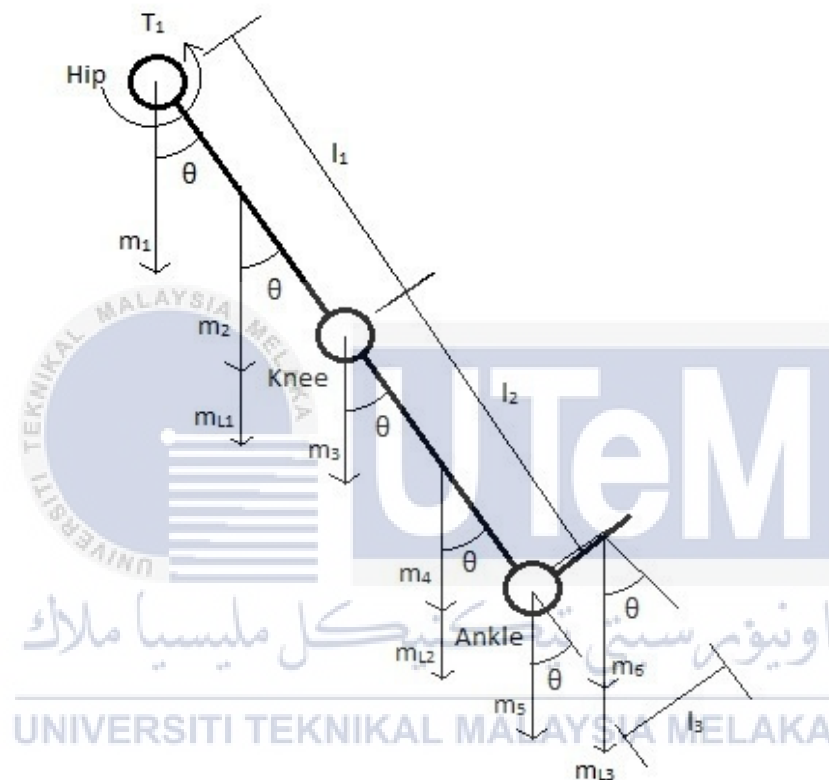
Figure 3.4: Forces acting at hip joint.
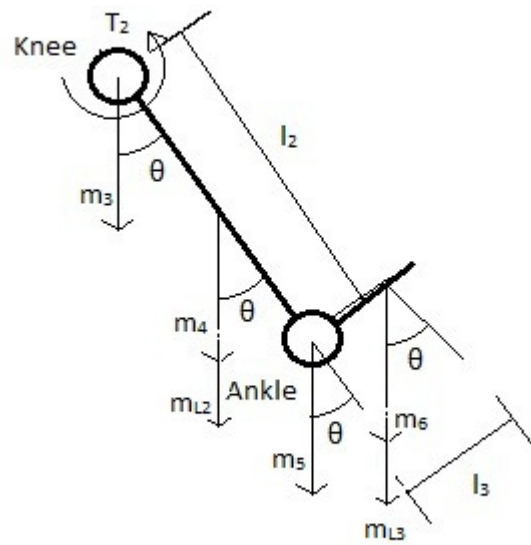
Figure 3.5: Forces acting at knee joint.
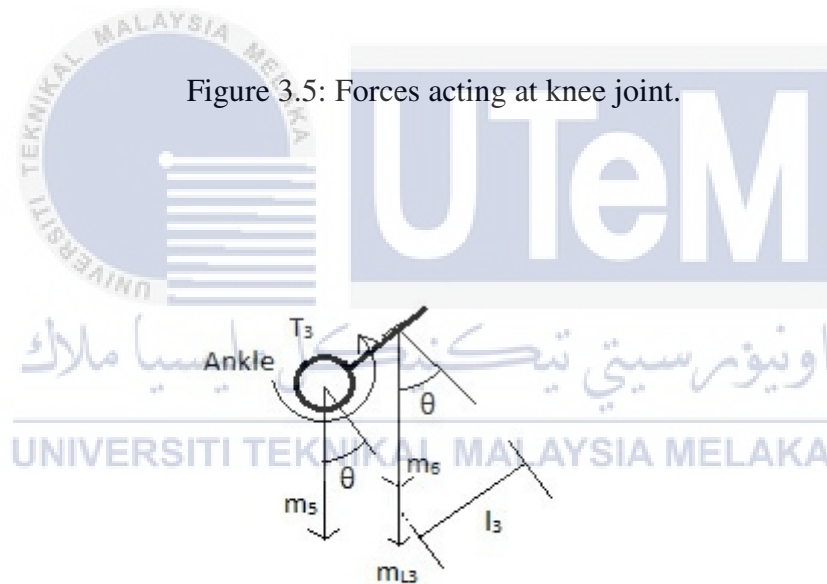
Figure 3.6: Forces acting at ankle joint.

The torque required to generate by the actuator at each joint can be determined as shown below.

Let

$m_1 = mass\ of\ actuator\ at\ hip\ joint$

$m_2 = mass\ of\ thigh$

$m_3 = mass\ of\ actuator\ at\ knee\ joint$

$m_4 = mass\ of\ shank$

$m_5 = mass\ of\ actuator\ at\ ankle\ joint$

$m_6 = mass\ of\ foot$

$m_{L1} = mass\ of\ thigh\ link$

$m_{L2} = mass\ of\ shank\ link$

$m_{L3} = mass\ of\ ankle\ link$

$l_1 = length\ of\ thigh$

$l_2 = length\ of\ shank$

$l_3 = length\ of\ foot$

$T_1 = torque\ required\ at\ hip\ joint$

$T_2 = torque\ required\ at\ knee\ joint$

$T_3 = torque\ required\ at\ ankle\ joint$

$$T_1 = sin\theta \left[(m_2 + m_{L1})g\left(\frac{l_1}{2}\right) + m_3g(l_1)\right]$$
$$+sin\theta \left[(m_4 + m_{L2})g\left(l_1 + \frac{l_2}{2}\right)\right] + sin\theta[m_5g(l_1 + l_2)]$$
$$+sin\theta[(m_6 + m_{L3})g(l_1 + l_2)] + cos\theta\left[(m_6 + m_{L3})g\left(\frac{l_3}{2}\right)\right]$$
(3.17)

$$T_2 = sin\theta\left[(m_4 + m_{L2})g\left(\frac{l_2}{2}\right)\right] + sin\theta[+m_5g(l_2)] + sin\theta[+m_6g(l_2)]$$
$$+cos\theta\left[(m_6 + m_{L3})g\left(\frac{l_3}{2}\right)\right]$$
(3.18)

$$T_3 = cos\theta\left[(m_6 + m_{L3})g\left(\frac{l_3}{2}\right)\right]$$
(3.19)

T_1, T_2 and T_3 can be found using these equations.

3.4 Design the lower limb exoskeleton.

Before designing the lower limb exoskeleton, several steps are taken to select the suitable component for the exoskeleton. First, motors and drive systems are selected based on the torque requirement calculated. The maximum torque produce by the combination of the motor and drive system must exceed the torque required to actuate the joints without the exoskeleton. Then, the reasonable estimation of the weight of the hip link, knee link and foot pad are done. The mass of the links are estimated by multiplying the volume of the link to the density of the material used. Finally, the weight of the motor, drive system and links are inserted into the equation to check if the maximum torque produced by the motors is able to actuate the joints or not. If the motor and drive system selected are not able to lift the user's limb, a higher torque producing motor and drive system will be selected. If the motor and drive system selected are able to actuate the joints, the design of exoskeleton will be started.

The mechanical design of the exoskeleton is designed using the software SolidWorks. The exoskeleton frame is designed to couple with the drive systems coupling. Details drawing of each part are drawn and assembled. At the end of this phase, assembly drawing of a complete lower limb exoskeleton is presented. The process flow of this phase is illustrated as shown in Figure 3.7.
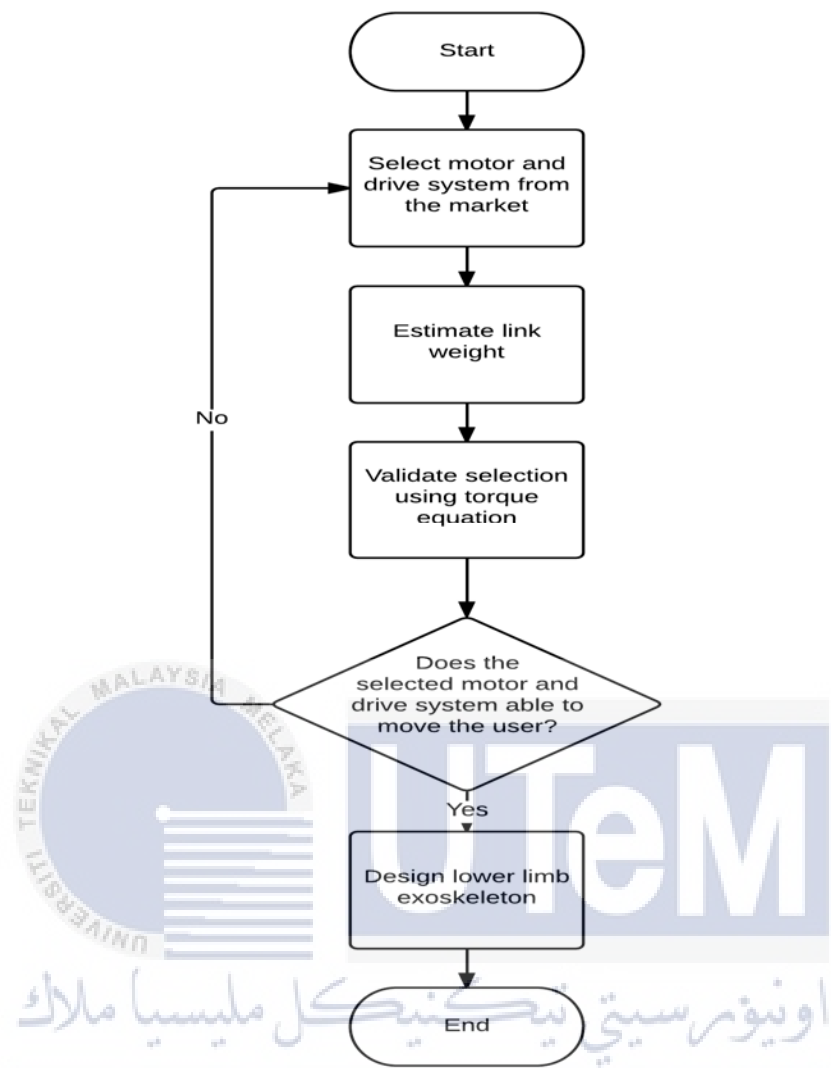
Figure 3.7: Flow chart of designing lower limb exoskeleton.

3.4.1 Actuator Selection

From the calculations, the torque required at hip, knee and ankle joint are 47.56Nm, 21.68Nm and 2.10Nm respectively to lift the user's limb for walking. Hence, the motor selected should produce more than the calculated value to be able to lift the exoskeleton and the user's limbs. In this project, brushless DC motors are selected for their efficiency and longer lifetime compared to other type of motors.[39] Since the exoskeleton requires more torque then speed, gearboxes or reducers are selected to couple with each motor to trade speed for more torque. This will decrease the output speed and increase the output torque significantly.

The brushless DC motors selected for the hip, knee and ankle joint are the flat series from Maxon which are EC90 Flat, EC60 Flat and EC45 Flat respectively. They produce a maximum continuous torque of 560mNm, 289mNm and 128mNm respectively. These motors are selected because they are one of the slimmest and the lightest designs available on the market, which makes them suitable to be used to actuate the exoskeleton. Besides that, these motors can be overdriven to produce more than 3 times the maximum continuous torque for a short amount of period should the circumstances required. Moreover, strain wave gearboxes with a gear ratio of 100:1 are selected to couple with each motor to amplify the output torque 100 times from the motor's output shaft. These sorts of reducers are manufactured by Harmonic Drive and the CSD series that are selected are one of the flattest and lightest reducer available. This makes the selected motor and gearbox combination suitable to be applied on wearable or exoskeleton robots. The motor and reducer combined to produce 56Nm, 28.9Nm and 12.8Nm at hip, knee and ankle joint respectively. The specification of the motors and reducers are summarized in Table 3.2 and 3.3.

Table 3.2: Specifications of selected motor.

	Hip	Knee	Ankle
Model	MAXON EC90 FLAT	MAXON EC60 FLAT	MAXON EC45 FLAT
Voltage	36V	24V	24V
Weight	600g	471g	141g
Max. Continuous Torque	560mNm	289mNm	128mNm

Table 3.3: Specifications of selected reducers.

	Hip	Knee	Ankle
Model	HARMONIC DRIVE CSD-25-100	HARMONIC DRIVE CSD-17-100	HARMONIC DRIVE CSD-14-100
Weight	240g	100g	60g
Reduction Ratio	100:1	100:1	100:1

3.4.2 Selection Verifications

As seen from the calculations, without including the weight of the actuator unit, the torque required at hip, knee and ankle joint are 47.56Nm, 21.68Nm and 2.10Nm respectively. After selecting the motors and reducers, the weight of the combined units are inserted into the torque equations to get the torque required with the inclusion of actuator's weight. The calculations show that the torque required are 50.19Nm, 22.73Nm and 2.10Nm for hip, knee and ankle joint respectively. By comparing the required torque to the maximum continuous torque that are able to produce by the actuators which are 56Nm, 28.9Nm and 12.8Nm, the torque required at each joint does not exceed the maximum continuous torque that can be produced. This comparison verified the selection of the motors and reducers on its ability to produce enough torque to fulfil the torque requirement. The comparison between required torques and maximum torques are summarized in Table 3.4

.

Table 3.4: Comparison between required torque and maximum continuous torque.

	Hip	Knee	Ankle
Torque Required At Joint (Without Actuators)	47.56Nm	21.68Nm	2.10Nm
Torque Required At Joint (With Actuators)	50.19Nm	22.73Nm	2.10Nm
Max. Continuous Torque That Can Be Produced By The Actuators	56.00Nm	28.90Nm	12.80Nm

3.4.3 Exoskeleton Design

The exoskeleton robot is designed using Computer-Aided Design software named SolidWorks. After selecting the actuators, the exoskeleton's dimension parameters are set according to the objective of this project. The exoskeleton is designed according to the anthropomorphic parameters of the human body to make sure that the joints of the exoskeleton are concentric with the user's joints. This will help in improving its compliance to the human body. The anthropomorphic parameters of the limbs are estimated using ratio obtained from [37] and [38] to determine the links length of the exoskeleton. Then, an accurate rendering and design of the parts and links are carried out using SolidWorks with reference to the parameters set.

The exoskeleton is designed to carry an able-bodied and healthy user with a maximum weight of 100kg and height of 185cm. The exoskeleton that includes all the actuator units and links weighs only 6.44kg. It is mainly made up of Aluminium-7075 which is light and strong at the same time. It is considered as a bipedal wearable robot with 3 degrees of freedom each limb which allows the hip, knee and ankle joint to be rotated and powered in the Sagittal plane. It consists of thigh link, shank link and foot pad for each limb of the exoskeleton like the human body. Each link is linked together by a pivot joint instead of using the actuator unit as the joint as shown in Figure 3.8. This design will help

in avoiding direct load applied to the motors and reducers which will damage the actuator unit as there are limitations to its overhung load. Besides that, it will help to shift the load applied by the user's limb to the pivot joint and thus increasing the lifetime of the actuator unit. Moreover, the pivot joint also limits the rotation of the joint mechanically to avoid any accident caused by the malfunction of the actuators. This is very important precaution to make the exoskeleton safe for the users.

There are special mounts designed to mount the actuators onto the exoskeleton to provide actuation to the joints as shown in Figure 3.9. The mount not only served as couples the link and the actuator but also serve as the coupling for the motor and reducer. The mounts are also made up of Aluminium-7075 which helps in saving weight. Apart from that, there are adjustable braces to strap onto the user's limb so that the limb moves with the exoskeleton. The braces are to be covered with Velcro straps for easy and fast fastening action. The exoskeleton's parts including link and mounts are designed using the standard thickness of the Aluminium sheet or bar on the market to make it easier and cheaper to be fabricated. Apart from that, the bolt and screw hole size used are in accordance to the standard size in the market for easy tapping and fabrication. The complete drawing of the exoskeleton is shown in Figure 3.10.
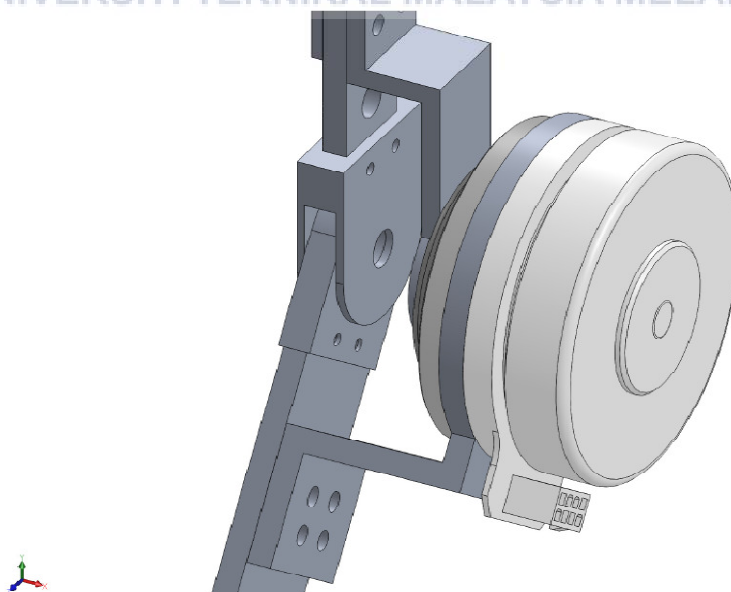

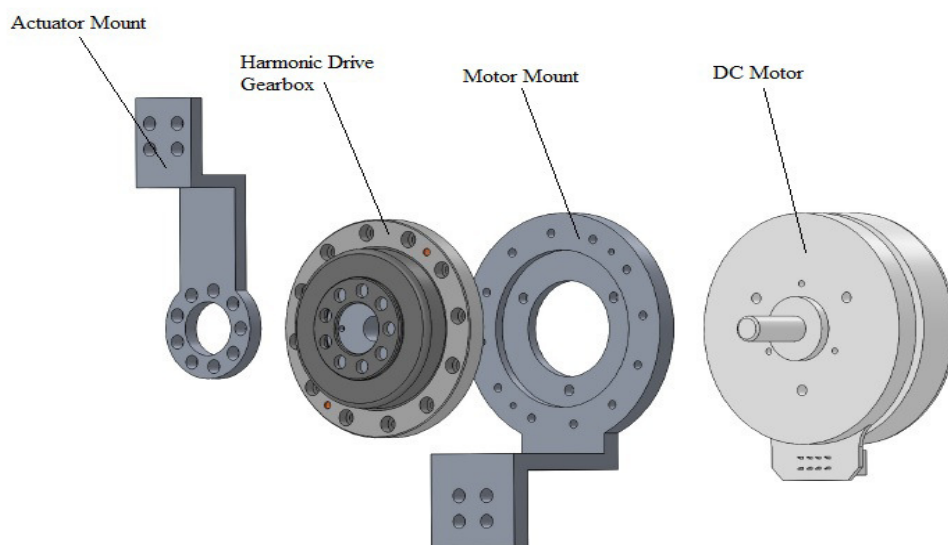Figure 3.8: Pivot joint and actuator mount design on the exoskeleton.

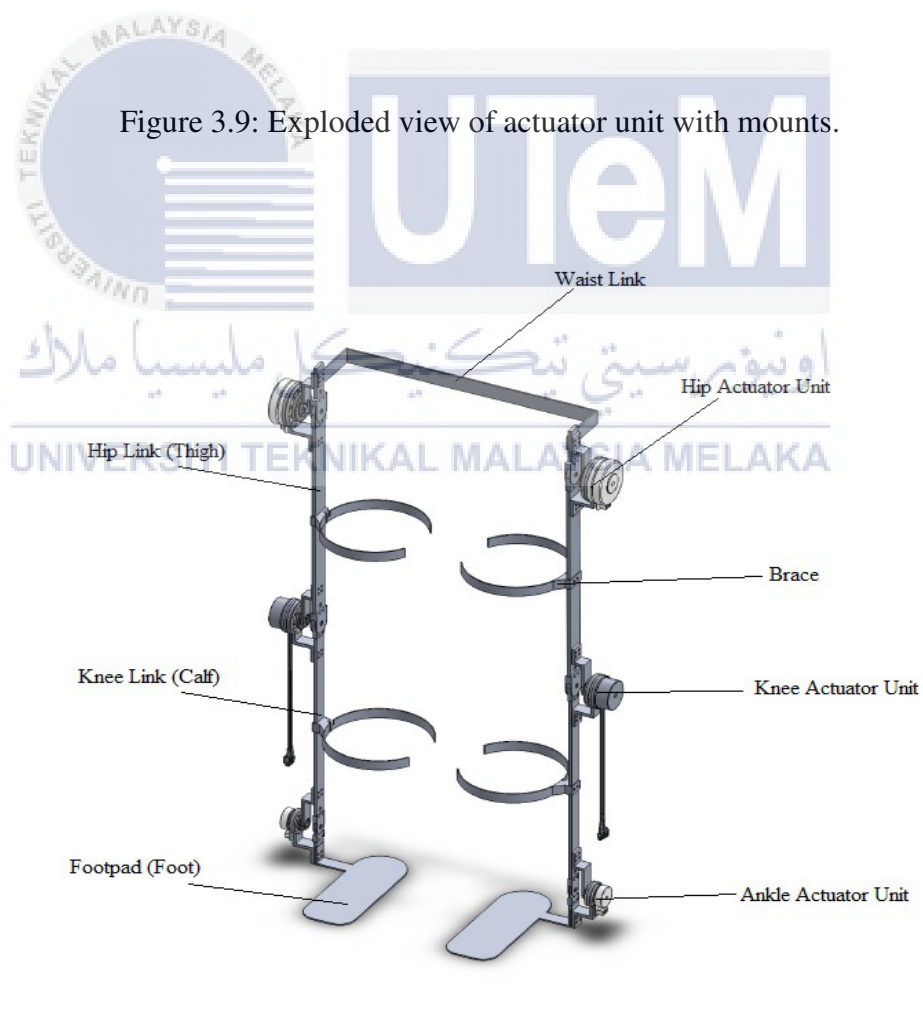Figure 3.9: Exploded view of actuator unit with mounts.
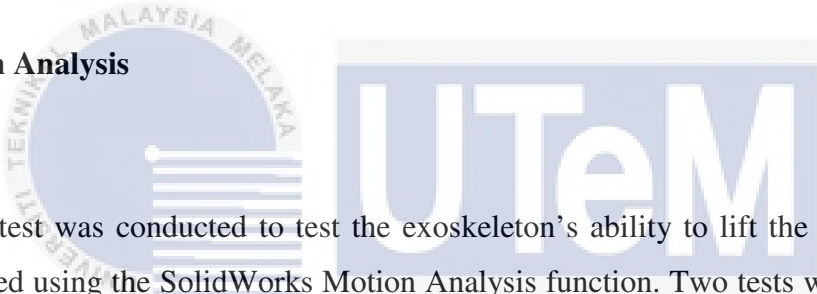
Figure 3.10: The assembly drawing of the designed exoskeleton.

3.5 Analysis of the designed exoskeleton

After designing the exoskeleton, two tests were conducted to test the exoskeleton using SolidWorks. Finite Element Analysis (FEA) was done to test the structural strength of the exoskeleton. This is to make sure that the exoskeleton links are strong enough to support a 100kg user. Apart from that, the motion analysis was done to test if the exoskeleton is able to actuate the lower limbs of the user with the weight of 100kg or not. This is done by obtaining the torque pattern for each joint during walking and examines the selected actuator units' ability to emulate the torque pattern respectively for each joint.

3.5.1 Motion Analysis

This test was conducted to test the exoskeleton's ability to lift the user's limb. It was conducted using the SolidWorks Motion Analysis function. Two tests were conducted to obtain the torque required to perform walking motion. First, the designed exoskeleton has a weight accurate humanoid dummy strap onto it to simulate the weight of the user. Then, trajectory planning is required to for the exoskeleton model to simulate the legs motion in a walking gait. In the first test, the exoskeleton model was required to perform leg swing movement according to the trajectory planning and obtain the torque value of taking one step. The torque value for each joint required to perform the leg swing motion are recorded and observed to verify the ability of the actuator selected to produce enough torque to support the user to take one step. The data acquired are also compared to the calculated values. For the second test, the exoskeleton model was required to perform two complete cycles of walking motion to obtain the torque values for a complete walking cycle. The torque value for each joint are recorded and analysed to further verify the exoskeleton's ability to support the user to walk.

3.5.1.1 Trajectory Planning

In this project, trajectory planning of the exoskeleton is done by using the functions that describe the position of the foot with respect to the time when performing the leg lift motion. These functions can be obtained from the studies done in [40] and it is used in gait generation by setting the parameters as shown in Figure 3.11.
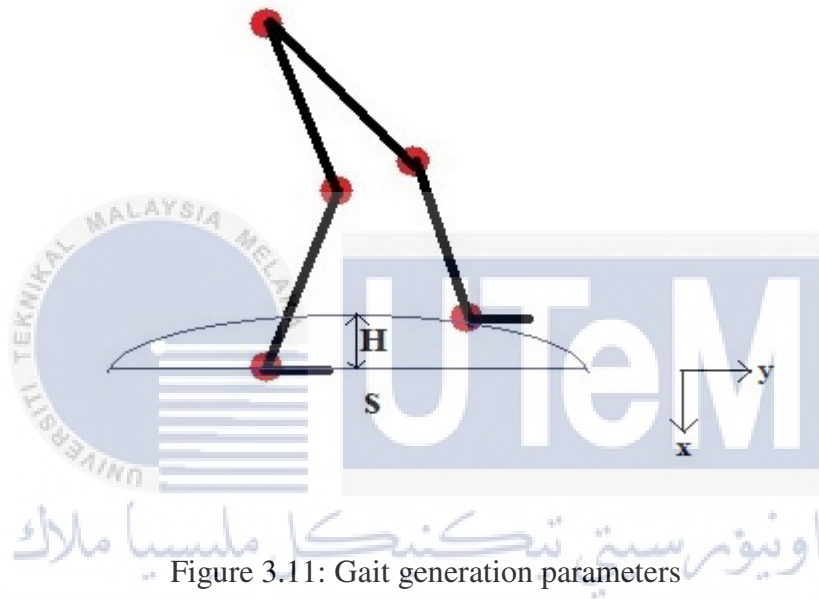
Figure 3.11: Gait generation parameters

$$P_y(t) = \left(\frac{s}{2}\right) sin\left[\frac{\pi}{T}\left(t - \frac{T}{2}\right)\right](u(t - 2T) - u(t - T)) \qquad (3.20)$$

$$P_x(t) = Hsin\left[\pi\left(\frac{P_x(t)}{s} + 0.5\right)\right](u(t - 2T) - u(t - T)) \qquad (3.21)$$

Where

$P_x = position\ of\ the\ foot\ \ in\ x - axis\ relative\ to\ the\ hip$

$P_y = position\ of\ the\ foot\ \ in\ y - axis\ relative\ to\ the\ hip$

$H = maximum\ lift\ height$

$s = step\ length$

$T = period\ time$

By inserting the gait generation parameters into equation 3.20 and 3.21, the position of the foot at any instantaneous moment in the time period can be determined. After obtaining the positions of the foot across the time period, the joint angles for all joints at any given moment in the time period are determined using the inverse kinematics equation derived. The time period, T is set to be 1s, whereas the maximum lift height, H is set to be 0.04m and the step length, s is set to be 0.78m which is the estimated value obtained from [41]. The data are calculated and tabulated as shown in Table 3.5.

Table 3.5: Sample of Walking gait data.

$t(s)$	$P_y(m)$	$P_x(m)$	$\theta_1(°)$	$\theta_2(°)$	$\theta_3(°)$
0	-0.3900	0.8591	-24.04	-0.76	-24.81
0.1	-0.3709	0.8560	-15.01	-17.17	-32.18
0.2	-0.3155	0.8473	-4.14	-33.23	-37.38
0.3	-0.2292	0.8350	7.57	-46.82	-39.25
0.4	-0.1205	0.8237	19.16	-56.16	-37.00
0.5	0.0000	0.8191	29.12	-59.52	-30.40
0.6	0.1205	0.8237	35.80	-56.16	-20.36
0.7	0.2292	0.8350	38.28	-46.82	-8.54
0.8	0.3155	0.8473	36.70	-33.23	3.47
0.9	0.3709	0.8560	31.84	-17.17	14.67
1.0	0.3900	0.8591	24.79	-0.76	24.03

3.5.1.2 One Step Leg Swing Motion

After planning the trajectory, rotary actuators are inserted to each joint of the exoskeleton model in SolidWorks Motion Analysis. Then, the data points of joint angles calculated are inserted into each individual rotary actuator with respect to time as shown in Figure 3.12. These data points will command the rotary actuator to rotate to desired angles calculated at a specific time and hence perform the leg swing motion of the walking gait. After inserting the data points, the motion simulation of the exoskeleton model is

conducted and desired data like torque at each joint are calculated. Next, the torque required at each joint to perform this motion are recorded and plotted into graphs for observation and comparison with the calculated value. The exoskeleton model's motion simulation is shown in Figure 3.13 with the trace path of the foot.
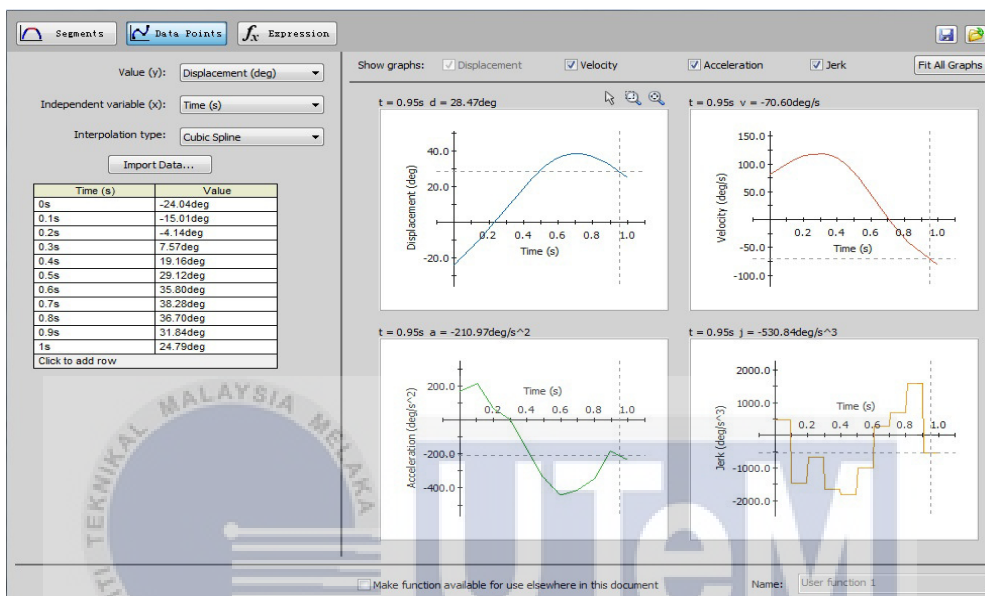

Figure 3.12: Data points inserted to each joints.

Figure 3.13: Exoskeleton model leg swing motion simulation.

3.5.1.3 Two Complete Cycle Walking Motion

In this test, the exoskeleton model is required to perform two steps of walking motion to get the torque data for each joint. This test's purpose is to find out the torque required for a 100kg user to walk with the exoskeleton strapped on. First, the trajectory paths of the feet are planned using the equations found in [40]. The trajectory planned for in this test are two steps walking motion for both legs and walking speed is set to 1.2m/s as this is the most effective walking speed as mentioned in [42]. Then, the joint angle data for each joint with respect to time are obtained using inverse kinematics equations. The data are then inserted as input to allow the exoskeleton model to perform the walking motion as shown in Figure 3.14. Besides that, the exoskeleton model was added with weight accurate human dummy to simulate the effect of user's weight on the joint torques. Essentially, this test repeats the process of the first test, but with even more data points to be inserted as the input for the rotary actuators. Next, the simulations for the exoskeleton to perform two walking steps are performed. The resulting torque data for each joint are recorded and plotted into graphs for illustration. Next, the results obtained are analysed accordingly to examine each actuator unit's ability to produce the torque pattern required for walking. The different phases of a walking motion are indicated with different coloured region in the graphs. The region coloured in blue represents the swing phase where the foot is lifted whereas the region coloured in red represents the stance phase where the foot is touching the ground at all time.
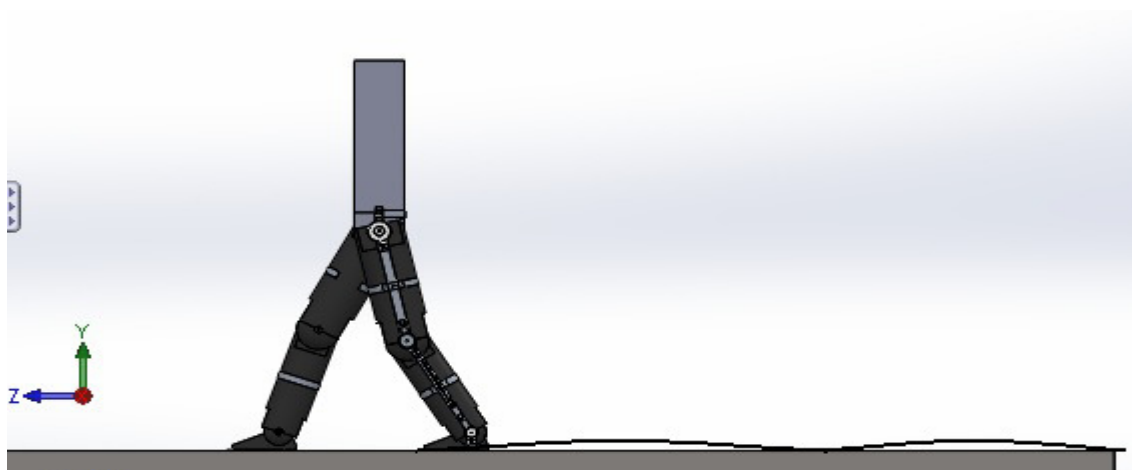
Figure 3.14: Exoskeleton model walking motion simulation.

3.5.2 Finite Element Analysis

This test will be conducted to test the exoskeleton's structural strength and to make sure that it's strong enough to support the user. The Finite Element Analysis (FEA) test will show the stress distributions on the links of the exoskeleton in loaded condition. First, the material of the exoskeleton's links will be selected. Then, suitable fixtures and loads are applied to the hip link, knee link and foot pad to simulate the load conditions of the exoskeleton when it is loaded during operations. Besides that, weight accurate limb models are also applied to emulate the weight on the exoskeleton. Apart from that, the gravity is set to be 9.81m/s^2. Then, the simulation models are applied with maximum torque for each joint obtained from the motion analysis to get the stress distributions on the links under extreme conditions. After that, the simulations are executed to get the stress distribution on the exoskeleton's link in terms of von Mises stress. Finally, the stress distribution diagrams obtained for each link are recorded and analysed. The maximum stress on the exoskeleton should be far less than the yield strength of the material. This is because when the stress exceeds the yield strength, the link will start to deform. If the result of the simulation is not satisfied, the exoskeleton's links will be strengthened at maximum stress areas. If the result of the simulation is satisfied, unnecessary area of the links can be removed to make the exoskeleton as light as possible.

CHAPTER 4

RESULT, ANALYSIS AND DISCUSSION

4.1 Mathematical model using kinematic analysis

The mathematical model derived from kinematic analysis is verified using robotic toolbox in Matlab. The Denavit-Hartenberg parameters are inserted into the program and the robotic model is plotted.
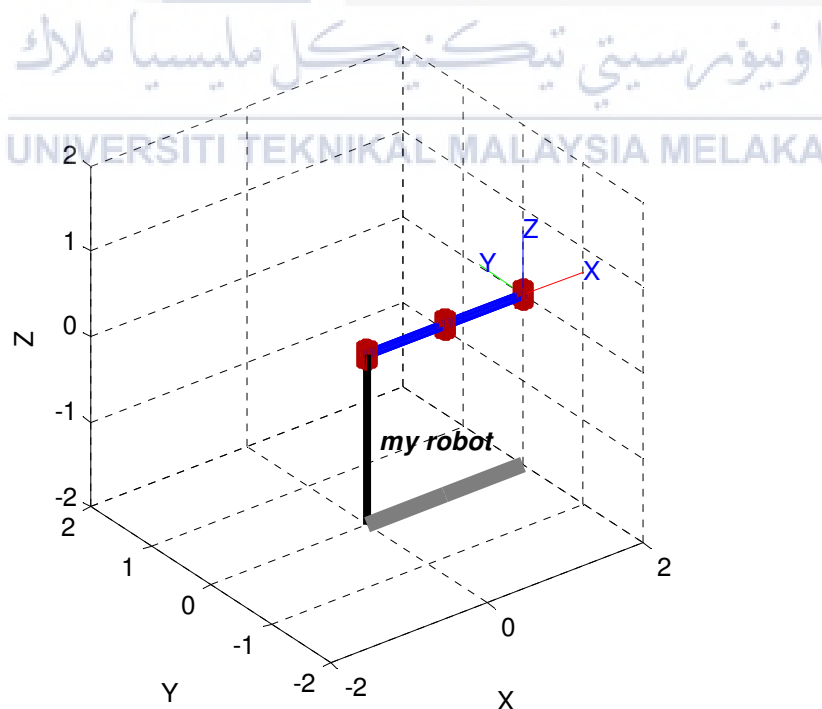
Figure 4.1: Robotic model generated in Matlab.

To verify the model derived from the kinematic analysis, joint angle values are substituted into the equations and data obtained from Matlab and manual calculations are compared. The length of each link is taken as 1m. The results obtained are shown in table 4.1.

Table 4.1: Result from calculations and Matlab simulations.

hip joint, θ_1(°)	knee joint, θ_2(°)	Position in of end effector in x-axis, x(m)		Position of end effector in y-axis, y(m)	
		Calculation	Simulation	Calculation	Simulation
0	0	2.00	2.0000	0.00	0.0000
10	10	1.92	1.9245	0.52	0.5157
30	30	1.37	1.3660	1.37	1.3660
50	50	0.47	0.4691	1.75	1.7509
70	70	-0.42	0.4240	1.58	1.5825
90	90	-1.00	-1.0000	1.00	1.0000

The results from calculations and simulations show the same answer. This means that the mathematical model derived from kinematic analysis is correct and can be used to represent the motion of the lower limb exoskeleton. The forward and inverse kinematic equations are used in trajectory planning to emulate human walking motion.

4.2 Joint Torque

This section contains the calculations of torque required for each joint. To calculate the torque required for each joint, the mass of the actuators is equal to zero and the link masses are estimated. The body segment parameters that be obtained from [37] and [38] are as shown below. Besides that, the maximum angle during walking for hip, knee and ankle joints are obtained from the study in [3] which are 32.2º, 73.5º and 30.0º respectively. The maximum required torque values during walking for each joint are calculated by inserting the maximum angle into joint torque equations for each joint.

$mass\ of\ thighs = 22.36\%\ of\ total\ mass$

$mass\ of\ shanks = 8.78\%\ of\ total\ mass$

$mass\ of\ feet = 3.66\%\ of\ total\ mass$

$\therefore mass\ of\ a\ single\ thigh = 11.18\%\ of\ total\ mass$

$\therefore mass\ of\ a\ single\ shank\ = 4.39\%\ of\ total\ mass$

$\therefore mass\ of\ a\ foot = 1.83\%\ of\ total\ mass$

$estimated\ mass\ of\ thigh\ link = 0.9kg$

$estimated\ mass\ of\ shank\ link = 0.8kg$

$estimated\ mass\ of\ feet\ link = 0.4kg$

$length\ of\ thigh = 26\%\ of\ total\ height$

$length\ of\ shank = 25\%\ of\ total\ height$

$length\ of\ foot = 12\%\ of\ total\ height$

Subject is taken to 100kg in weight and 185cm in height.

$$T_1 = sin\theta \left[(m_2 + m_{L1})g\left(\frac{l_1}{2}\right) + m_3 g(l_1)\right]$$
$$+ sin\theta\left[(m_4 + m_{L2})g\left(l_1 + \frac{l_2}{2}\right)\right] + sin\theta[m_5 g(l_1 + l_2)]$$
$$+ sin\theta[(m_6 + m_{L3})g(l_1 + l_2)] + cos\theta\left[(m_6 + m_{L3})g\left(\frac{l_3}{2}\right)\right]$$
$$= sin\theta[(0.1118 \times 100 + 0.9)(9.81)(0.2405) + (0.0439 \times 100 + 0.8)(9.81)(0.481 + 0.23125)$$
$$+ (0.0183 \times 100 + 0.4)(9.81)(0.481 + 0.4625)] + cos\theta[(0.0183 \times 100 + 0.4)(9.81)(0.111)]$$
$$= sin\theta(90.33) + cos\theta(2.43)$$

For hip joint, maximum angle during walking is $\theta = 32.2°$

$\therefore \boldsymbol{T_1 = 47.56Nm}$

$$T_2 = sin\theta \left[(m_4 + m_{L2})g\left(\frac{l_2}{2}\right)\right] + sin\theta[+m_5g(l_2)] + sin\theta[+m_6g(l_2)]$$

$$+cos\theta \left[(m_6 + m_{L3})g\left(\frac{l_3}{2}\right)\right]$$

$$= sin\theta[(0.0439 \times 100 + 0.8)(9.81)(0.23125) + (0.0183 \times 100 + 0.4)(9.81)(0.4625)]$$

$$+cos\theta[(0.0183 \times 100 + 0.4)(9.81)(0.111)]$$

$$= sin\theta(22.99) + cos\theta(2.43)$$

For knee joint, maximum angle during walking is $\theta = 73.5°$

$\therefore \boldsymbol{T_2 = 21.68Nm}$

$$T_3 = cos\theta \left[(m_6 + m_{L3})g\left(\frac{l_3}{2}\right)\right]$$

$$= cos\theta[(0.0183 \times 100 + 0.4)(9.81)(0.111)]$$

$$= cos\theta(2.43)$$

For hip joint, maximum angle during walking is $\theta = 30.0°$

$\therefore \boldsymbol{T_3 = 2.10\ Nm}$

From the calculation, the torque required at the hip joint is 47.56 Nm; the torque required at the knee joint is 21.68 Nm whereas the torque required at the ankle is 2.10 Nm. Therefore, the motor and drive system should produce more torque than the calculated torque values to lift both the user's limb and the exoskeleton.

4.3 Exoskeleton design

The exoskeleton is designed using SolidWorks with all the parts required like links, couplings, mounts and pivot joints. Each part is drawn part by part and then assembled to form the complete exoskeleton design. The complete assembly drawing of the exoskeleton is as shown in Figure 4.2 and the details about the design are discussed in Chapter 3. Besides that, the detailed drawings of each part with dimensions are attached in the appendix for further development and fabrication.
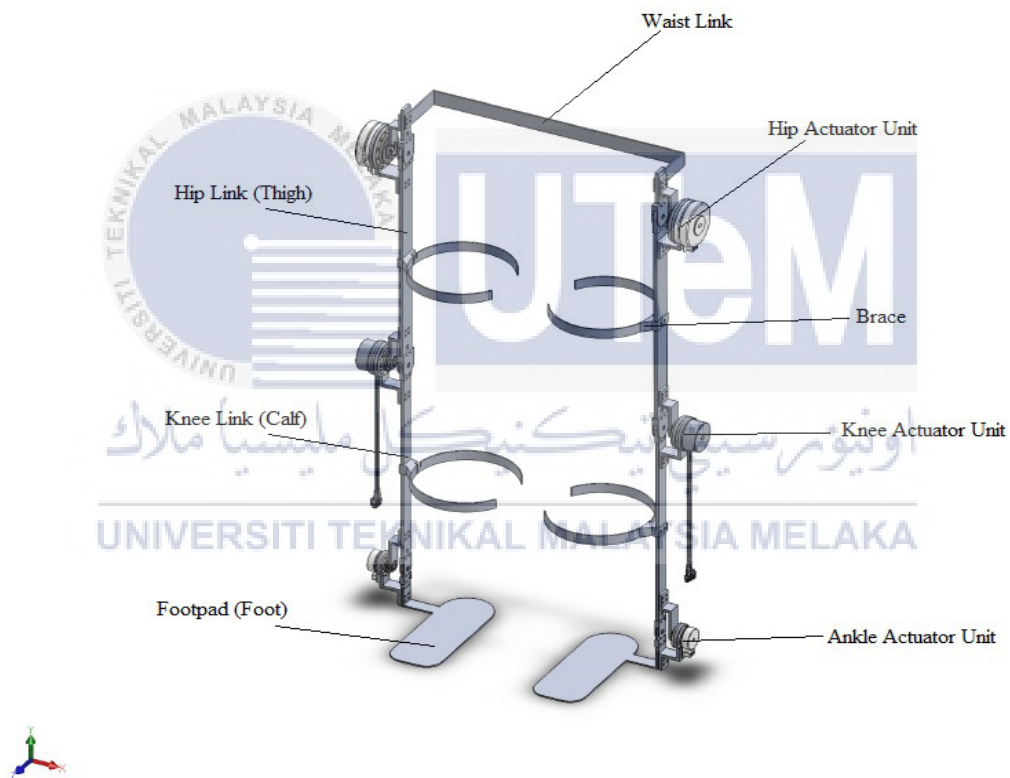

Figure 4.2: Isometric view of the exoskeleton.

4.4 Motion Analysis

This section contains the torque data collected from both tests in motion analysis. The data obtained from the simulations or calculations are plotted into graphs for analysing purpose. Besides that, detailed analyses on the result obtained from simulations are also included in this section to verify of the performance of the exoskeleton.

4.4.1 One Step Leg Swing Motion

In this section, the exoskeleton model was required to perform one leg swing motion in SolidWorks Motion Analysis. The data obtained from required torque calculation and torque data obtained from SolidWorks Motion Analysis for all 3 joints are recorded and tabulated as shown in Table 4.2, Table 4.3 and Table 4.4. Besides that, the data collected are also plot into graphs for better illustration as shown in Figure 4.3, Figure 4.4 and Figure 4.5. These torque data accounts for one stepping motion of a walking gait.

4.4.1.1 Hip Joint

The data for hip joint are tabulated and plotted into graph as shown in Table 4.2 and Figure 4.3. Table 4.2 shows the torque data collected from both calculations and simulations whereas Figure 4.3 shows the graph of torque value against time for both calculations and simulations.

Table 4.2: Torque data required in the hip joint.

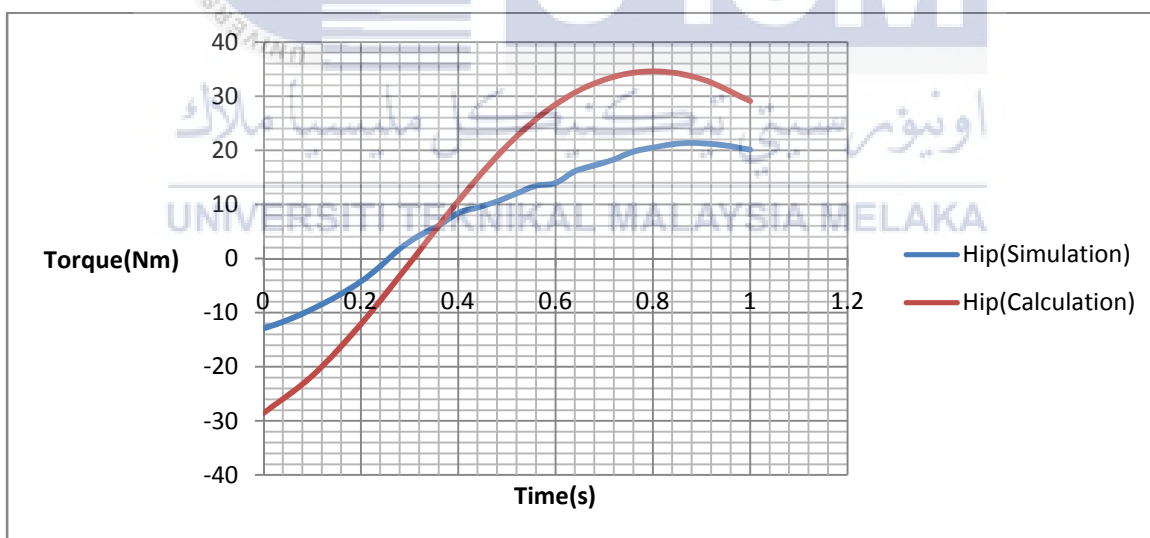| $time, t(s)$	$hip\ angle, \theta_1(°)$	$calculated\ torque, T_c(Nm)$	$simulated\ torque, T_s(Nm)$
0	-24.04	-28.55	-12.87
0.1	-15.01	-21.67	-9.31
0.2	-4.14	-12.1	-4.24
0.3	7.57	-0.92	3.03
0.4	19.16	10.59	8.41
0.5	29.12	20.8	11.29
0.6	35.80	28.44	13.95
0.7	38.28	33.01	17.76
0.8	36.70	34.55	20.48
0.9	31.84	33.14	21.23
1.0	24.79	29.06	20.09

Figure 4.3: Graph of torque against time for hip joint.

The data from calculation shows a gradual increase from -28.55Nm initially to 34.55Nm at 0.8s and then gradually decrease to 29.06Nm at 1.0s. The data obtained from simulation exhibits the same partial sinusoidal pattern as the calculated torque value.

However, the value obtained from the simulation varies in a smaller scale. The torque value starts at -12.87 Nm initially and then gradually increased to 21.32 Nm at 0.88s and then decreased to 20.10Nm at 1.0s. This difference in magnitude is most likely to be caused by the dynamic factors that are ignored in the calculations as the calculations are made in static form. The factors like momentum, angular velocity and accelerations that are ignored in the calculations are most likely to be the cause for the difference in magnitude between the calculated values and simulated values.

Moreover, the maximum value of torque in terms of magnitude for hip joint obtained from simulation and calculation are 21.32Nm and 34.55Nm respectively. This means that the hip joint actuator unit selected is able to support the user to take a step as the torque required does not exceed the maximum continuous torque of actuator unit which is 56 Nm.

4.4.1.2 Knee Joint

The data for knee joint are tabulated and plotted into graph as shown in Table 4.3 and Figure 4.4. Table 4.3 shows the torque data collected from both calculations and simulations whereas Figure 4.4 shows the graph of torque value against time for both calculations and simulations.

Table 4.3: Torque data required at knee joint.

time, $t(s)$	knee angle, $\theta_2(°)$	calculated torque, $T_c(Nm)$	simulated torque, $T_s(Nm)$
0	-0.76	0.33	1.16
0.1	-17.17	2.44	4.94
0.2	-33.23	4.50	8.33
0.3	-46.82	6.48	10.13
0.4	-56.16	6.61	10.64
0.5	-59.52	5.05	10.38
0.6	-56.16	4.09	9.34
0.7	-46.82	1.59	7.39
0.8	-33.23	-2.44	4.34
0.9	-17.17	-6.34	0.61
1.0	-0.76	-9.39	-3.37
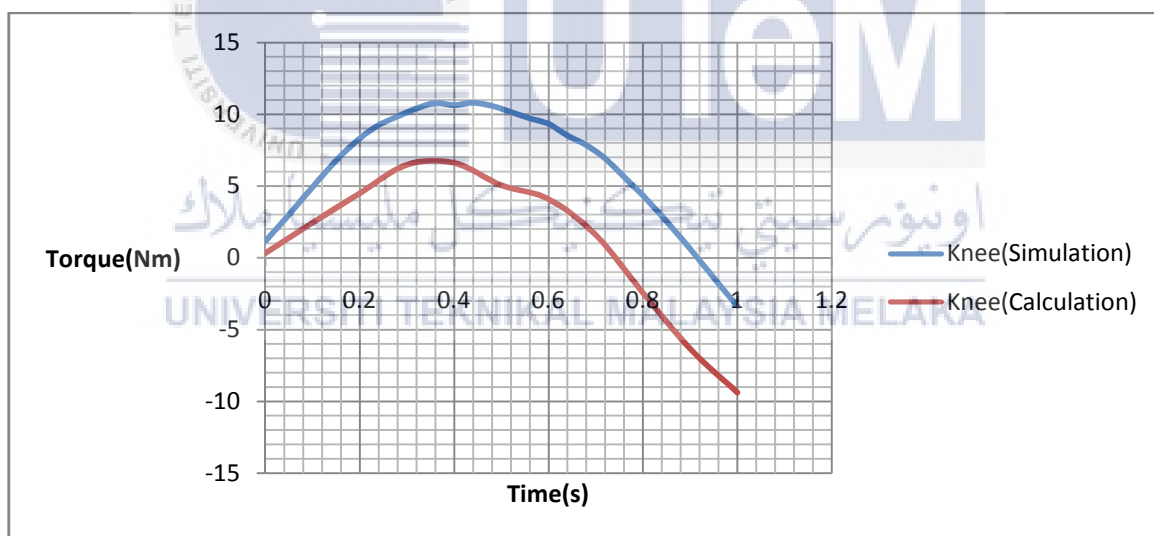
Figure 4.4: Graph of torque against time for knee joint.

For the knee joint, the data obtained from calculations shows a gradual increase from 0.33Nm initially to 6.61 Nm at 0.80s and then decrease gradually to -9.39 Nm at 1.00s. As for the data obtained from simulation also shows a gradual increase from 1.16 Nm at 0s to 10.64 Nm at 0.4s and then gradually decrease to -3.37 Nm. Both data shows a similar bell shaped pattern, but varies in a different magnitude and reaches a different

maximum value. This difference in magnitude is likely to be caused by the negligence of dynamic factors as the calculations are made in static equilibrium. The factors like momentum, angular velocity and acceleration are most likely to cause the difference in magnitude and yet exhibit the similar pattern for both calculated and simulated values.

Besides that, the absolute maximum value for both calculated and simulated torque values are 9.39Nm and 10.64Nm respectively. The maximum value for the simulation does not exceed the maximum continuous torque of the knee joint actuator unit selected which is 28.9 Nm. This means that the knee joint actuator units selected are able to support the user to take a step forward.

4.4.1.3 Ankle Joint

The data for hip joint are tabulated and plotted into graph as shown in Table 4.4 and Figure 4.5. Table 4.4 shows the torque data collected from both calculations and simulations whereas Figure 4.5 shows the graph of torque value against time for both calculations and simulations.

Table 4.4: Torque data required at ankle joint.

$time, t(s)$	$ankle\ angle, \theta_3(°)$	$calculated\ torque, T_c(Nm)$	$simulated\ torque, T_s(Nm)$
0	-24.81	-0.84	-1.18
0.1	-32.18	-1.06	-1.21
0.2	-37.38	-1.21	-1.13
0.3	-39.25	-1.26	-1.02
0.4	-37.00	-1.20	-0.87
0.5	-30.40	-1.01	-0.74
0.6	-20.36	-0.69	-0.65
0.7	-8.54	-0.30	-0.60
0.8	3.47	0.12	-0.57
0.9	14.67	0.50	-0.54
1.0	24.03	0.81	-0.51

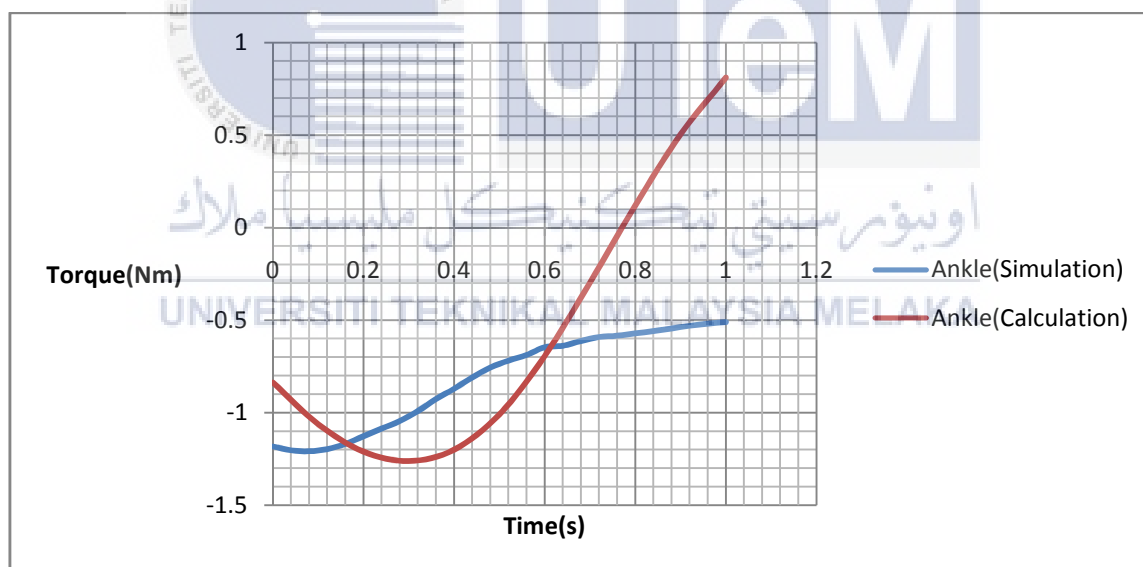Figure 4.5: Graph of torque against time for ankle joint.

For the ankle joint, the data obtained from calculations shows a gradual decrease from -0.84 Nm initially to -1.26 Nm at 0.30s and then increase gradually to 0.81Nm at 1.0s. The data obtained from simulation shows a similar pattern with calculated data but with a less steep and more gradual slope. The torque value from simulation starts at -1.18Nm

initially and then decrease to -1.21Nm at 0.10s. After that, the value increased gradually from -1.21Nm to -0.51Nm at 1.00s. The difference in steepness of slope is likely to be caused by the dynamic factors ignored in calculation as mentioned above as it is done in only considering static equilibrium. Factors like momentum, angular velocity and acceleration are not considered in the calculation are most likely the cause of the difference in the magnitude of the gradient and values.

The absolute maximum torque value for both calculation and simulation are 1.26Nm and 1.21Nm respectively. This indicates that the ankle joint actuator units selected are able to handle and support the user to take a step forward. This is because the value does not exceed the maximum continuous torque of the ankle joint actuator unit selected which is 12.80Nm
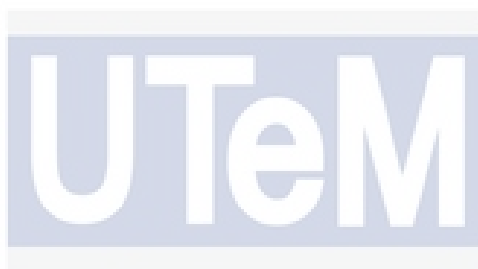
4.4.1.4 Summary

From the result, all the actuator units selected are able to swing a 100kg user's leg to take a step. This is because the maximum torque required at all 3 joints to swing the user's leg does not exceed the maximum continuous torque that can be produced by their respective actuator units. However, the torque value obtained from the calculation deviates from the simulation in terms of scale even though they exhibit similar patterns. This is because the equation only considers for the static component, but does not consider the dynamic factors like momentum, angular velocity and acceleration. Therefore, the joint torque equations require further improvement to provide a much more accurate estimation of torque required.

4.4.2 Two Complete Cycle Walking Motion

In this section, the exoskeleton model was required to perform two complete cycle walking motion in SolidWorks Motion Analysis. The torque data obtained from SolidWorks Motion Analysis for all 6 joints are recorded and also plotted into graphs for better illustration as shown in Figure 4.6, Figure 4.7, Figure 4.8, Figure 4.9, Figure 4.10 and Figure 4.11. These torque data account for two complete cycle walking motion for each joint of the lower limbs. The different phases of a walking motion are indicated with different coloured region in the graphs. The region coloured in blue represents the swing phase where the foot is lifted whereas the region coloured in red represents the stance phase where the foot is touching the ground at all time.

4.4.2.1 Left Hip Joint

The torque data for left hip joint obtained from the simulation are plotted into graph as shown in Figure 4.6. Figure 4.6 shows the torque value recorded for left hip joint in two complete walking cycle walking motion. For the first step, the left leg starts with the swing phase.
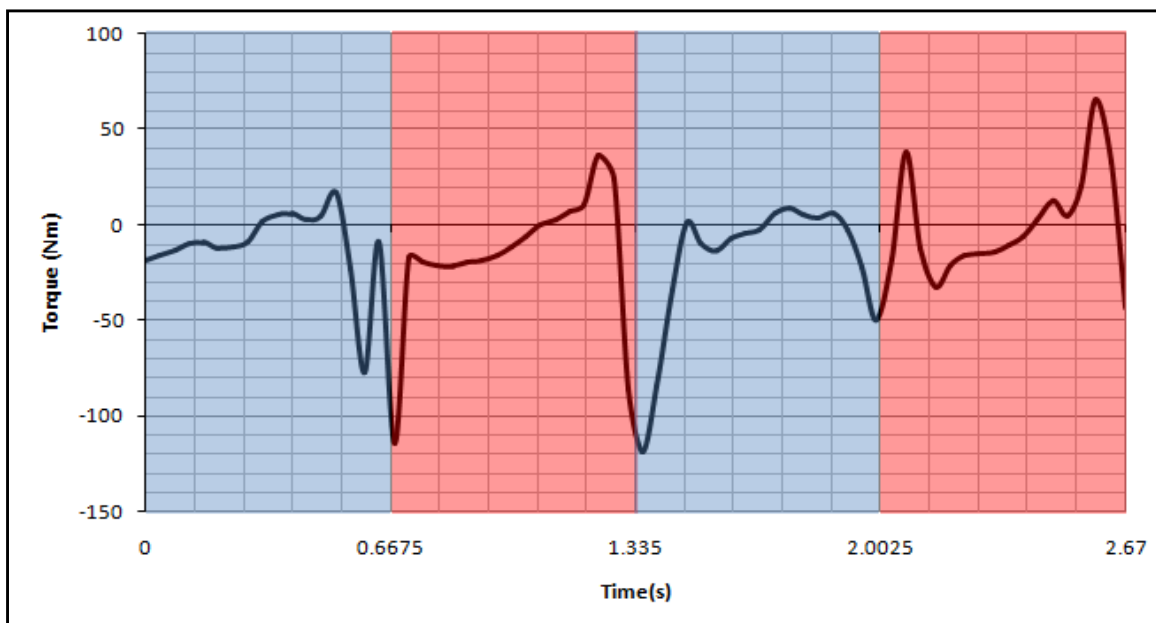
Figure 4.6: Torque value for left hip joint in two step walking motion.

The torque values exert similar pattern for each phase. The torque value shows a fluctuated increase in swing phase and a gradual increase in stance phase. Most of the time, the magnitude of torque values is within the range of 56Nm which is the maximum continuous torque of the hip actuator unit. However, the torque value shows some spikes during the transitions between phases. These spikes are caused by the rapid deceleration of the leg to a brief halt during the transition between phases. This is because the joint requires a large amount of torque to decelerate and then accelerate in the opposite direction during the transition which explains the surge and recover of the torque value. From the Figure 4.6, there are multiple spikes shown in 0.67s and 2.00s which can be caused by a jerk during the deceleration of the joint. This indicates that the transitions were rough which could be caused by the planned trajectory. On the other hand, the singular spike shown in 1.34s indicates a smooth deceleration and acceleration during transition. For a brief moment, the spikes can reach a maximum value of 120Nm which is about two times the maximum continuous torque of the hip actuator unit can produce. Hence, the actuator unit will need to be overdriven in order to mimic the torque pattern of walking motion.

4.4.2.2 Left Knee Joint

The torque data for left knee joint obtained from the simulation are plotted into graph as shown in Figure 4.7. Figure 4.7 shows the torque value recorded for left knee joint in two complete walking cycle walking motion. For the first step, the left leg starts with the swing phase.
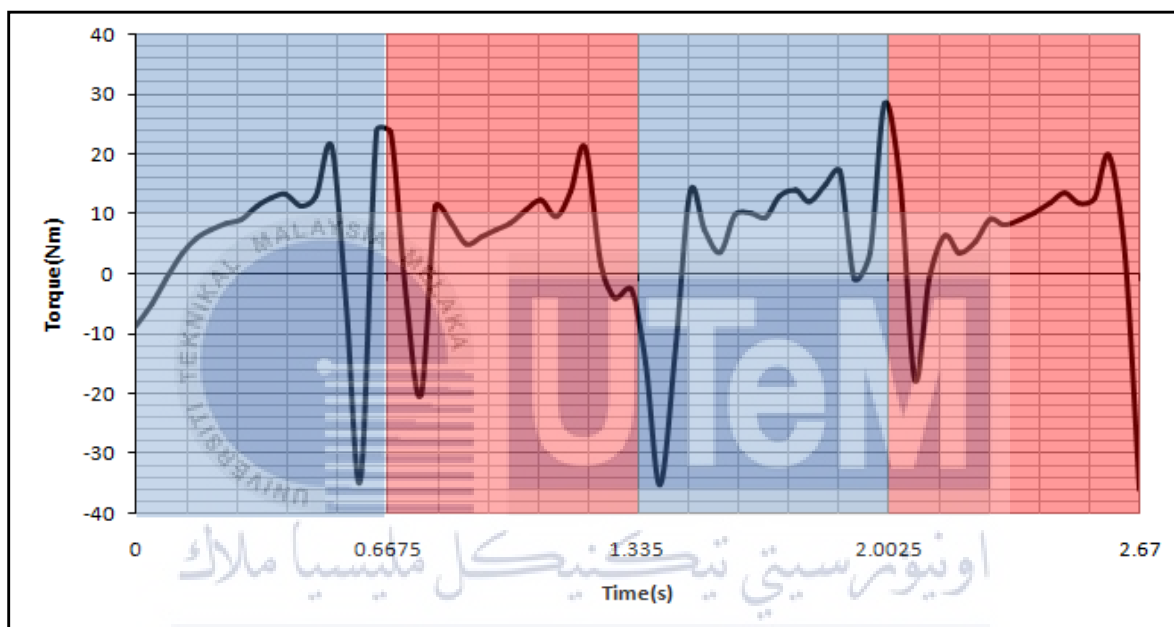

Figure 4.7: Torque value for left knee joint in two step walking motion.

The torque values exert similar pattern for both phases. The torque value shows a fluctuated increase in both swing phase and stance phase. Most of the time, the magnitude of torque values is within the range of 28.9Nm which is the maximum continuous torque of the knee actuator unit. However, the torque value also shows some spikes during the transitions between phases. These spikes are caused by the rapid deceleration of the leg to a brief halt during the transition between phases. During the transition between swing phase and stance phase, the joint required a large amount of torque to stop the leg and then accelerate in the opposite direction. This rapid deceleration and acceleration causes the fluctuations in torque value. As shown in Figure 4.7, there are multiple spikes shown in 0.67s and 2.00s, which are caused by jerking motion during the deceleration of the joint.

This indicates a rough deceleration during transitions which could be caused by the trajectory itself. The spike shown in 1.34s indicates a smooth stopping motion with a slight jerk during transition. For a brief moment, the spikes can reach a maximum value of 36Nm which is about 1.25 times the maximum continuous torque of the knee actuator unit can produce. Due to the fact that the knee actuator unit can only supply a maximum continuous torque of 28.9Nm, the actuator unit will need to be overdriven to emulate the walking motion.

4.4.2.3 Left Ankle Joint

The torque data for the left ankle joint obtained from the simulation are plotted into graph as shown in Figure 4.8. Figure 4.8 shows the torque value recorded for the left ankle joint in two complete walking cycle walking motion. For the first step, the left leg starts with the swing phase.
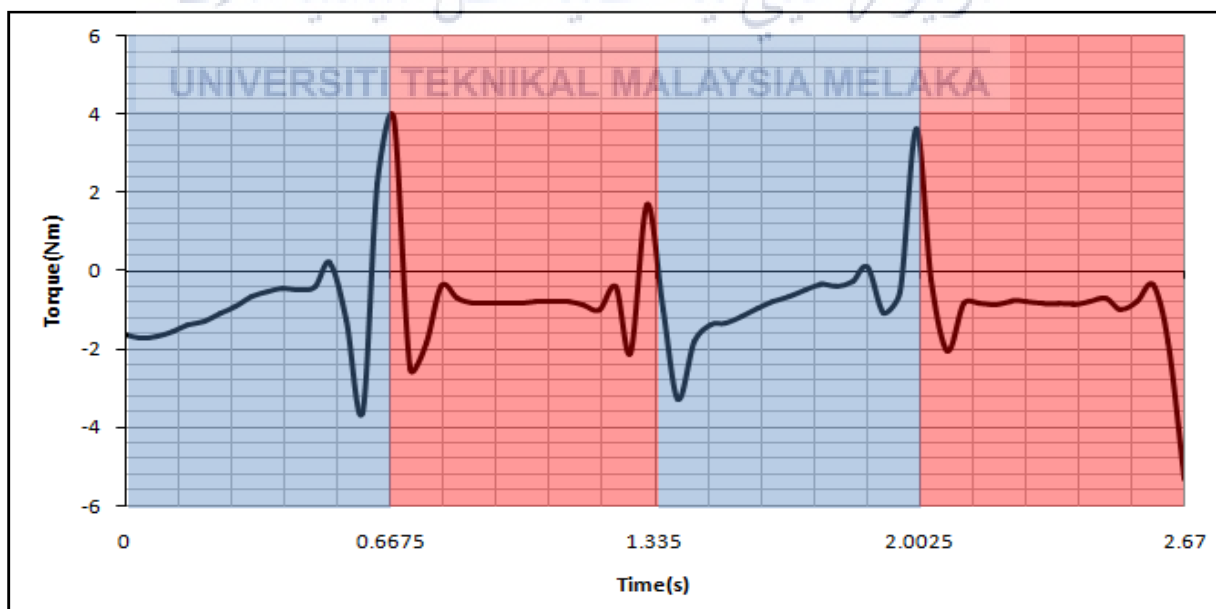

Figure 4.8: Torque value for left ankle joint in two step walking motion.

The torque values exert similar pattern for each phase. The torque value shows a gradual increase in swing phase, but the value remains almost constant for stance phase. However, the torque value also shows some spikes during the transitions between phases. These spikes are caused by the rapid deceleration of the leg to a brief stop during the transition between phases. The torque value fluctuates during the transition between phases because the joint need to stop and accelerate in the opposite direction. Besides that, there are multiple spikes shown in 0.67s, 1.34s, and 2.00s, which are caused by jerks during the deceleration of the joint. These jerks are caused by rough deceleration which could be subsequently caused by the planned trajectory itself. For a brief moment, the spikes can reach a maximum value of 4Nm but it does not exceed the maximum continuous torque that can be produced by the ankle actuator unit. This means that the ankle actuator unit does not need to be overdriven to mimic the torque pattern of ankle joint during walking.

4.4.2.4 Right Hip Joint

The torque data for right hip joint obtained from the simulation are plotted into graph as shown in Figure 4.9. Figure 4.9 shows the torque value recorded for right hip joint in two complete walking cycle walking motion. For the first step, the right leg starts with the stance phase.
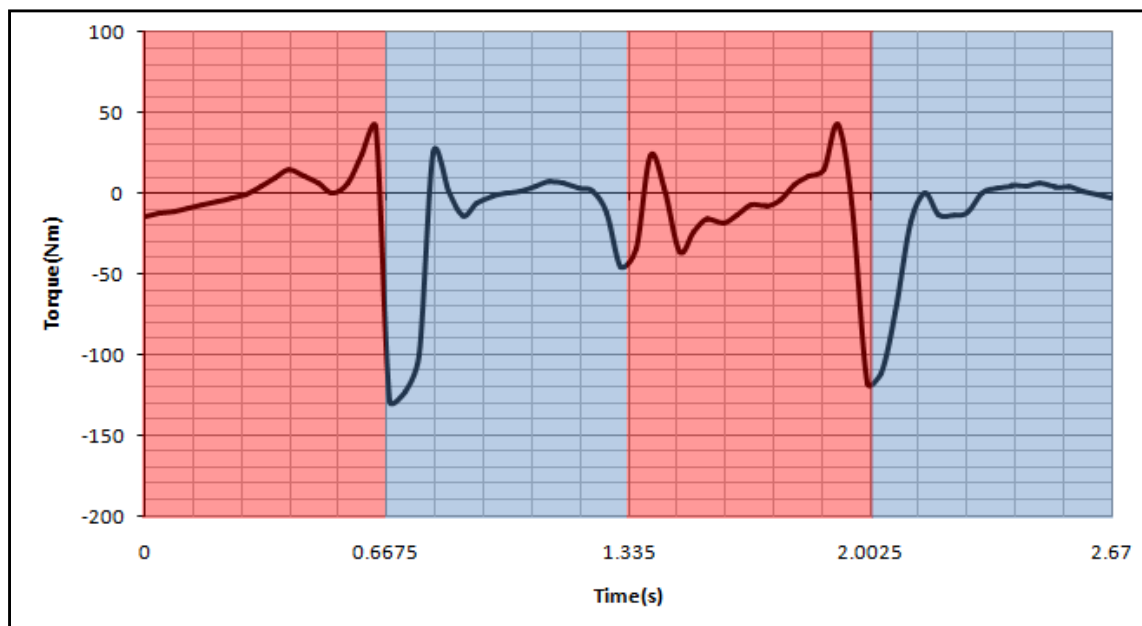
Figure 4.9: Torque value for right hip joint in two step walking motion.

The torque values exert similar pattern for each phase. The torque value shows a gradual increase in stance phase, but the value increased and then decreased gradually for stance phase. Most of the time, the magnitude of torque values is within the range of 56Nm which is the maximum continuous torque of the hip actuator unit. However, the torque value shows some spikes during the transitions between phases. These spikes in the torque value occurred because of the sudden deceleration of the leg to a brief halt during transition between phases. This is because a large amount of torque is required to stop the leg and then accelerate it in the opposite direction. From Figure 4.9, there are singular spikes shown in 0.67sand 2.00s, which shows that the joint decelerated and accelerated in a smooth manner. However, the multiple spikes shown in 1.34s indicate that there are jerks during the transition of phases. This indicates a rough deceleration during transitions which could be caused by the trajectory itself. For a brief moment, the spikes can reach a maximum value of 130Nm which is about two times the maximum continuous torque of the hip actuator unit can produce. Hence, the hip actuator unit will need to overdriven to mimic the torque pattern during walking.

4.4.2.5 Right Knee Joint

The torque data for right hip joint obtained from the simulation are plotted into graph as shown in Figure 4.10. Figure 4.10 shows the torque value recorded for right knee joint in two complete walking cycle walking motion. For the first step, the right leg starts with the stance phase.
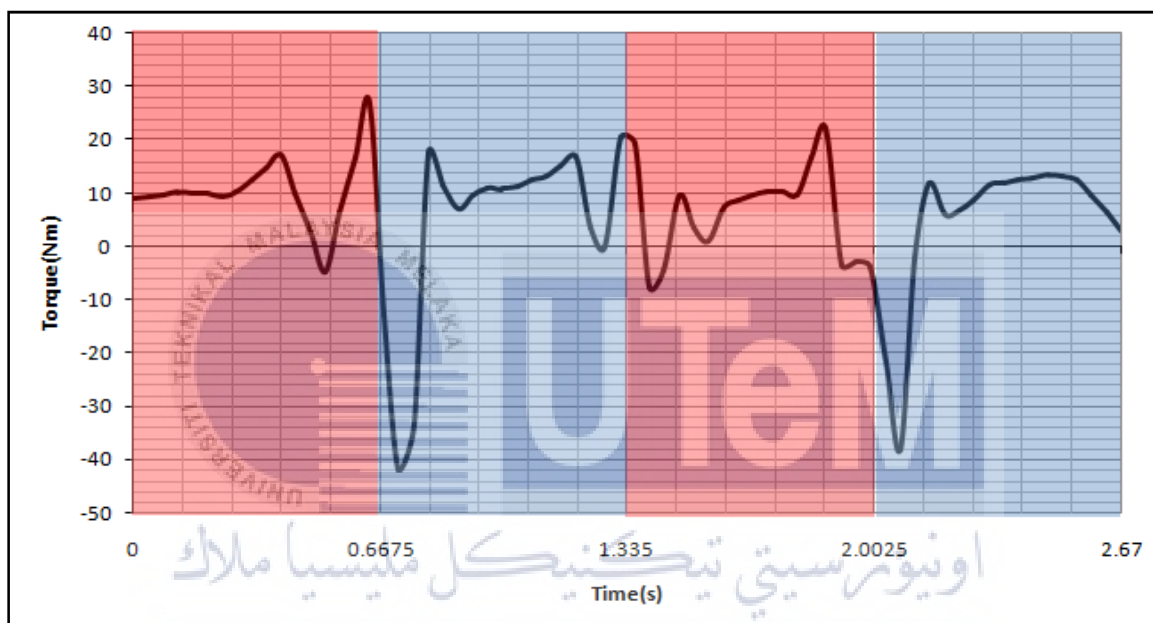

Figure 4.10: Torque value for right knee joint in two step walking motion.

The torque values exert similar pattern for both phases. The torque value shows a gradual increase in both the stance phase and stance phase. Most of the time, the magnitude of torque values is within the range of 28.9Nm which is the maximum continuous torque of the knee actuator unit. However, the torque value shows some spikes during the transitions between phases. These spikes are caused by the rapid deceleration of the leg to a brief halt during the transition between phases. During the transition between swing phase and stance phase, the joint required a large amount of torque to stop the leg and then accelerate in the opposite direction. This rapid deceleration and acceleration causes the fluctuations in torque value. There are multiple spikes shown in 0.67s and 1.34s, which can be caused by jerks during the deceleration of the joint. This indicates a rough

deceleration during transitions which could be caused by the trajectory itself. On the other hand, the spike shown in 2.00s indicates a smooth stopping motion with a slight jerk during transition. For a brief moment, the spikes can reach a maximum value of 42Nm which is about 1.5 times the maximum continuous torque of the knee actuator unit can produce. Thus, the knee actuator unit needs to be overdriven to mimic the torque pattern of walking motion since it only produces a maximum continuous torque of 28.9Nm.

4.4.2.6 Right Ankle Joint

The torque data for right ankle joint obtained from the simulation are plotted into graph as shown in Figure 4.9. Figure 4.9 shows the torque value recorded for right ankle joint in two complete walking cycle walking motion. For the first step, the right leg starts with the stance phase.
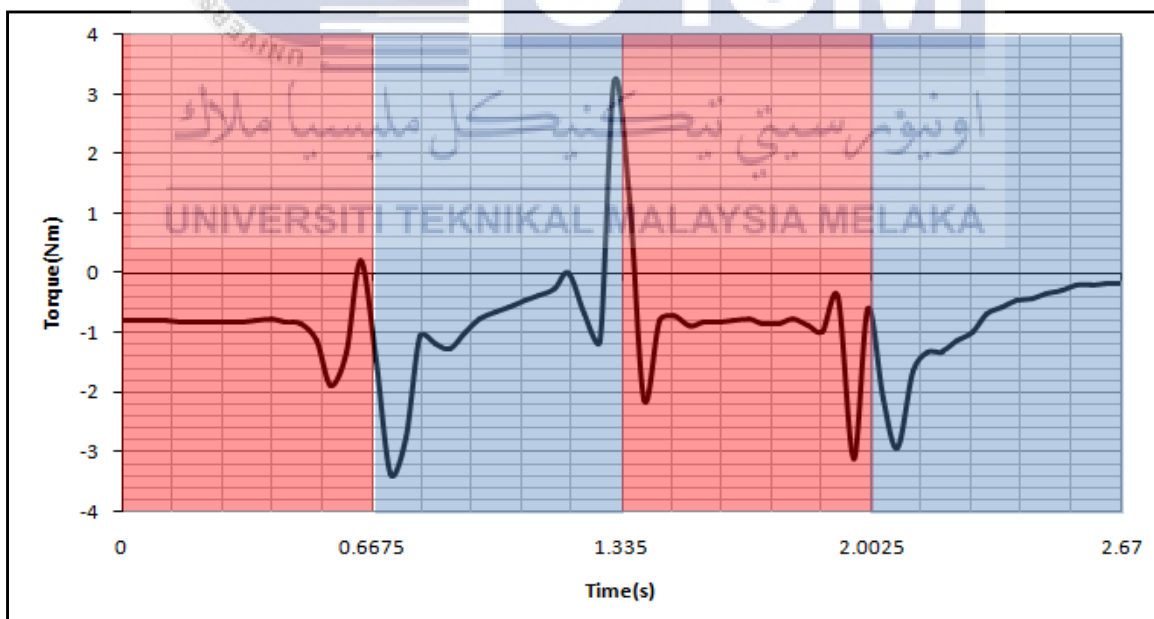

Figure 4.11: Torque value for right knee joint in two step walking motion.

The torque values exert similar pattern for each phase. The torque value shows a gradual increase in the swing phase, but it remains constant in stance phase. However, the

torque value shows some spikes during the transitions between phases. As mentioned before, they are caused by the rapid deceleration of the leg during the transition between phases. During a transition between walking phases, the joints are required to come to a halt and then move in the opposite direction. Hence, this causes the fluctuation in the torque value as large amount of torque is required to stop the moving body part. There are fluctuating spikes in 0.67s, 1.34s and 2.00s because there are jerks during the transition. This indicates a rough deceleration during transitions which could be caused by the trajectory itself. For a brief moment, the spikes can reach a maximum value of 3.4Nm but it does not exceed the maximum continuous torque of the ankle actuator unit can produce. In other words, the ankle actuator unit does not need to be overdriven to emulate the torque pattern of walking.

4.4.2.7 Summary

From the result, the torque required during a walking motion does not exceed the maximum continuous torque able to produce by the actuators in different phases of walking except for the transition period between phases. All the joints show some spikes in the torque value during the transition period between swing phase and stance phase of walking motion. This is caused by the sudden decelerations of the joints during transitions between phases. During the transition between phases, the moving legs of the user need to decelerate to a standstill and then accelerate in the opposite direction. Therefore, the spikes in torque value are braking torque applied to decelerate the user's legs to a halt. The maximum continuous torque value for hip, knee and ankle joints are 56Nm, 28.9Nm and 12.8Nm respectively. However, for hip and knee joints, the braking torque required is about two times the maximum continuous torque able to produce by the each actuator unit.

To overcome this problem, one of the advantages of DC motor can be utilised to provide braking torque for the walking. The DC motor chosen can be overdriven to produce more than twice the maximum continuous torque for a limited amount of time

continuously before overheating. The DC motor chose for hip joints are able to produce twice the maximum continuous torque for about 230s continuously before overheating. As for the DC motor chosen for the knee joint, it can produce twice the maximum continuous torque for about 200s continuously before overheating. From the graphs, the average total time span for spikes in one walking step is 0.4s while torque value does not exceed the maximum continuous torque value for the rest of the time. This means that, the average overdrive time span in one step is 0.4s whereas the average non-overdrive time span one step is 0.94s. This will allow the actuator units cool down between the spikes and allows the exoskeleton to work for some time before overheating occurs. Hence, although the actuator units selected are able to provide actuation to a 100kg user, but there is a limitation. This limitation can be overcome by deploying a better control system to smoothen the walking motion of the exoskeleton especially during the transition between phases. A better trajectory control is required to help in producing a smoother walking trajectory of the legs so that the deceleration is less rapid and less jerks. Besides that, the limitation can also be eliminated by adding a braking mechanism or a spring mechanism help in the deceleration of the exoskeleton. Apart from that, a torque control demonstrated in [27] is also required to overcome this problem by controlling the torque produced by actuator unit and avoid the overshoot of torque produced.

In summary, the actuator units selected are able to actuate the lower limb of the user most of the time, but it needs to be overdriven during transition period between phases unless a better trajectory control system or braking system is applied.

4.5 Finite Element Analysis

This section contained the results of Finite Element Analysis for each exoskeleton link. The diagram indicates the stress distribution on the link when appropriate load and torque are applied to the links. The torque applied on each link is the maximum value of torque for each joint obtained from the motion analysis. Hence, the torque applied on the hip, knee and ankle link are 130Nm, 50Nm and 6Nm respectively. By analysing the stress distribution diagrams, the structural strengths of all the exoskeleton links under extreme load are examined in this section.
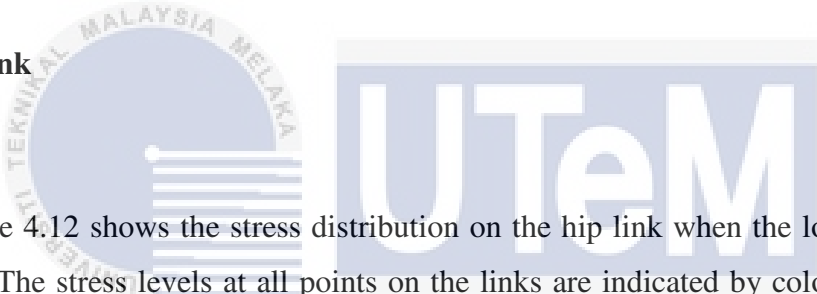
4.5.1 Hip Link

Figure 4.12 shows the stress distribution on the hip link when the load and torque are applied. The stress levels at all points on the links are indicated by colours where red indicates maximum stress and blue indicates minimum stress as shown by the legend in Figure 4.12. The stress distribution shows a high stress level exerted on regions like the motor mount, the upper part of the link as well as the pivot joint. However, the maximum stress occurs at the motor mount with pressure of 319MN/m^2 is lower than the yield strength of Aluminium-7075, 515MN/m^2 by about 38.25%.
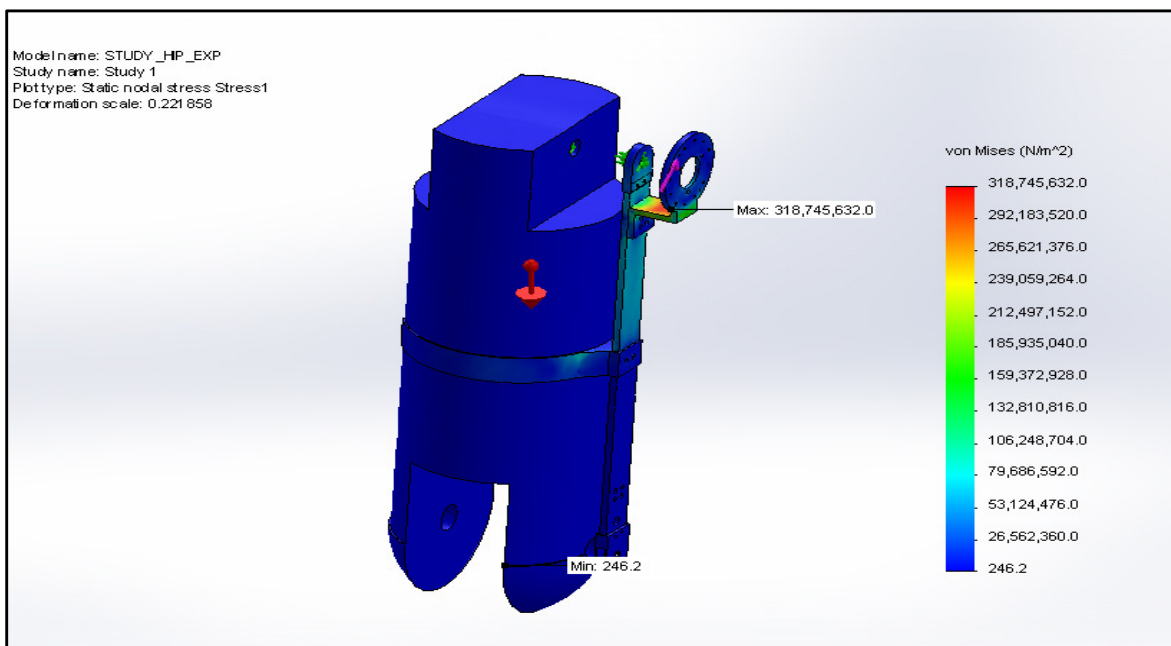
Figure 4.12: Stress distribution on the hip link.

4.5.2 Knee Link

Figure 4.13 shows the stress distribution on the knee link when the load and torque are applied. The stress levels at all points on the links are indicated by colours where red indicates maximum stress and blue indicates minimum stress as shown by the legend in Figure 4.13. The stress distribution shows a high stress level exerted on regions like the motor mount, the upper part of the link as well as the pivot joint. However, the maximum stress occurs at the motor mount with pressure of 171MN/m^2 is significantly lower than the yield strength of Aluminium-7075, 515MN/m^2 by about 66.80%.

Figure 4.13: Stress distribution on the knee link

4.5.3 Foot Pad

Figure 4.14 shows the stress distribution on the foot pad when the load and torque are applied. The stress levels at all points on the links are indicated by colours where red indicates maximum stress and blue indicates minimum stress as shown by the legend in Figure 4.14. The stress distribution shows a high stress level exerted on regions like the foot pad link as well as the pivot joint. However, the maximum stress occurs at the pivot joint with pressure of 78MN/m^2 is significantly lower than the yield strength of Aluminium-7075, 515MN/m^2 by about 84.85%.
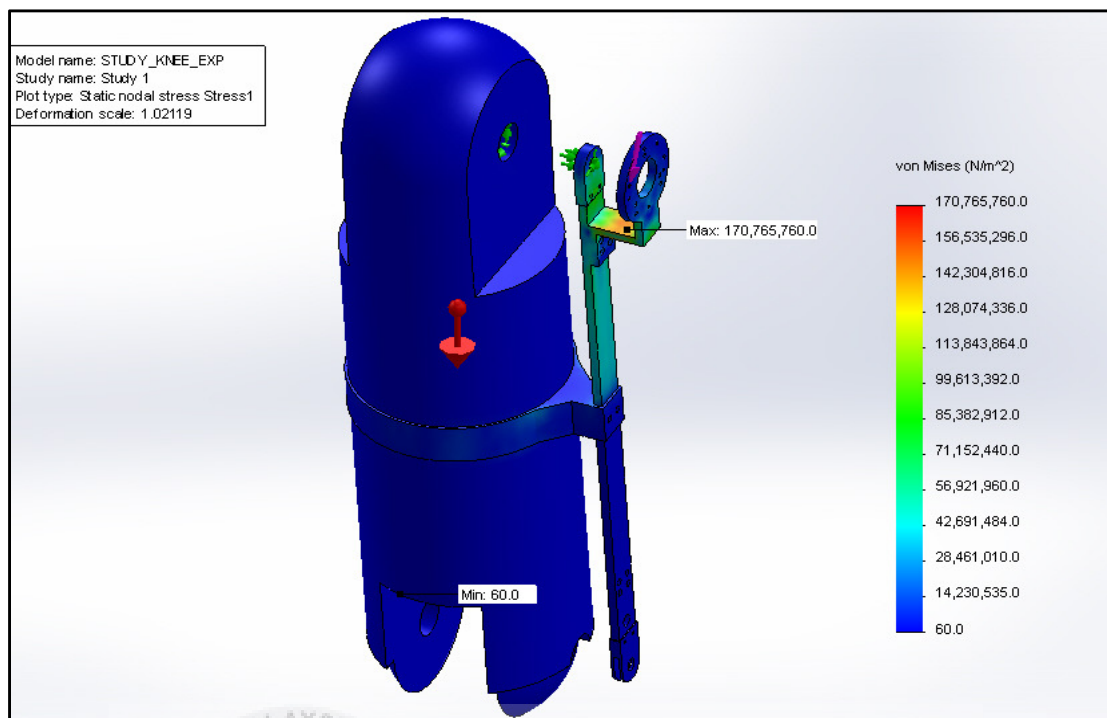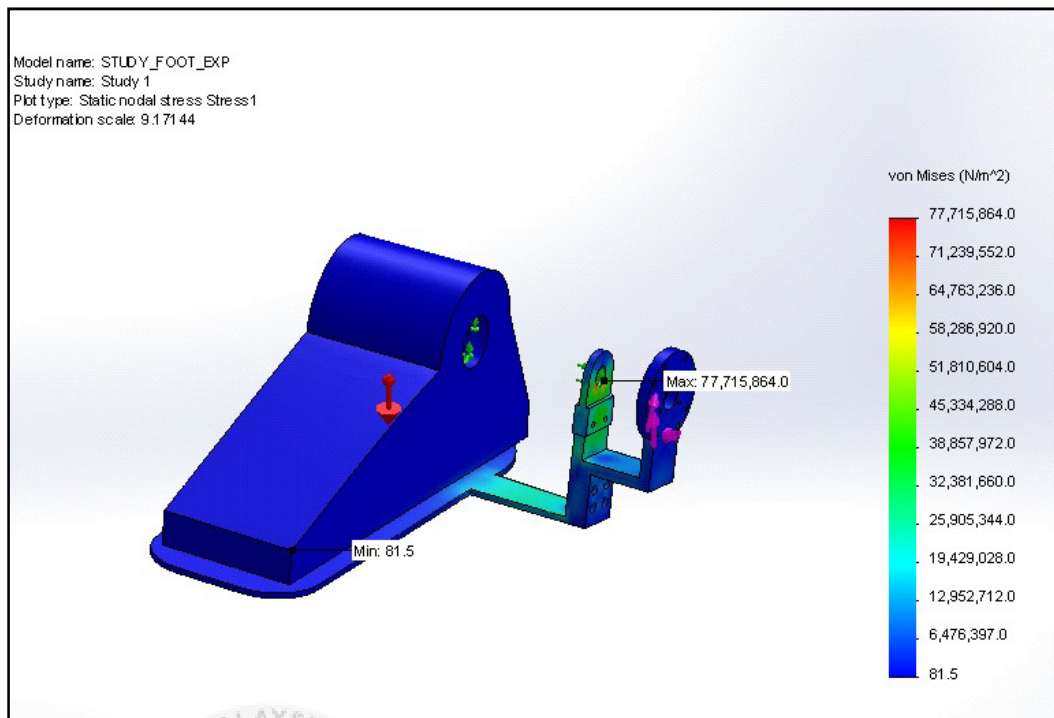
Figure 4.14: Stress distribution on the footpad.

4.5.4 Summary

From the result, all the maximum stress exerted on the links does not exceed the yield strength of the Aluminium-7075 used to construct the links. This means that, the links will not deform or fracture under extreme conditions like for instance when the maximum torque is applied to the links. Hence, the links are able to support the 100kg user when torque is applied during the walking motion.

CHAPTER 5

CONCLUSION AND RECOMMENDATIONS

5.1 Conclusion

Based on the objectives, the mathematical model and torque equations are derived to study the motion of the lower limb exoskeleton and determine the torque required at joints. The mathematical model is verified using Matlab and the torque required for each joint are calculated. Besides that, the exoskeleton is designed by selecting actuator units available on the market using the calculations obtained from the torque equations. DC motors and gearboxes are selected for each joint according to the torque requirement at different joints and the selections are verified with calculations. Apart from that, the structural strength of the designed exoskeleton's links is tested by applying appropriate loads and torque to the links. The test shows that all exoskeleton's links are able to withstand the maximum torque produced when walking with 100kg user strap onto it. Moreover, the exoskeleton underwent motion analysis to test its ability to support the user for walking. The tests show that the actuator units selected for each joint are able to fulfil all torque requirements for walking via overdrive which further verified the actuator selections. This means that the exoskeleton robot designed is strong enough to support the user's limbs and it produces enough torque to actuate the limbs of the user but with a certain limitation. Unless the trajectory is smoothen, otherwise the actuator units will need to be overdriven to mimic the torque patterns. In conclusion, all the objectives of this project are achieved, but the exoskeleton robot also requires improvements in terms of the

control system. The future works should focus on the sensory system, trajectory control system as well as power consumption of the exoskeleton to further improve the design.

5.2 Recommendations

To solve the problem caused by torque value spikes during the transition between walking phases, a braking mechanism should be incorporated into the design of the exoskeleton to help the actuator units decelerate. Besides that, a spring mechanism can also be incorporated into the design of the exoskeleton to store and release energy during the transitions of walking phases. These two designs can help the actuator units to brake without generating braking torque by themselves, which helps to avoid the use of overdrive during operations. Other than that, a good trajectory control system should also be implemented to make the walking motion smoother as well as decelerate less rapidly. This will help in reducing the torque value spikes during the transition of walking phases. Nevertheless, future studies should also work on the sensory system and control system to make sure that the exoskeleton performs as it intended. Any imperfection found in the exoskeleton design should also be corrected and improved to make sure that it is safe to be operated by the user. The actual exoskeleton robot can only be fabricated and assembled after thorough studies and researches for further testing.

REFERENCE

[1] J. R. Jones; C. S. Huxtable; J. T. Hodgson. *Self-reported work-related illness in 2004/05: Results from the Labour Force Survey,* [online]. Available at: http://www.hse.gov.uk/statistics/swi/swi0405.pdf [accessed 22 October 2014]

[2] Health and Safety Laboratory, Health and Safety Executive. *Lower limb MSD*, [online]. Available at: http://www.hse.gov.uk/research/rrpdf/rr706.pdf [accessed 22 October 2014]

[3] Zoss, AB.; Kazerooni, H.; Chu, A, "Biomechanical design of the Berkeley lower extremity exoskeleton (BLEEX)," *Mechatronics, IEEE/ASME Transactions* on, vol.11, no.2, pp.128,138, April 2006

[4] Zoss, AB.; Kazerooni, H, "Design of an electrically actuated lower extremity exoskeleton," *Advanced Robotics*, Vol. 20, No. 9, pp. 967–988, 2006

[5] JM. Hollerbach; IW. Hunter; J. Ballantyne, "A comparative analysis of actuator technologies for robotics," *The Robotics Review*, Vol. 2, Pages 299-342, 1992

[6]Kazerooni, H., "Exoskeletons for human power augmentation," *Intelligent Robots and Systems, 2005. (IROS 2005). 2005 IEEE/RSJ International Conference on* , vol., no., pp.3459,3464, 2-6 Aug. 2005

[7]Bock, T.; Linner, T. ; Ikeda, W.," Exoskeleton and Humanoid Robotic Technology in Construction and Built Environment," *The Future of Humanoid Robots - Research and Applications,2012.* vol., no., pp 111-146, 20 Jan. 2012.

[8]Herr, H., "Exoskeletons and orthoses: classification, design challenges and future directions," *Journal of NeuroEngineering and Rehabilitation, 2009.* vol., no., pp 1-9, 18 June 2009.

[9]Fleischer, C.; Wege, A.; Kondak, K.; Hommel, G., "Application of EMG signals for controlling exoskeleton robots," *Biomed Tech 2006.* vol., no., pp 314-319, Dec. 2006.

[10] Pratt, G.A.; Williamson, M.M., "Series elastic actuators," *Intelligent Robots and Systems 95. 'Human Robot Interaction and Cooperative Robots', Proceedings. 1995 IEEE/RSJ International Conference on* , vol.1, no., pp.399,406 vol.1, 5-9 Aug 1995

[11] Jiménez-Fabián, R.; Verlinden, O., "Review of control algorithms for robotic ankle systems in lower-limb orthoses, prostheses, and exoskeletons.," *Medical Engineering & Physics 2012.* vol. 34, no. 4, pp397-408, 19 Dec. 2011.

[12] Singh, RM.; Chatterji, S.; "Trends and Challenges in EMG Based Control Scheme of Exoskeleton Robots-A Review," *International Journal of Scienctific and Engineering Research, 2012.* vol. 3, no. 8, pp1-8, August 2012.

[13]Hong, Y. W.; King, Y. J.; Yeo, W. H.; Ting, C. H.; Chuah, Y. D.; Lee, J. V.; Chok, E. T., " Lower Extremity Exoskeleton: Review and Challenges Surrounding the Technology and its Role in Rehabilitation of Lower Limbs," *Australian Journal of Basic and Applied Sciences.* vol.7, no.7, pp520-524, 2013.

[14] Sawicki, G.; Domingo, A.; Ferris, D.; "The effects of powered ankle–foot orthoses on joint kinematics and muscle activation during walking in individuals with incomplete spinal cord injury," *Journal of NeuroEngineering and Rehabilitation.* vol.3, no.3, 28 Feb. 2006

[15] Rosengrant, B.; Kostik, B. *Potentiometers: A Proven Position Sensing Solution that Every Engineer Needs to Consider in Modern Designs,* [online]. Available at: http://www.sensorsmag.com/sensors/position-presence-proximity/potentiometers-a-proven-position-sensing-solution-every-engi-9038 [accessed 28 October 2014]

[16] Ramsdale, R. *Mechanical Components - Potentiometers, Encoders, LVDTs,* [online]. Available at: http://www.engineershandbook.com/Components/positionsensors.htm [accessed 28 October 2014]

[17] Harmonic Drive LLC. *Advantages,* [online]. Available at: http://harmonicdrive.net/reference/advantages/ [accessed 28 October 2014]

[18] Sanz-Merodio, D.; Cestari, M.; Arevalo, J.C.; Garcia, E., "A lower-limb exoskeleton for gait assistance in quadriplegia," *Robotics and Biomimetics (ROBIO), 2012 IEEE International Conference on ,* vol., no., pp.122,127, 11-14 Dec. 2012

[19] Xianggang Zhang; Zenghe Xiang; Qingxia Lin; Qifang Zhou, "The design and development of a lower limbs rehabilitation exoskeleton suit," *Complex Medical Engineering (CME), 2013 ICME International Conference on ,* vol., no., pp.307,312, 25-28 May 2013

[20] Banchadit, W.; Temram, A; Sukwan, T.; Owatchaiyapong, P.; Suthakorn, J., "Design and implementation of a new motorized-mechanical exoskeleton based on CGA Patternized Control," *Robotics and Biomimetics (ROBIO), 2012 IEEE International Conference on ,* vol., no., pp.1668,1673, 11-14 Dec. 2012

[21] Onen, U.; Botsali, F.M.; Kalyoncu, M.; Tinkir, M.; Yilmaz, N.; Sahin, Y., "Design and Actuator Selection of a Lower Extremity Exoskeleton," *Mechatronics, IEEE/ASME Transactions on ,* vol.19, no.2, pp.623,632, April 2014

[22] Stopforth, R., "Customizable Rehabilitation Lower Limb Exoskeleton System.," *Int J Adv Robotic Sy*, vol. *9, no.*152, 2012.

[23] Marcheschi, S.; Salsedo, F.; Fontana, M.; Bergamasco, M., "Body Extender: Whole body exoskeleton for human power augmentation," *Robotics and Automation (ICRA), 2011 IEEE International Conference on ,* vol., no., pp.611,616, 9-13 May 2011

[24] Hayashi, T.; Kawamoto, H.; Sankai, Y., "Control method of robot suit HAL working as operator's muscle using biological and dynamical information," *Intelligent Robots and*

Systems, 2005. (IROS 2005). 2005 IEEE/RSJ International Conference on , vol., no., pp.3063,3068, 2-6 Aug. 2005

[25] Walsh, C.J.; Paluska, D.; Pasch, K.; Grand, W.; Valiente, A; Herr, H., "Development of a lightweight, underactuated exoskeleton for load-carrying augmentation," *Robotics and Automation, 2006. ICRA 2006. Proceedings 2006 IEEE International Conference on* , vol., no., pp.3485,3491, 15-19 May 2006

[26] Low, K. H.; Xiaopeng Liu; Haoyong Yu, "Development of NTU wearable exoskeleton system for assistive technologies," *Mechatronics and Automation, 2005 IEEE International Conference* , vol.2, no., pp.1099,1106 Vol. 2, 29 July-1 Aug. 2005

[27] Kawamoto, H.; Suwoong Lee; Kanbe, S.; Sankai, Y., "Power assist method for HAL-3 using EMG-based feedback controller," *Systems, Man and Cybernetics, 2003. IEEE International Conference on* , vol.2, no., pp.1648,1653 vol.2, 5-8 Oct. 2003

[28] Zoss, AB.; Kazerooni, H.; Chu, A, "Biomechanical design of the Berkeley lower extremity exoskeleton (BLEEX)," *Mechatronics, IEEE/ASME Transactions on* , vol.11, no.2, pp.128,138, April 2006

[29] Chu, A; Kazerooni, H.; Zoss, A, "On the Biomimetic Design of the Berkeley Lower Extremity Exoskeleton (BLEEX)," *Robotics and Automation, 2005. ICRA 2005. Proceedings of the 2005 IEEE International Conference on* , vol., no., pp.4345,4352, 18-22 April 2005

[30] Zoss, A; Kazerooni, H.; Chu, A, "On the mechanical design of the Berkeley Lower Extremity Exoskeleton (BLEEX)," *Intelligent Robots and Systems, 2005. (IROS 2005). 2005 IEEE/RSJ International Conference on* , vol., no., pp.3465,3472, 2-6 Aug. 2005

[31] Kaiser Aluminium. *Rod and Bar Alloy 2024,*[online]. Available at: https://online.kaiseraluminum.com/depot/PublicProductInformation/Document/1022/Kaiser_Aluminum_2024_Rod_and_Bar.pdf [accessed 1 November 2014]

[32] Kaiser Aluminium. *Rod and Bar Alloy 7075,*[online]. Available at: https://online.kaiseraluminum.com/depot/PublicProductInformation/Document/1028/Kaiser_Aluminum_7075_Rod_and_Bar.pdf [accessed 1 November 2014]

[33] Kaiser Aluminium. *Rod and Bar Alloy 7068,*[online]. Available at: https://online.kaiseraluminum.com/depot/PublicProductInformation/Document/1027/Kaiser_Aluminum_7068_Rod_and_Bar.pdf [accessed 1 November 2014]

[34] Walsh, C. J., "Biomimetic design of an under-actuated leg exoskeleton for load-carrying augmentation," PhD. dissertation, Dept. of Mech. Eng, Massachusetts Institute of Technology, Cambridge, MA, 2006.

[35] Schmidler, C., Health Pages. *Anatomical Reference Planes,* [online]. Available at http://www.healthpages.org/anatomy-function/anatomy-terms/ [accessed 1 November 2014]

[36] Lim, T. O.; Ding, L. M.; Zaki, M.; Suleiman, A. B.; Fatimah, S.; Siti, S.; ... & Maimunah, A. H., "Distribution of body weight, height and body mass index in a national sample of Malaysian adults," *Medical Journal of Malaysia*, vol.55, no. 1, pp 108-128. 2000

[37] Drillis, R.; Contini, R.; Bluestein, M. , "Body segment parameters," *Artificial limbs*, vol. 8, no.1, pp 44-66. 1964

[38] Tawakal Hasnain Baluch, A. M.; Iqbal, J., Izhar, U.; & Khan, U. S., "Kinematic and Dynamic Analysis of a Lower Limb Exoskeleton," *World Academy of Science, Engineering and Technology.* vol. 6, no., pp 812-816. 23Sept. 2012

[39]M. Bortole., "Design And Control Of A Robotic Exoskeleton For Gait Rehabilitation", Master, Universidad Carlos III De Madrid, 2015.

[40] N. L. Shaari., "Parameter Study of Stable Walking Gaits For NAO Humanoid Robot", IJRET, vol. 02, no. 08, pp. 16-23, 2013.

[41]K. Crosby, 'Walking with Attitude - Article - How to Measure Stride or Step Length for your Pedometer', Walkingwithattitude.com, 2015. [Online]. Available: https://www.walkingwithattitude.com/articles/features/how-to-measure-stride-or-step-length-for-your-pedometer. [Accessed: 21- Dec- 2014].

[42] R. Neptune, K. Sasaki and S. Kautz., "The effect of walking speed on muscle function and mechanical energetic", Gait & Posture, vol. 28, no. 1, pp. 135-143, 2008.
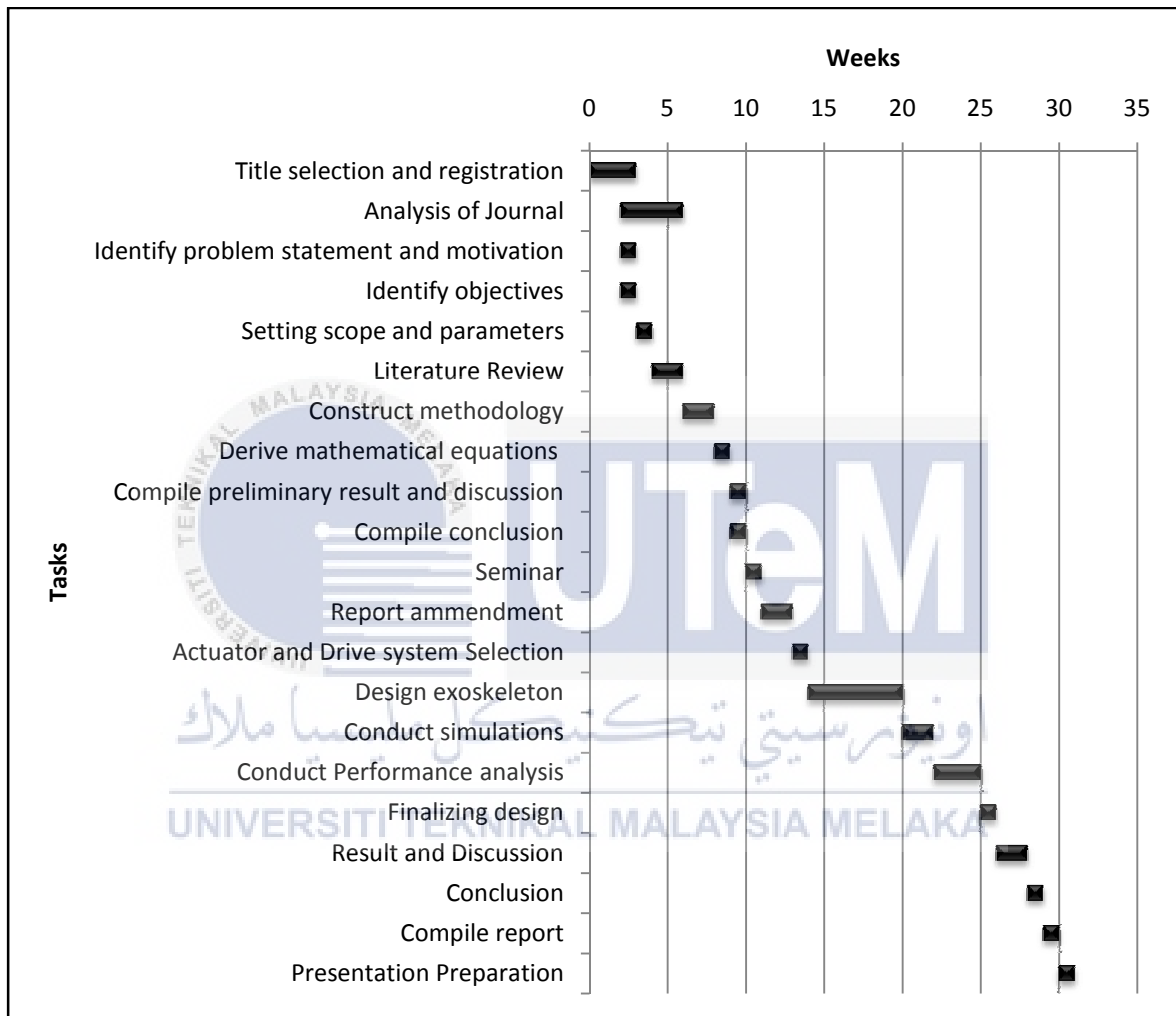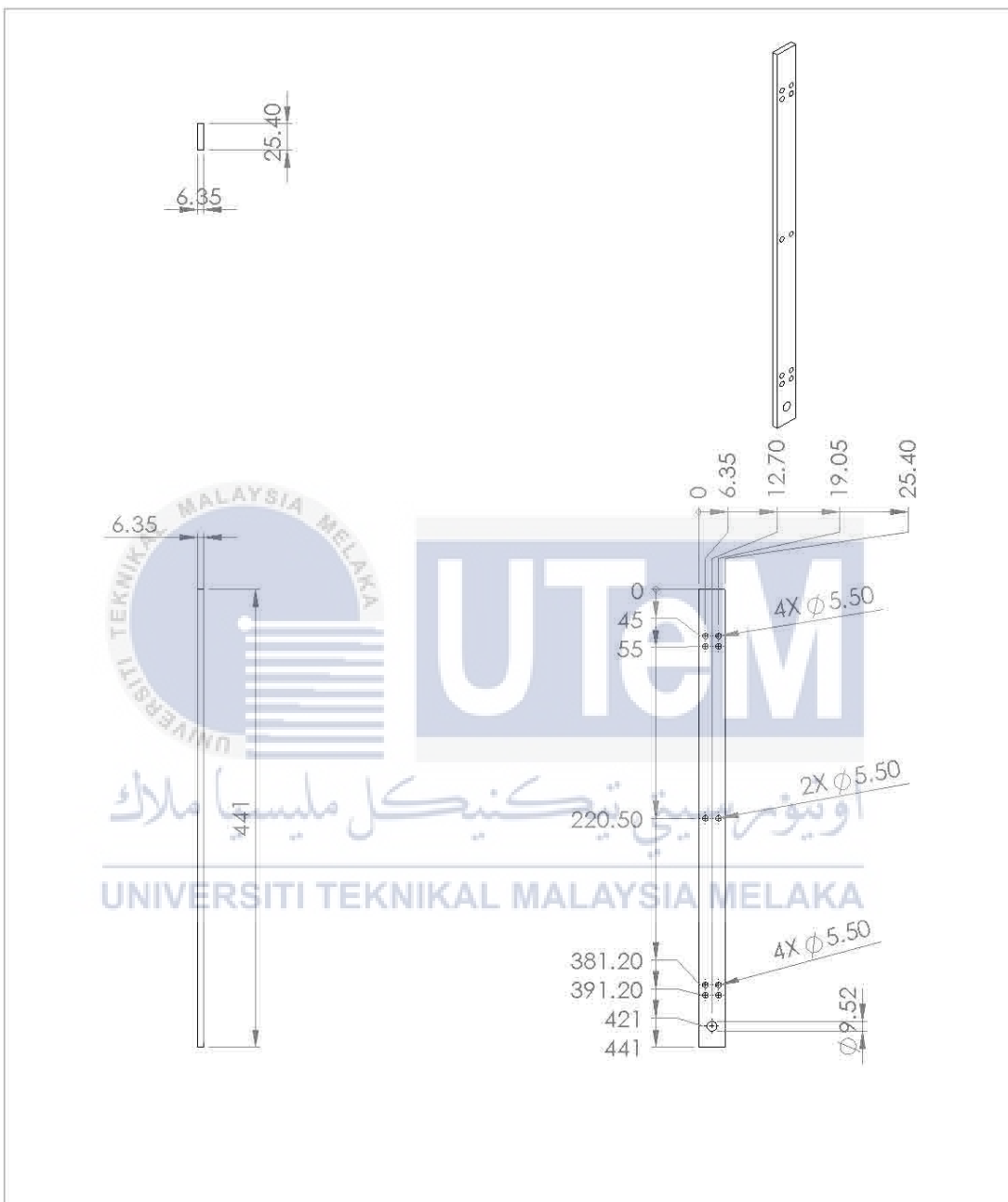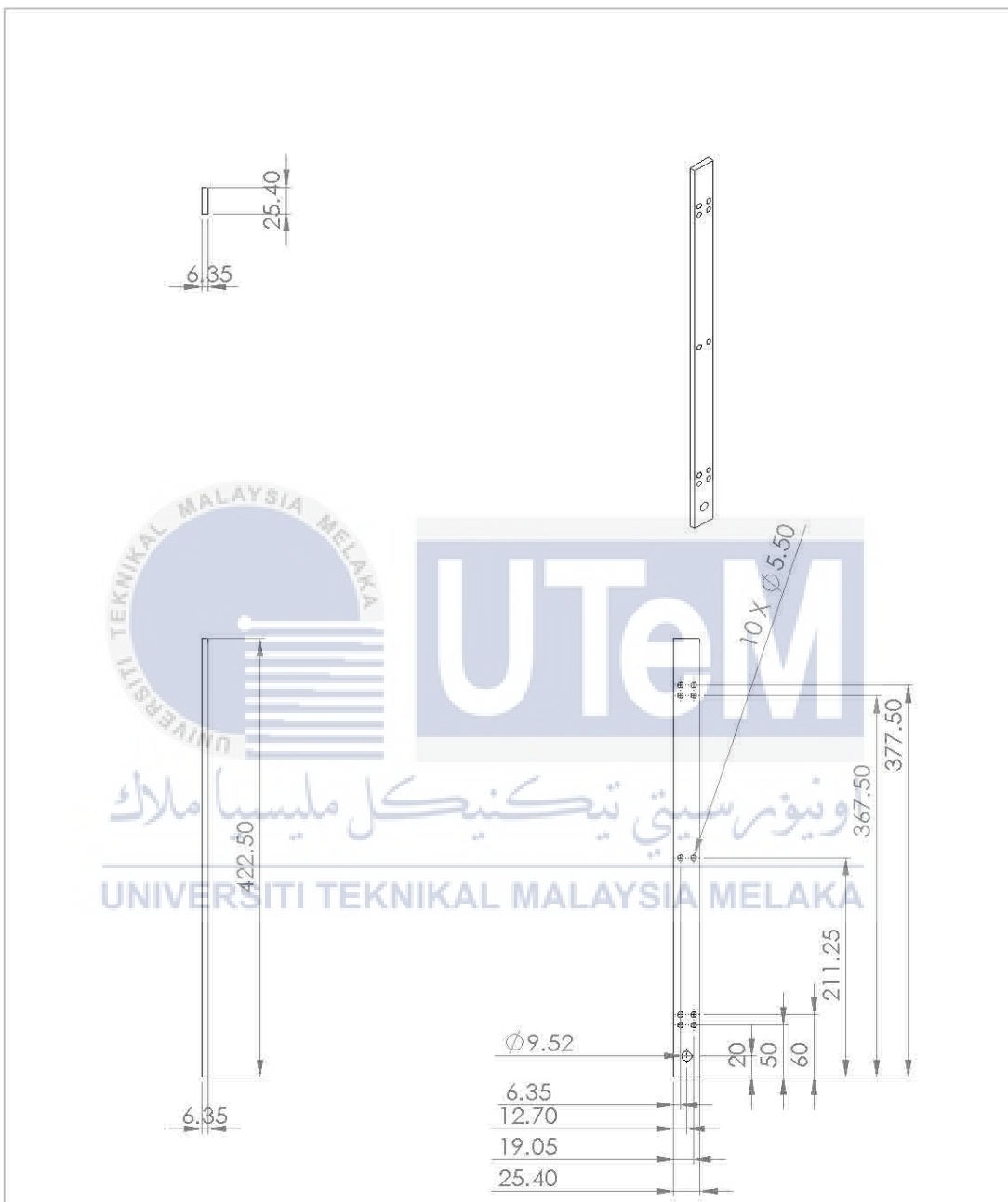
APPENDICES

APPENDIX A

Gantt Chart

APPENDIX B

Engineering Drawing of Hip Link

	NAME	SIGNATURE	DATE				TITLE:			
DRAWN										
CHK'D										
APPV'D										
MFG										
Q.A				MATERIAL:			DWG NO.	HIP_LINK		A4
				WEIGHT:			SCALE:1:5		SHEET 1 OF 1	

UNLESS OTHERWISE SPECIFIED: DIMENSIONS ARE IN MILLIMETERS SURFACE FINISH: TOLERANCES: LINEAR: ANGULAR:

FINISH:

DEBUR AND BREAK SHARP EDGES

DO NOT SCALE DRAWING

REVISION

APPENDIX C

Engineering Drawing of Knee Link

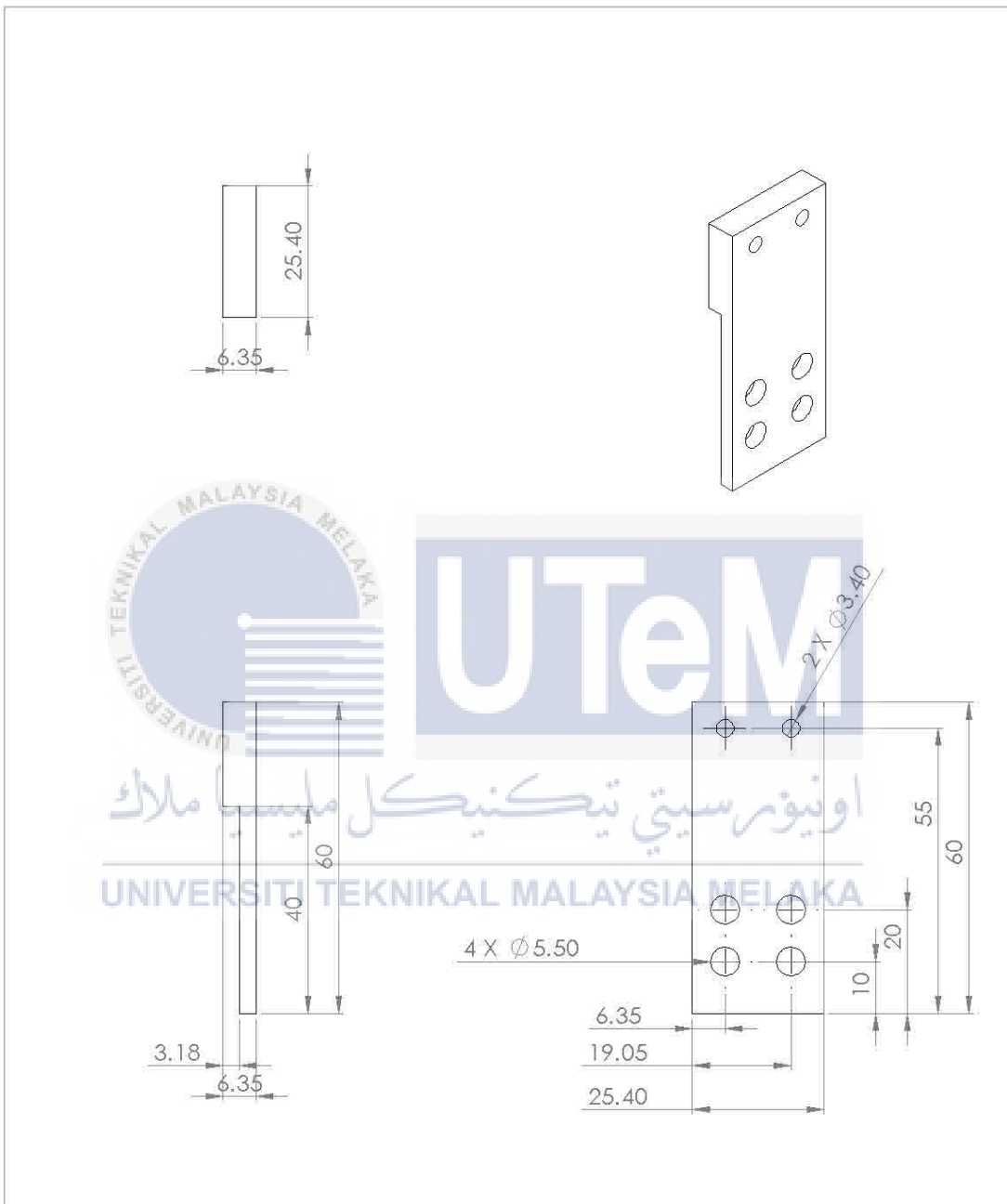|	NAME	SIGNATURE	DATE				TITLE:		
DRAWN									
CHK'D									
APPV'D									
MFG									
Q.A				MATERIAL:			DWG NO.	KNEE_LINK	A4
				WEIGHT:			SCALE:1:5		SHEET 1 OF 1

UNLESS OTHERWISE SPECIFIED:
DIMENSIONS ARE IN MILLIMETERS
SURFACE FINISH:
TOLERANCES:
  LINEAR:
  ANGULAR:

FINISH:

DEBUR AND
BREAK SHARP
EDGES

DO NOT SCALE DRAWING

REVISION

APPENDIX D

Engineering Drawing of Foot Link

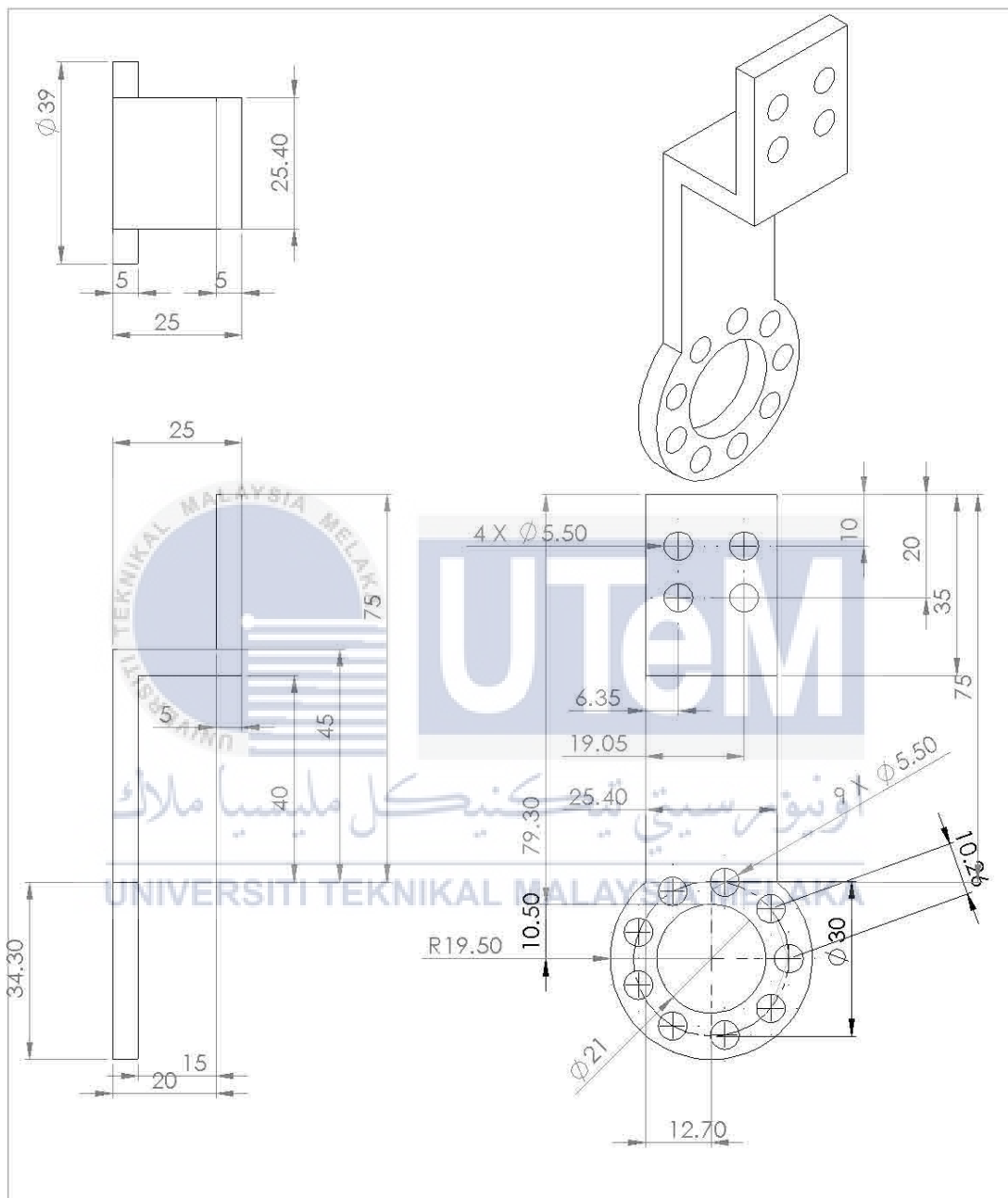|		NAME	SIGNATURE	DATE			TITLE:		
DRAWN									
CHK'D									
APPV'D									
MFG									
Q.A					MATERIAL:		DWG NO.	FOOT_LINK	A4
					WEIGHT:		SCALE:1:1	SHEET 1 OF 1	

UNLESS OTHERWISE SPECIFIED:
DIMENSIONS ARE IN MILLIMETERS
SURFACE FINISH:
TOLERANCES:
 LINEAR:
 ANGULAR:

FINISH:

DEBUR AND BREAK SHARP EDGES

DO NOT SCALE DRAWING

REVISION

APPENDIX E

Engineering Drawing of Link Coupling 1

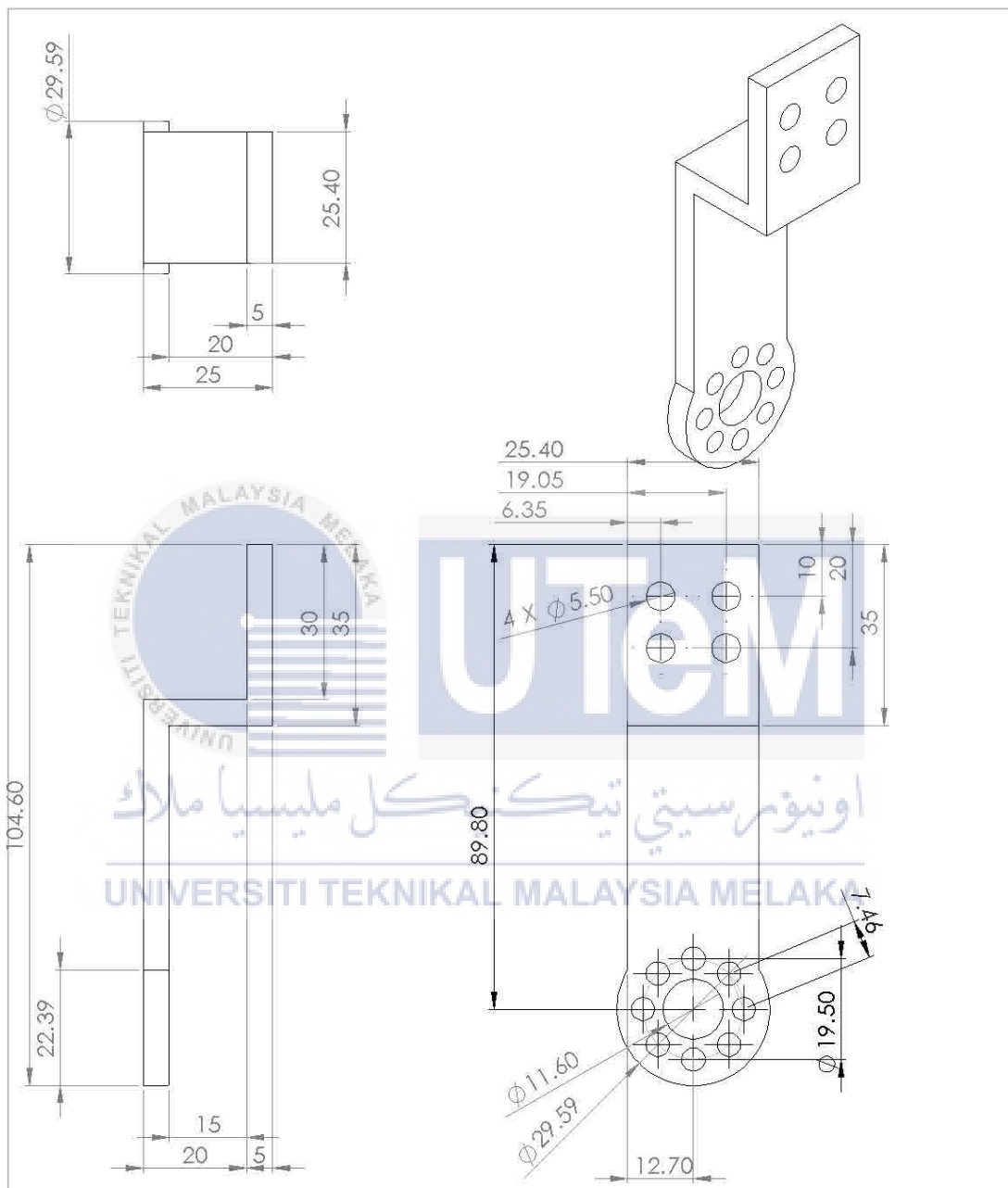|	NAME	SIGNATURE	DATE			TITLE:		
DRAWN								
CHK'D								
APPV'D								
MFG								
Q.A			MATERIAL:			DWG NO. LINK_COUPLING_1	A4	
			WEIGHT:			SCALE:1:1	SHEET 1 OF 1	

UNLESS OTHERWISE SPECIFIED:
DIMENSIONS ARE IN MILLIMETERS
SURFACE FINISH:
TOLERANCES:
 LINEAR:
 ANGULAR:

FINISH:

DEBUR AND
BREAK SHARP
EDGES

DO NOT SCALE DRAWING

REVISION

APPENDIX F

Engineering Drawing of Link Coupling 2

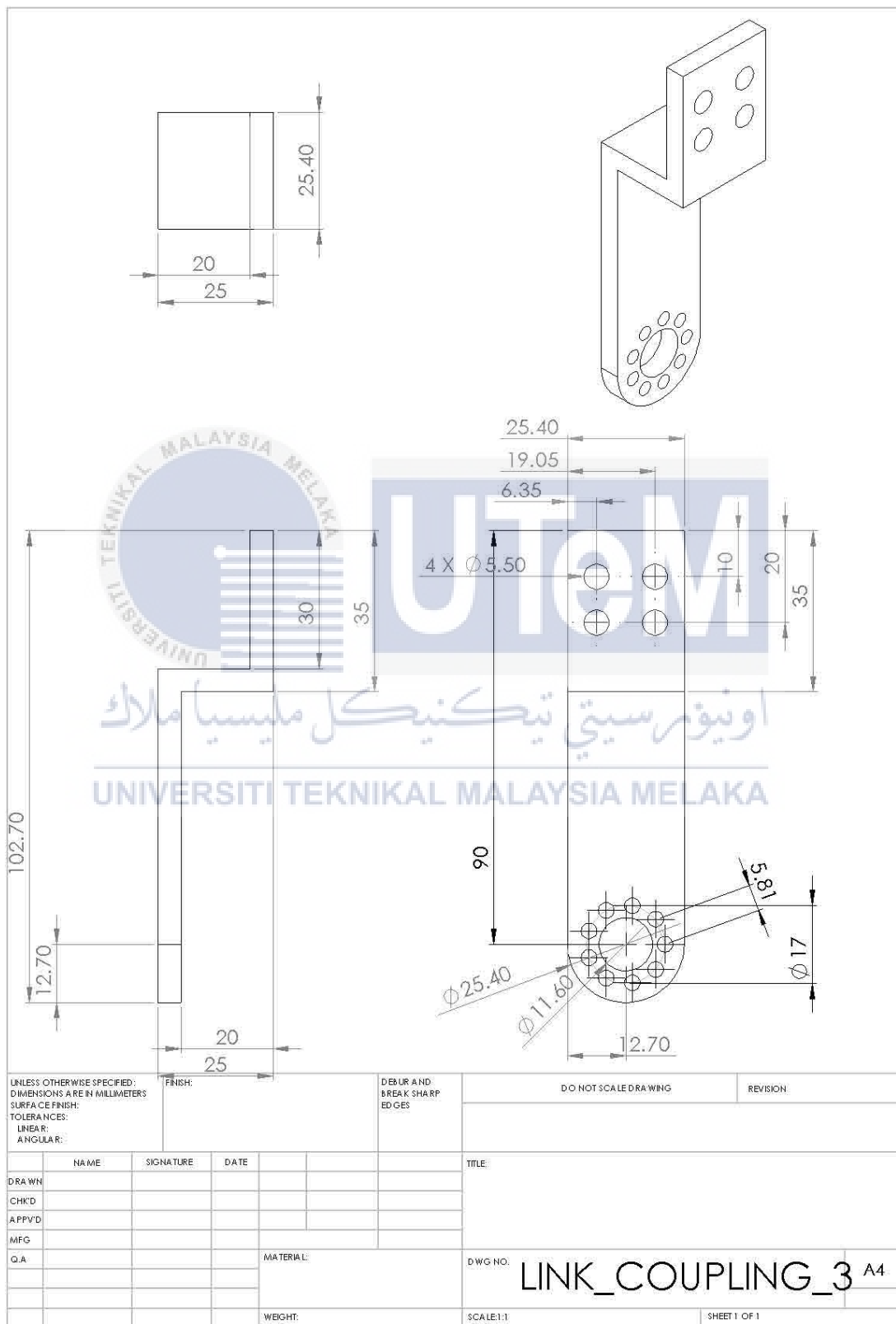|	NAME	SIGNATURE	DATE				TITLE:
DRAWN							
CHK'D							
APPV'D							
MFG							
Q.A							

UNLESS OTHERWISE SPECIFIED:
DIMENSIONS ARE IN MILLIMETERS
SURFACE FINISH:
TOLERANCES:
 LINEAR:
 ANGULAR:

FINISH:

DEBUR AND
BREAK SHARP
EDGES

DO NOT SCALE DRAWING

REVISION

MATERIAL:

WEIGHT:

DWG NO. LINK_COUPLING_2 A4

SCALE:1:1

SHEET 1 OF 1

APPENDIX G

Engineering Drawing of Link Coupling 3

	NAME	SIGNATURE	DATE			TITLE:		
DRAWN								
CHK'D								
APPV'D								
MFG								
Q.A				MATERIAL:		DWG NO. LINK_COUPLING_3	A4	
				WEIGHT:		SCALE:1:1	SHEET 1 OF 1	

UNLESS OTHERWISE SPECIFIED:
DIMENSIONS ARE IN MILLIMETERS
SURFACE FINISH:
TOLERANCES:
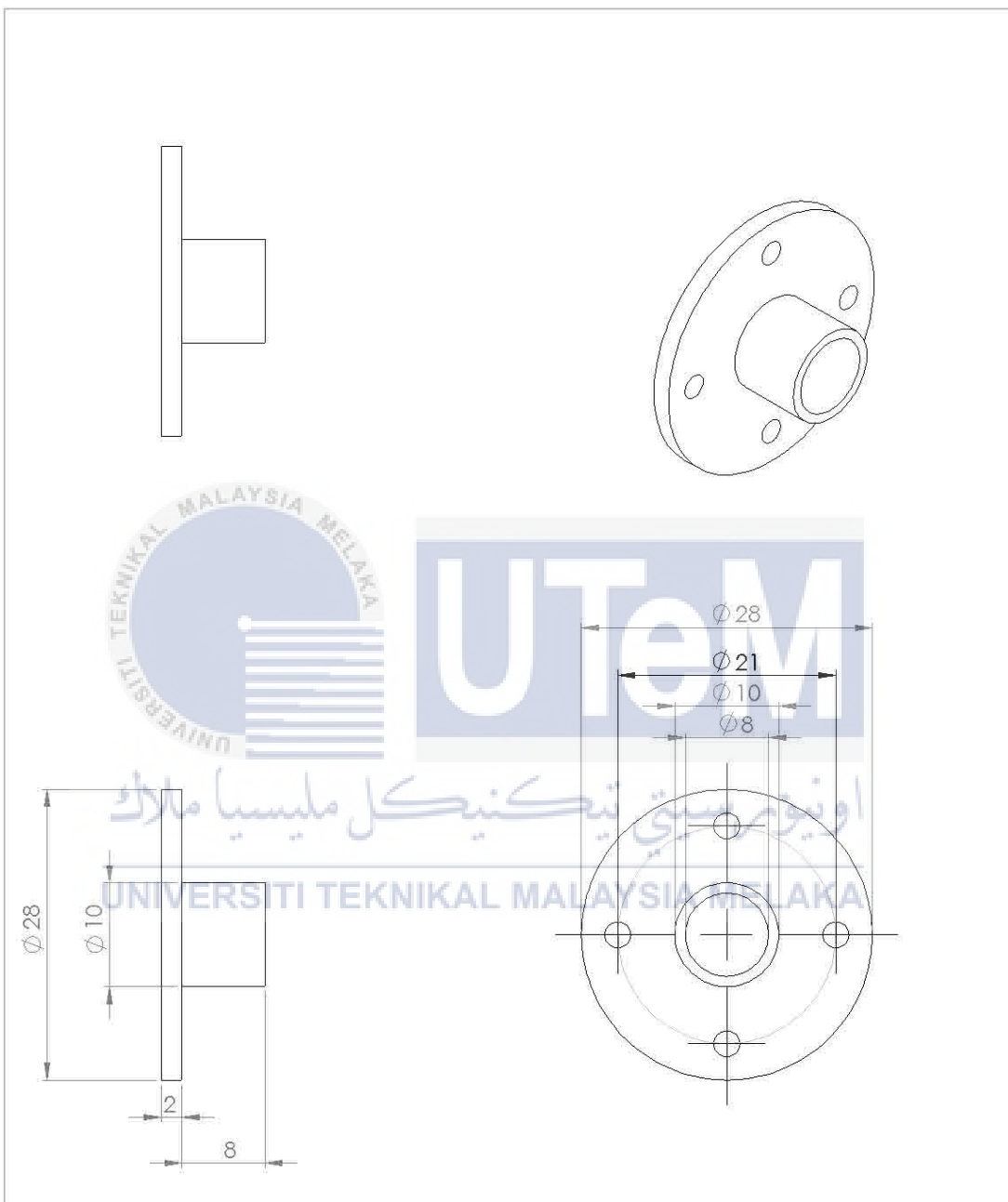 LINEAR:
  ANGULAR:

FINISH:

DEBUR AND
BREAK SHARP
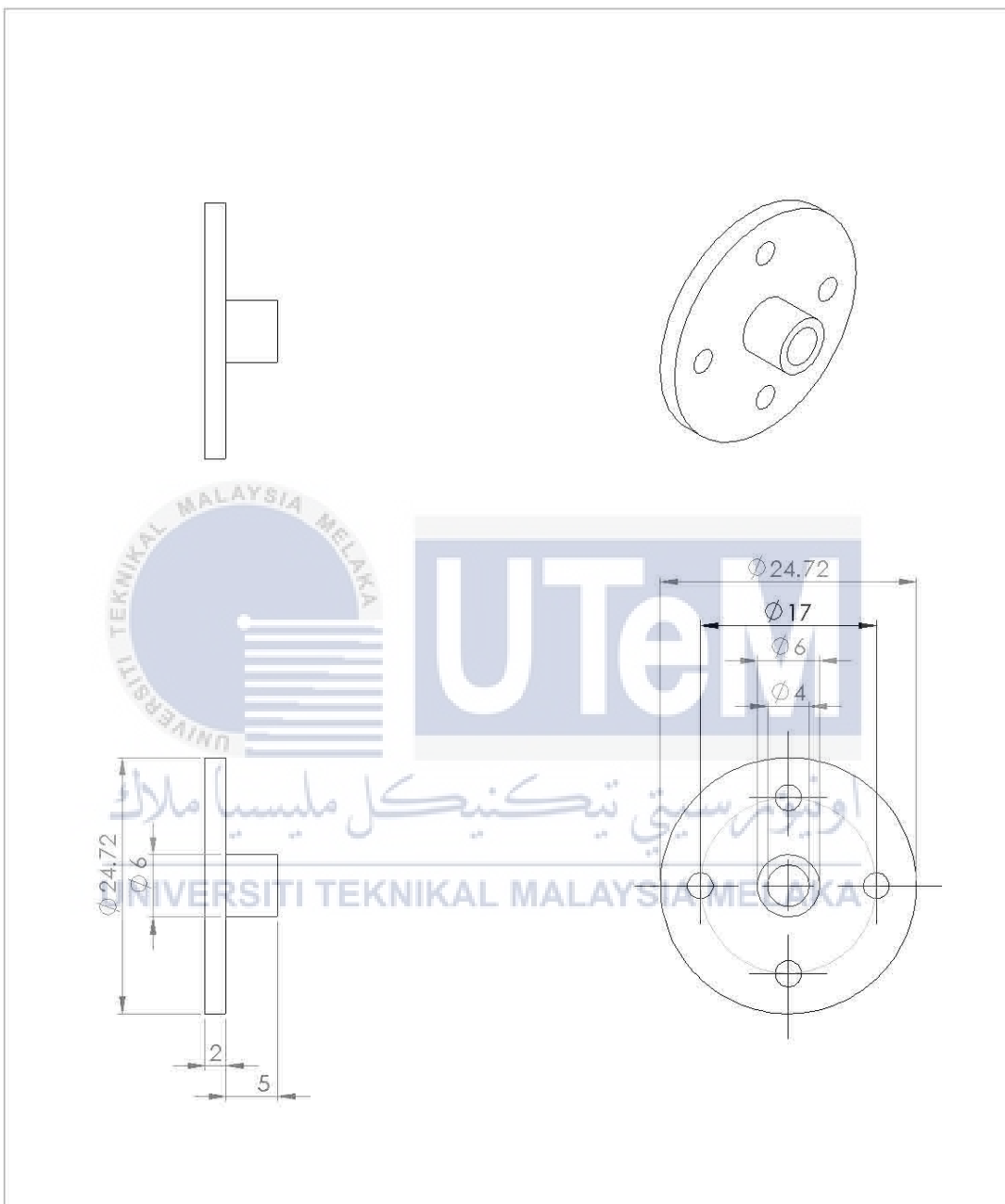EDGES

DO NOT SCALE DRAWING

REVISION

APPENDIX H

Engineering Drawing of Motor Coupling 1

UNLESS OTHERWISE SPECIFIED: DIMENSIONS ARE IN MILLIMETERS SURFACE FINISH: TOLERANCES: LINEAR: ANGULAR:		FINISH:			DEBUR AND BREAK SHARP EDGES		DO NOT SCALE DRAWING		REVISION
	NAME	SIGNATURE	DATE			TITLE:			
DRAWN									
CHK'D									
APPV'D									
MFG									
Q.A			MATERIAL:			DWG NO. MOTOR_COUPLING_1			A4
			WEIGHT:			SCALE:1:1		SHEET 1 OF 1	

APPENDIX I

Engineering Drawing of Motor Coupling 2

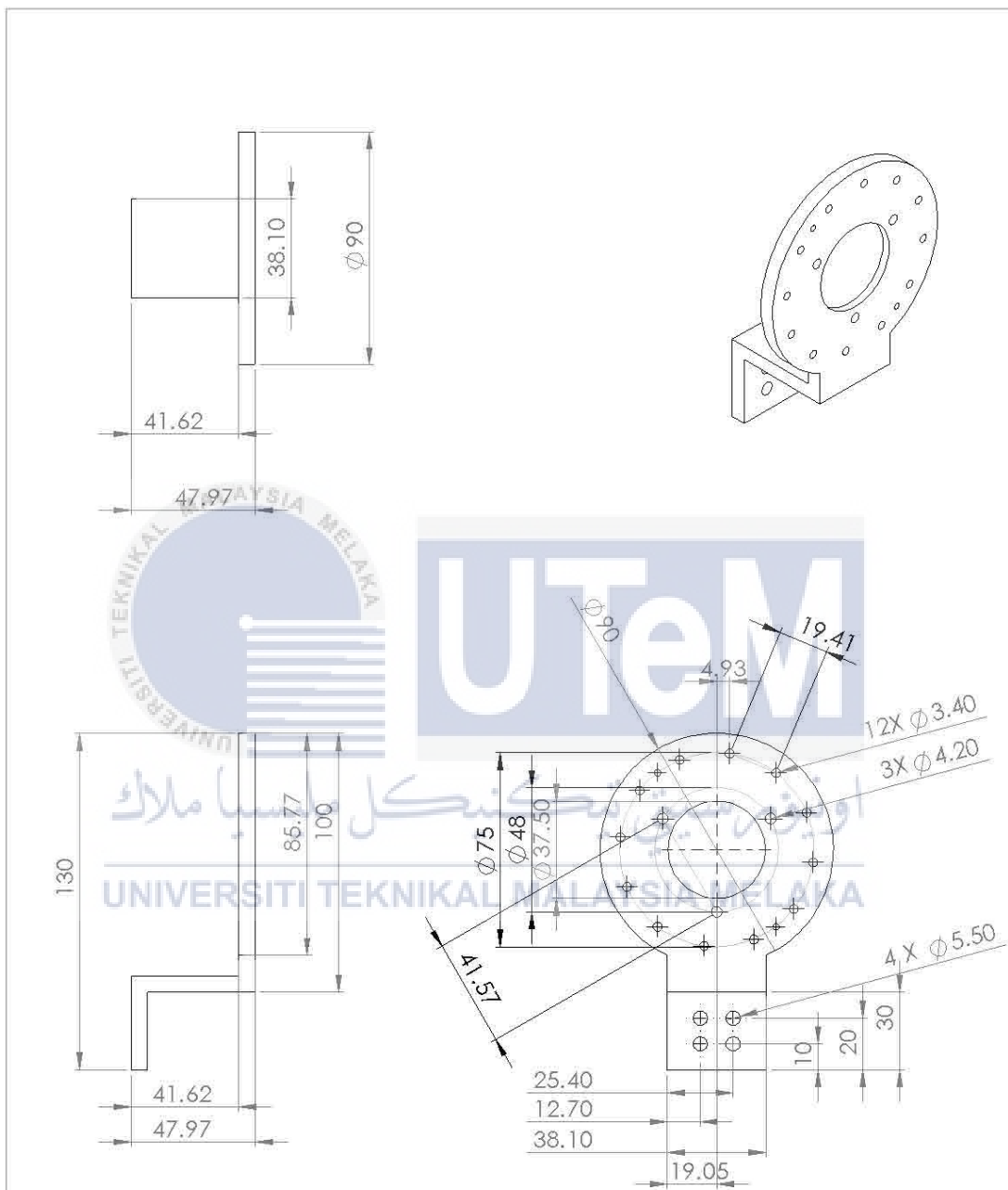|	NAME	SIGNATURE	DATE			TITLE:		
DRAWN								
CHK'D								
APPV'D								
MFG								
Q.A				MATERIAL:		DWG.NO. MOTOR_COUPLING_2		
				WEIGHT:		SCALE:2:1	SHEET 1 OF 1	

UNLESS OTHERWISE SPECIFIED:
DIMENSIONS ARE IN MILLIMETERS
SURFACE FINISH:
TOLERANCES:
   LINEAR:
   ANGULAR:

FINISH:

DEBUR AND
BREAK SHARP
EDGES

DO NOT SCALE DRAWING

REVISION

APPENDIX J

Engineering Drawing of Motor Coupling 3

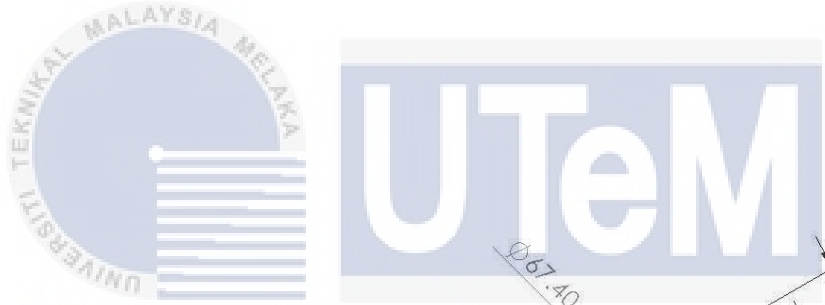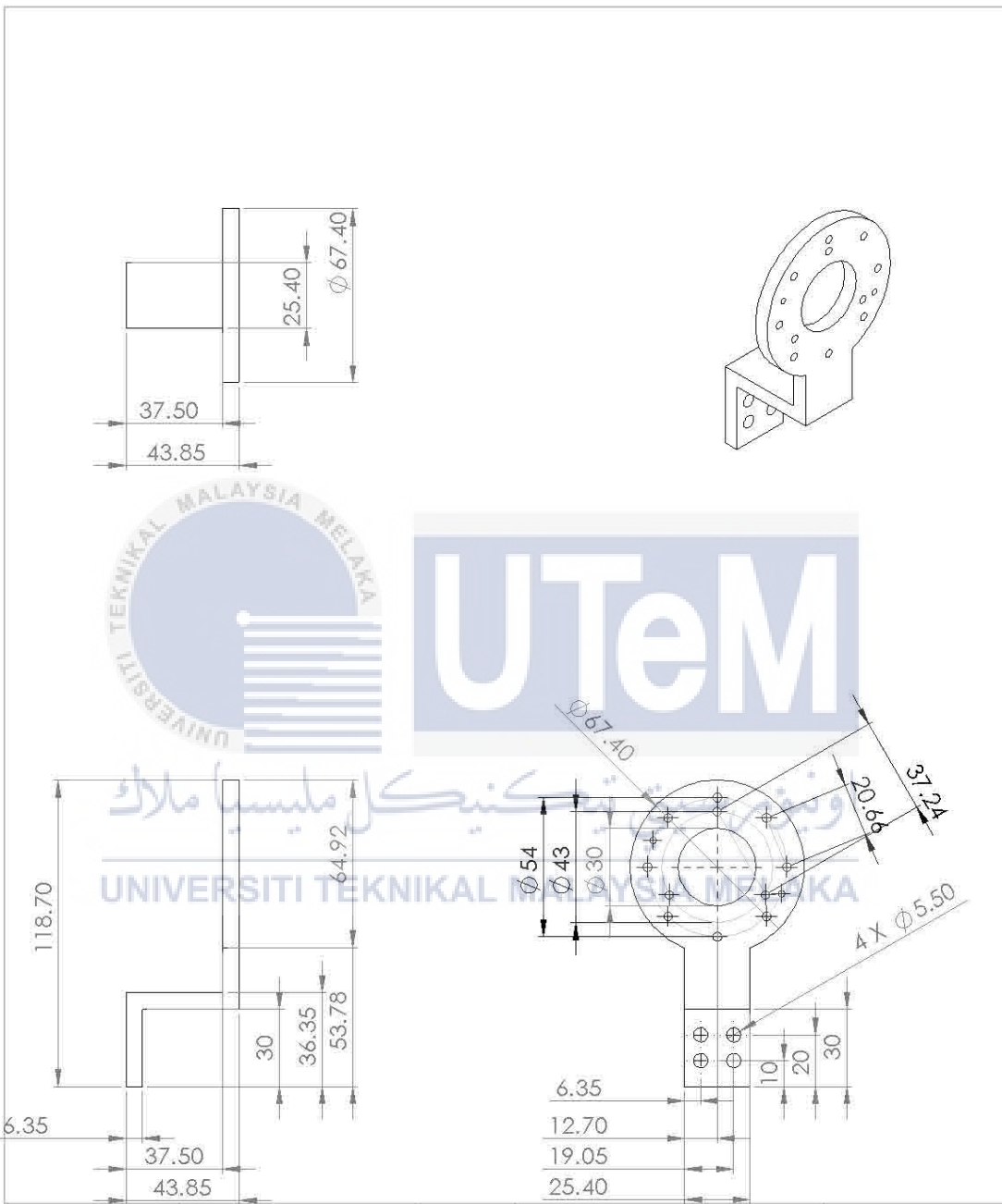|	NAME	SIGNATURE	DATE			TITLE:
DRAWN						
CHK'D						
APPV'D						
MFG						
Q.A			MATERIAL:			DWG NO. MOTOR_COUPLING_3
			WEIGHT:			SCALE:2:1 SHEET 1 OF 1

UNLESS OTHERWISE SPECIFIED: DIMENSIONS ARE IN MILLIMETERS SURFACE FINISH: TOLERANCES: LINEAR: ANGULAR:

FINISH:

DEBUR AND BREAK SHARP EDGES

DO NOT SCALE DRAWING

REVISION

Ø24.72 Ø17 Ø6 Ø4 Ø24.72 Ø6 2 5

APPENDIX K

Engineering Drawing of Motor Mount 1

	NAME	SIGNATURE	DATE
DRAWN			
CHK'D			
APPV'D			
MFG			
Q.A			

UNLESS OTHERWISE SPECIFIED:
DIMENSIONS ARE IN MILLIMETERS
SURFACE FINISH:
TOLERANCES:
  LINEAR:
  ANGULAR:

FINISH:

DEBUR AND BREAK SHARP EDGES

DO NOT SCALE DRAWING

REVISION

TITLE:

MATERIAL:

DWG NO. MOTOR_MOUNT_1 A4

WEIGHT:

SCALE:1:2

SHEET 1 OF 1

APPENDIX L

Engineering Drawing of Motor Mount 2

APPENDIX M

Engineering Drawing of Motor Mount 3

APPENDIX N

Engineering Drawing of Left Foot Pad

UNLESS OTHERWISE SPECIFIED: DIMENSIONS ARE IN MILLIMETERS SURFACE FINISH: TOLERANCES: LINEAR: ANGULAR:	FINISH:		DEBUR AND BREAK SHARP EDGES	DO NOT SCALE DRAWING	REVISION

	NAME	SIGNATURE	DATE			TITLE:
DRAWN						
CHK'D						
APPV'D						
MFG						
Q.A				MATERIAL:		DWG NO. FOOT_PAD_LEFT	A4
				WEIGHT:		SCALE:1:5	SHEET 1 OF 1

APPENDIX O

Engineering Drawing of Right Foot Pad

2 X R50

2 X R30

3.18

187.30
212.70
220

30

62.32
92.32
112.32
132.32

36.82
40

62.32
92.32
132.32
162.32

30

4 X Ø5.50

187.30
193.65
206.35
212.70
220
270

20
30
36.82
40

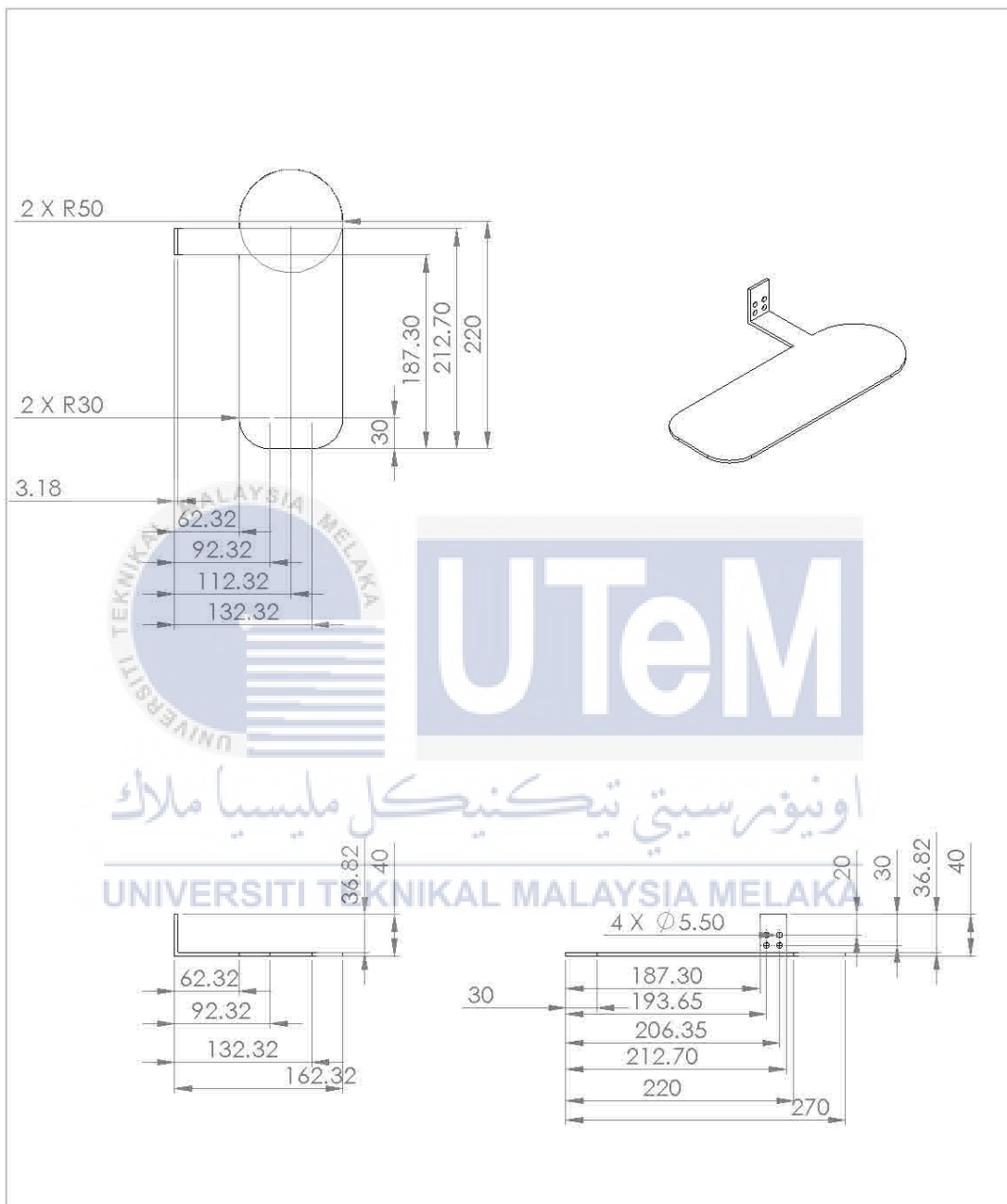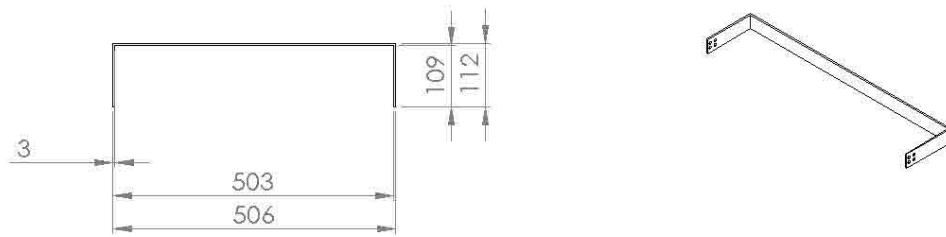|	NAME	SIGNATURE	DATE				TITLE:		
DRAWN									
CHK'D									
APPV'D									
MFG									
Q.A			MATERIAL:				DWG NO. FOOT_PAD_RIGHT	A4	
			WEIGHT:				SCALE:1:5	SHEET 1 OF 1	

UNLESS OTHERWISE SPECIFIED:
DIMENSIONS ARE IN MILLIMETERS
SURFACE FINISH:
TOLERANCES:
  LINEAR:
  ANGULAR:

FINISH:

DEBUR AND
BREAK SHARP
EDGES

DO NOT SCALE DRAWING

REVISION

APPENDIX P

Engineering Drawing of Belt

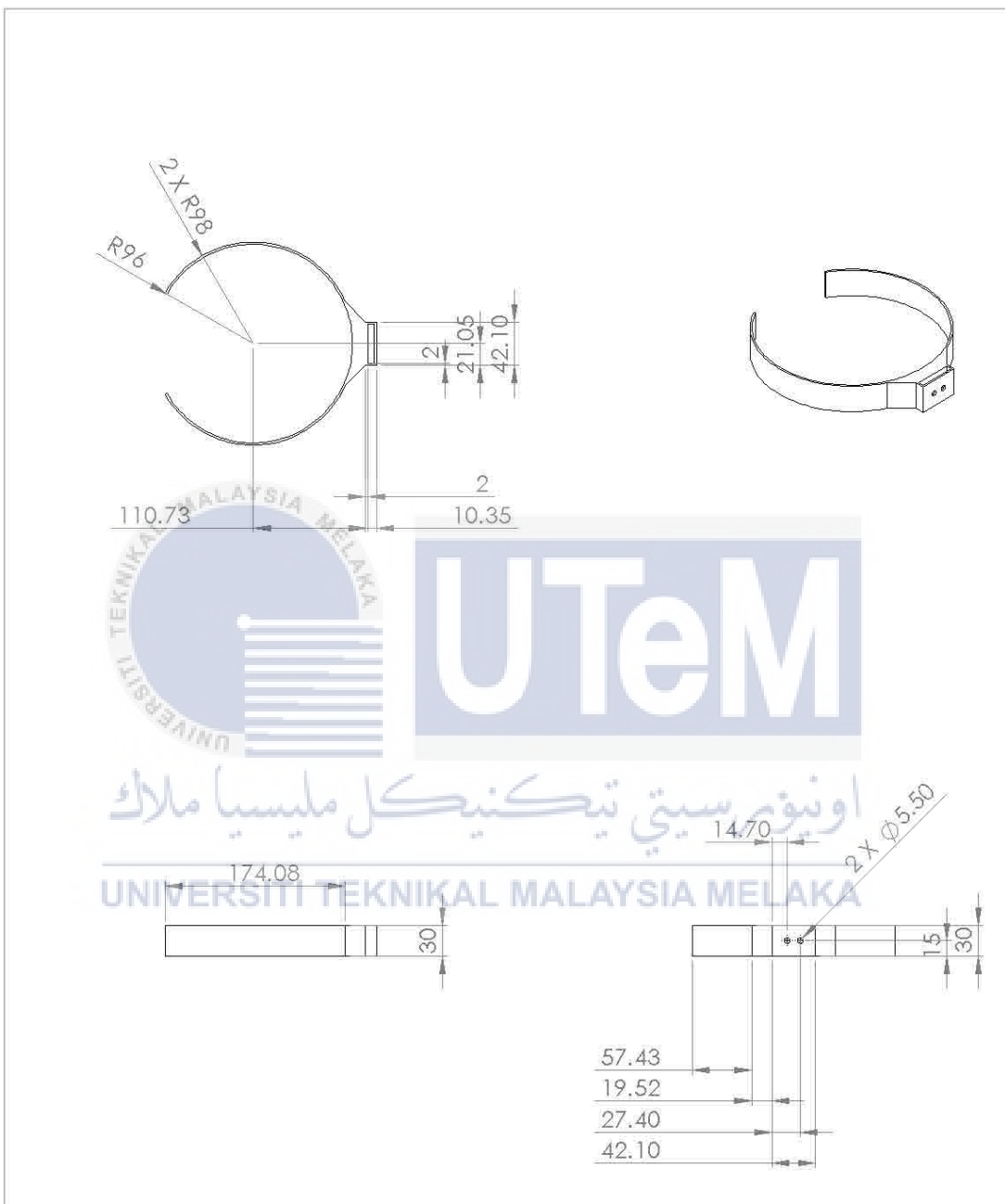|	NAME	SIGNATURE	DATE			TITLE		
DRAWN								
CHK'D								
APPV'D								
MFG								
Q.A			MATERIAL:			DWG NO.	BELT	A4

UNLESS OTHERWISE SPECIFIED:
DIMENSIONS ARE IN MILLIMETERS
SURFACE FINISH:
TOLERANCES:
  LINEAR:
  ANGULAR:

FINISH:

DEBUR AND BREAK SHARP EDGES

DO NOT SCALE DRAWING   REVISION

WEIGHT: SCALE:1:10   SHEET 1 OF 1

APPENDIX Q

Engineering Drawing of Brace

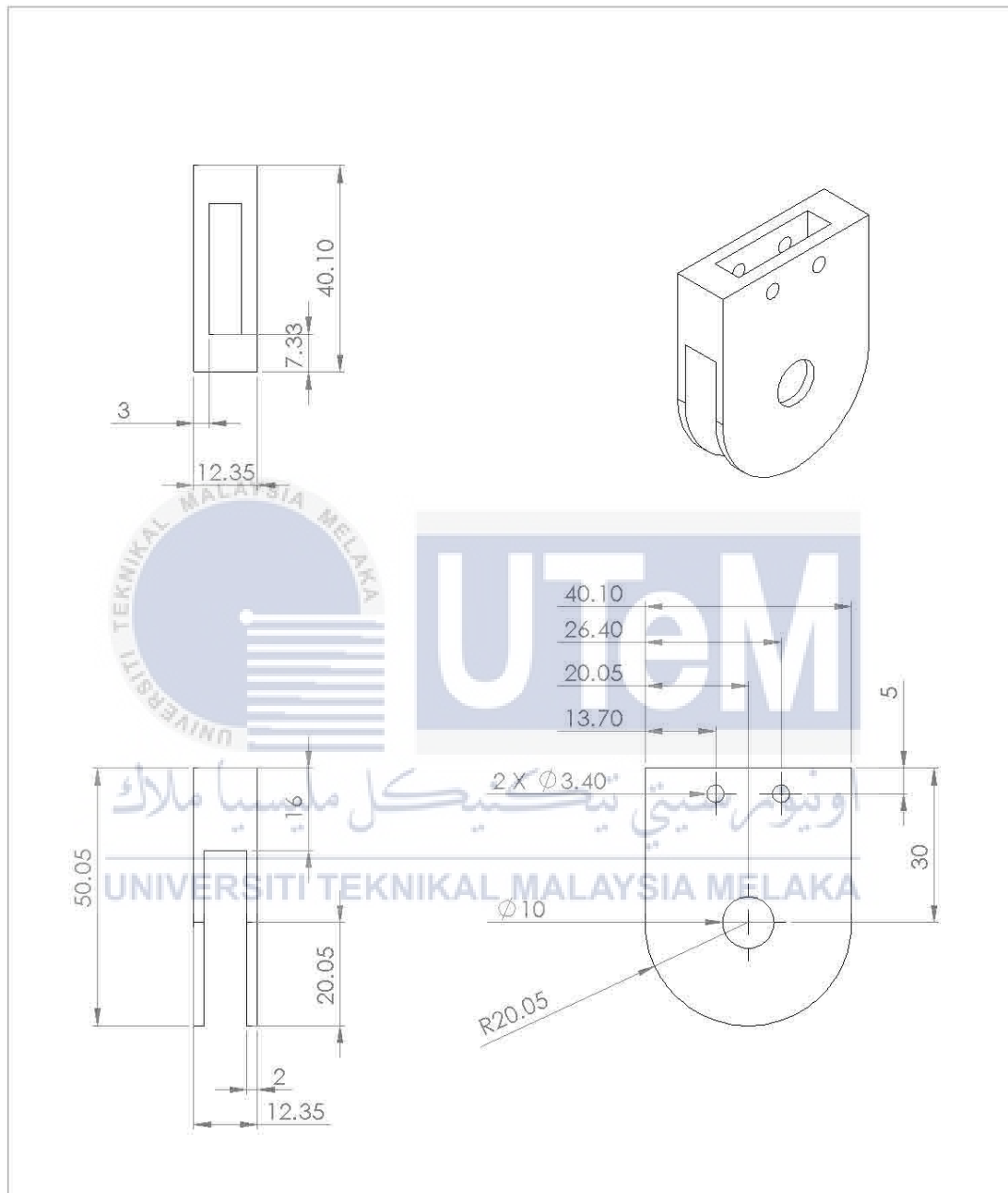|	NAME	SIGNATURE	DATE				TITLE:			
DRAWN										
CHK'D										
APPV'D										
MFG										
Q.A				MATERIAL:			DWG NO.	BRACE_1		A4
				WEIGHT:			SCALE:1:5		SHEET 1 OF 1	

UNLESS OTHERWISE SPECIFIED:
DIMENSIONS ARE IN MILLIMETERS
SURFACE FINISH:
TOLERANCES:
  LINEAR:
  ANGULAR:

FINISH:

DEBUR AND
BREAK SHARP
EDGES

DO NOT SCALE DRAWING   REVISION

APPENDIX R

Engineering Drawing of Pivot Base 1

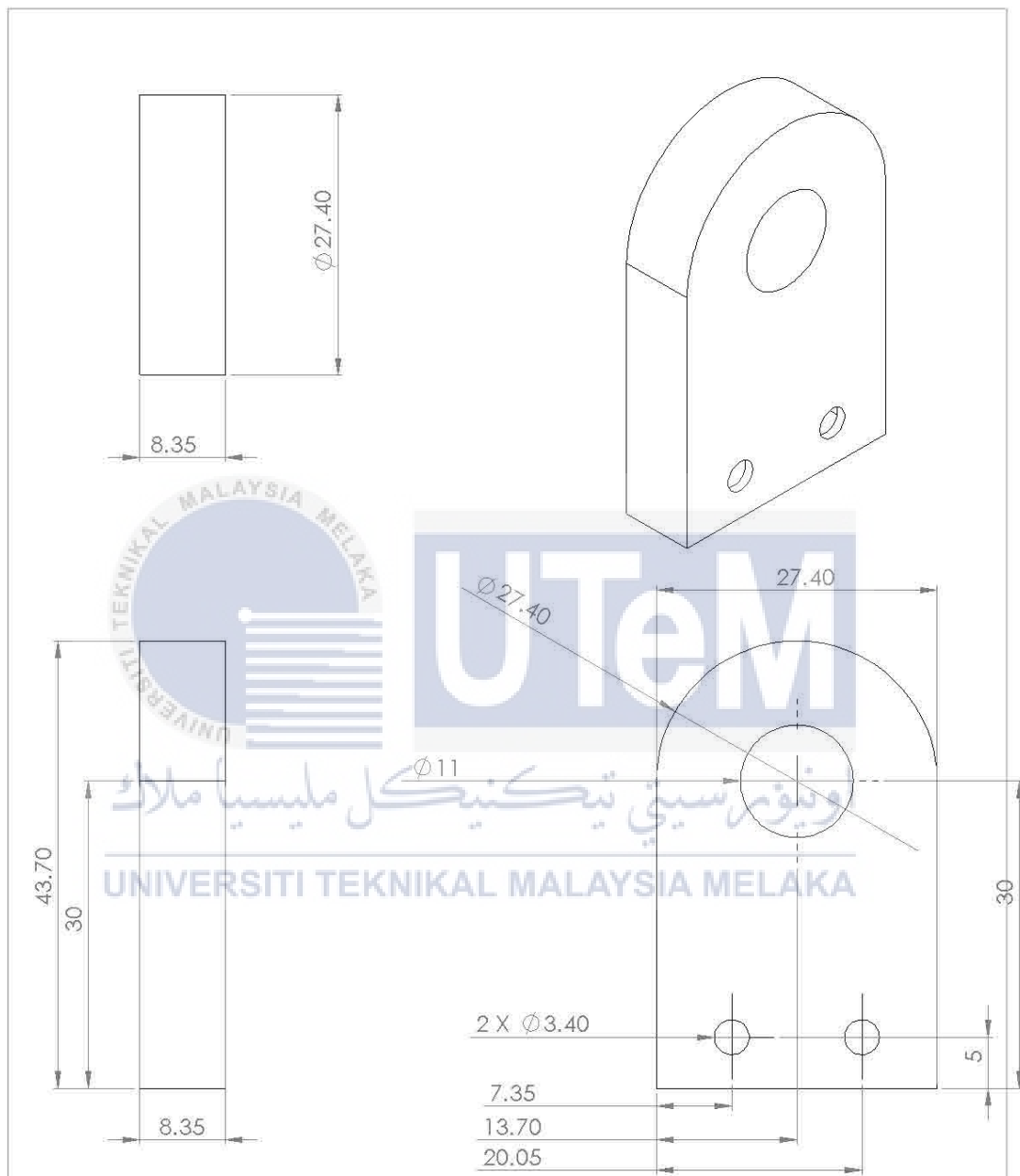|	NAME	SIGNATURE	DATE				TITLE:		
DRAWN									
CHK'D									
APPV'D									
MFG									
Q.A				MATERIAL:			DWG NO.	PIVOT_BASE	A4
				WEIGHT:			SCALE:1:1		SHEET 1 OF 1

UNLESS OTHERWISE SPECIFIED:
DIMENSIONS ARE IN MILLIMETERS
SURFACE FINISH:
TOLERANCES:
   LINEAR:
   ANGULAR:

FINISH:

DEBUR AND
BREAK SHARP
EDGES

DO NOT SCALE DRAWING   REVISION

APPENDIX S

Engineering Drawing of Pivot Effector 1

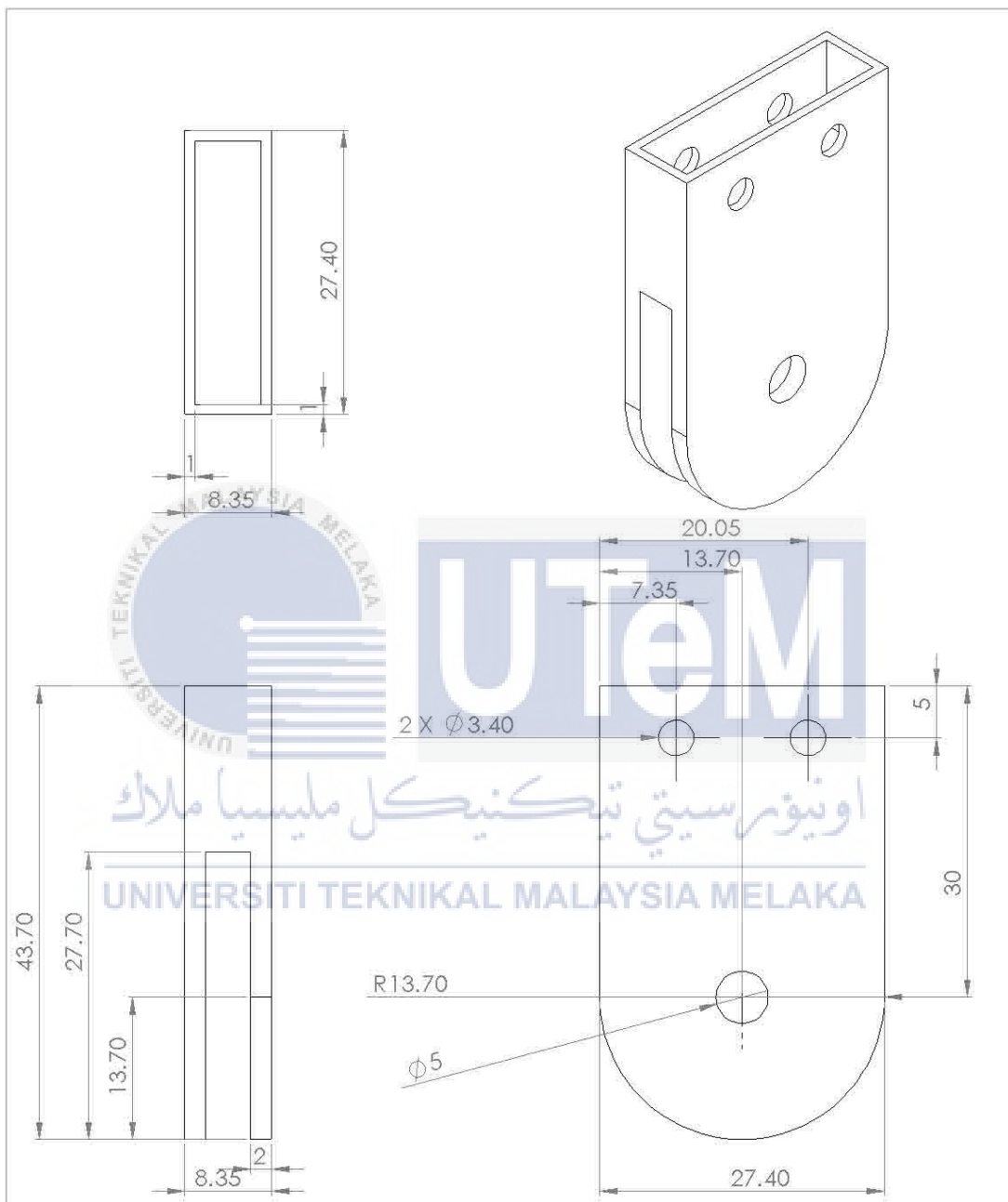|	NAME	SIGNATURE	DATE				TITLE:
DRAWN							
CHK'D							
APPV'D							
MFG							
Q.A			MATERIAL:				DWG NO.

UNLESS OTHERWISE SPECIFIED:
DIMENSIONS ARE IN MILLIMETERS
SURFACE FINISH:
TOLERANCES:
 LINEAR:
 ANGULAR:

FINISH:

DEBUR AND
BREAK SHARP
EDGES

DO NOT SCALE DRAWING

REVISION

PIVOT_EFFECTOR   A4

WEIGHT: SCALE:2:1   SHEET 1 OF 1

APPENDIX T

Engineering Drawing of Pivot Base 2

APPENDIX U

Engineering Drawing of Pivot Effector 2

27.40

8.35

27.40

Ø27.40

Ø6

30

43.70

30

16

16

5

2.18   2.18

8.35

2 X Ø3.40

7.35   7.35

13.70

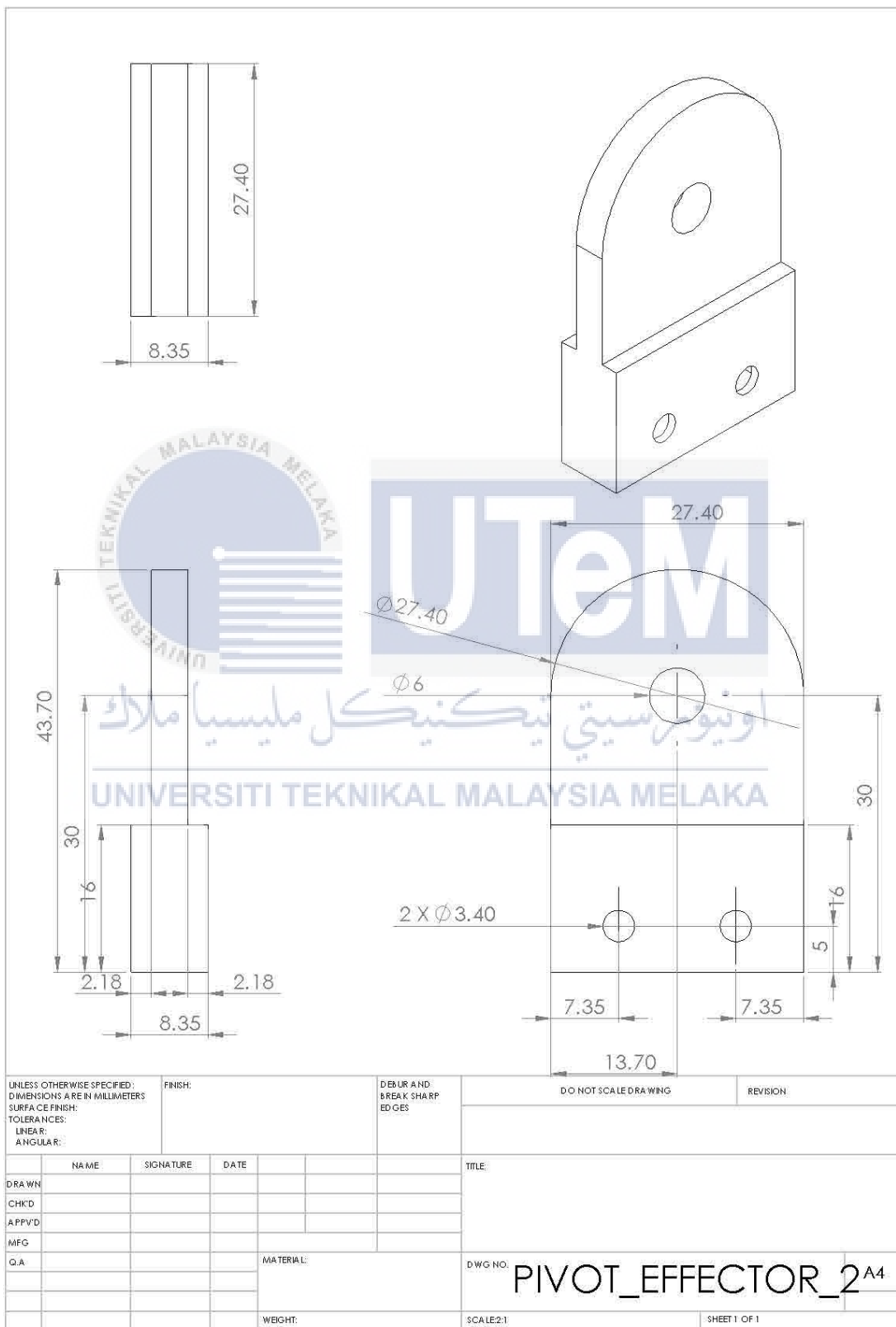|	NAME	SIGNATURE	DATE			
DRAWN						
CHK'D						
APPV'D						
MFG						
Q.A						

UNLESS OTHERWISE SPECIFIED:
DIMENSIONS ARE IN MILLIMETERS
SURFACE FINISH:
TOLERANCES:
  LINEAR:
  ANGULAR:

FINISH:

DEBUR AND
BREAK SHARP
EDGES

DO NOT SCALE DRAWING

REVISION

TITLE:

MATERIAL:

DWG NO. PIVOT_EFFECTOR_2 A4

WEIGHT:

SCALE:2:1

SHEET 1 OF 1

APPENDIX V

Engineering Drawing of Pivot Base 3

27.40

1

1

8.35

43.70

27.70

13.70

2

8.35

2 X Ø3.40

20.05

13.70

7.35

5

30

R13.70

Ø5

27.40

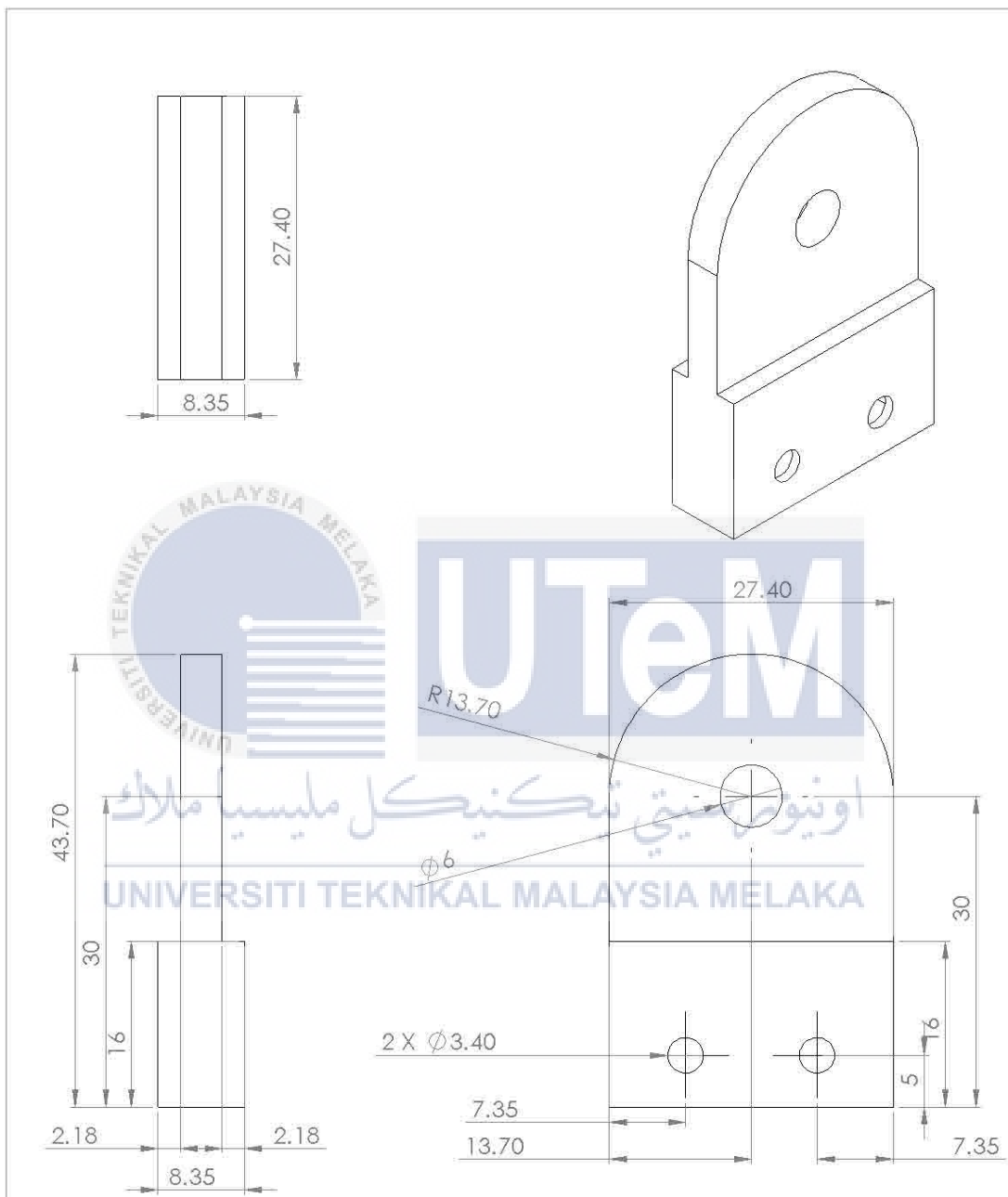|	NAME	SIGNATURE	DATE			TITLE:		
DRAWN								
CHK'D								
APPV'D								
MFG								
Q.A			MATERIAL:			DWG NO.	PIVOT_BASE_3	A4
			WEIGHT:			SCALE:2:1		SHEET 1 OF 1

UNLESS OTHERWISE SPECIFIED: DIMENSIONS ARE IN MILLIMETERS SURFACE FINISH: TOLERANCES: LINEAR: ANGULAR:

FINISH:

DEBUR AND BREAK SHARP EDGES

DO NOT SCALE DRAWING

REVISION

APPENDIX W

Engineering Drawing of Pivot Effector 3

	NAME	SIGNATURE	DATE			TITLE:	
DRAWN							
CHK'D							
APPV'D							
MFG							
Q.A			MATERIAL:			DWG NO. PIVOT_EFFECTOR_3	A4
			WEIGHT:			SCALE:2:1	SHEET 1 OF 1

UNLESS OTHERWISE SPECIFIED:
DIMENSIONS ARE IN MILLIMETERS
SURFACE FINISH:
TOLERANCES:
  LINEAR:
  ANGULAR:

FINISH:

DEBUR AND BREAK SHARP EDGES

DO NOT SCALE DRAWING

REVISION

APPENDIX X

Engineering Drawing of Waist Link